12-2019

Functional Importance of Lipin Phosphorylation

Stephanie Elizabeth Hood
University of Arkansas, Fayetteville

Functional Importance of Lipin Phosphorylation

A thesis submitted in partial fulfillment
of the requirements for the degree of
Master of Science in Cell and Molecular Biology

by

Stephanie E. Hood
Fairfield University
Bachelor of Science in Biology, 2013

December 2019
University of Arkansas

This thesis is approved for recommendation to the Graduate Council.

_____
Michael H. Lehmann, Ph.D.
Thesis Director

_____
Timothy A. Evans, Ph.D.
Committee Member

_____
Francis Millett, Ph.D.
Committee Member

Abstract

Highly conserved throughout evolution, lipins are dual functioning proteins found from yeast to humans. Functioning in the cytoplasm as phosphatidate phosphatase enzymes (PAP), lipins produce diacylglycerol that serves as a precursor for neutral fats and membrane phospholipids. Alternatively, nuclear lipins are responsible for the regulation of metabolic genes. Interestingly, both the mammalian lipin 1 paralog and the single *Drosophila* Lipin ortholog are highly phosphorylated proteins. Target of rapamycin (TOR) has previously been identified as one of the kinases that controls the subcellular localization of both lipin 1 and *Drosophila* Lipin. However, other serine and threonine kinases are predicted to be important for the phosphorylation of Lipin. Here, I implement both the GAL4/UAS system as well as CRISPR/Cas9 mutagenesis to systematically mutate individual amino acid residues or clusters of phosphorylation sites of *Drosophila* Lipin to identify their functional importance. Phenotypic characterization of the phosphosite mutants included fat body histology and fat droplet staining, triglyceride and protein content, starvation resistance, and potential developmental delays. Lipin antibody staining was employed to reveal intracellular distribution of the mutant protein. Results support the prediction that these phosphorylation sites are important for both nuclear function and the role of the protein in fat storage. Data reported here will support the understanding of how the activities of these proteins could be specifically targeted.

Acknowledgements

I would like to thank my graduate committee for their support and guidance throughout my degree. In particular, I would like to thank my advisor, Michael Lehmann his mentorship and constant encouragement.

Additionally, to my family and friends who have encouraged me throughout my degree, thank you! You have all made this moment possible. I would like to especially thank my husband Nick, who has supported me throughout every step of this journey; thank you for your patience and understanding when many nights and weekends were spent in the lab.

Dedication

For my grandfather, Patrick J. Greene, who passed away as I was finishing my degree. Without your guidance, I would not be the scientist I am today. Thank you for showing me that anything is possible with hard work and dedication.

Table of Contents

II. Materials and Methods (Cont.)

III. Results (Cont.)

List of Tables

List of Figures

List of Figures (Cont.)

List of Figures (Cont.)

I. Introduction

1. Functions of Lipin

Lipins are dual-function proteins that act according to their subcellular localization (Fig. 1) (Reue et al. 2009; Péterfy et al. 2010). In the cytoplasm, lipins function in the glycerol-3-phosphate pathway where they work as enzymes aiding in the production of diacylglycerol (DAG), the direct precursor for triacylglycerol (TAG), the main energy store used by eukaryotes (Fig. 2) (Csaki et al. 2013). Additionally, cytoplasmic Lipin is responsible for to synthesis of phospholipids, phosphatidylserine, phosphatidylethanolamine, and phosphatidylcholine. Nuclear lipins function as transcriptional coactivators and are responsible for the regulation of metabolic genes (Reue, 2009; Peterson et al., 2011).

Phosphatidic phosphatase activity (PAP) of Lipin has been well studied and is necessary for survival. Animals which lack PAP activity experience deficiencies in TAG synthesis (Harris et al., 2011). As mentioned, PAP activity of Lipin plays a fundamental role in the glycerol-3 phosphate pathway resulting in the production of TAG. TAG is then stored in specialized cells referred to as fat droplets. Membrane bound phospholipids are also a product of the PAP activity of Lipin, as the DAG produced serves as a precursor for their production (Csaki et al., 2013). In addition, PAP activity of Lipin is also required for normal insulin pathway activity in the *Drosophila* fat body (Schmitt et al., 2015).

The nuclear functions of Lipin, however, remain somewhat elusive. In mammals, Target of rapamycin complex 1 (TORC1) is a kinase responsible for the phosphorylation of lipin 1, inhibiting its translocation to the nucleus under fed conditions. However, during times of starvation, TORC1 is downregulated, and lipin 1 is able to enter the nucleus to act as a transcriptional co-regulator for metabolic genes (Peterson et al., 2011). Lipin in the fat body of

Drosophila melanogaster has also been observed to translocate into the cell nucleus during times of starvation and also when TORC1 is down-regulated by RNAi (Schmitt et al., 2015).

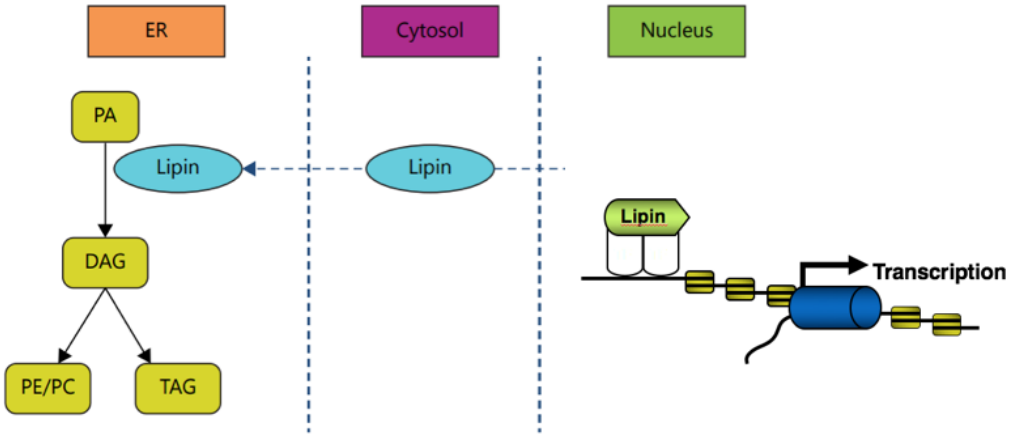

Fig 1. Lipin is a dual functioning protein. In the cytoplasm, specifically, the endoplasmic reticulum (ER), Lipin serves as a PAP enzyme and is responsible for the production DAG. In the nucleus, Lipin works as a transcriptional co-regulator. Figure from adapted from Chen et al., 2014.

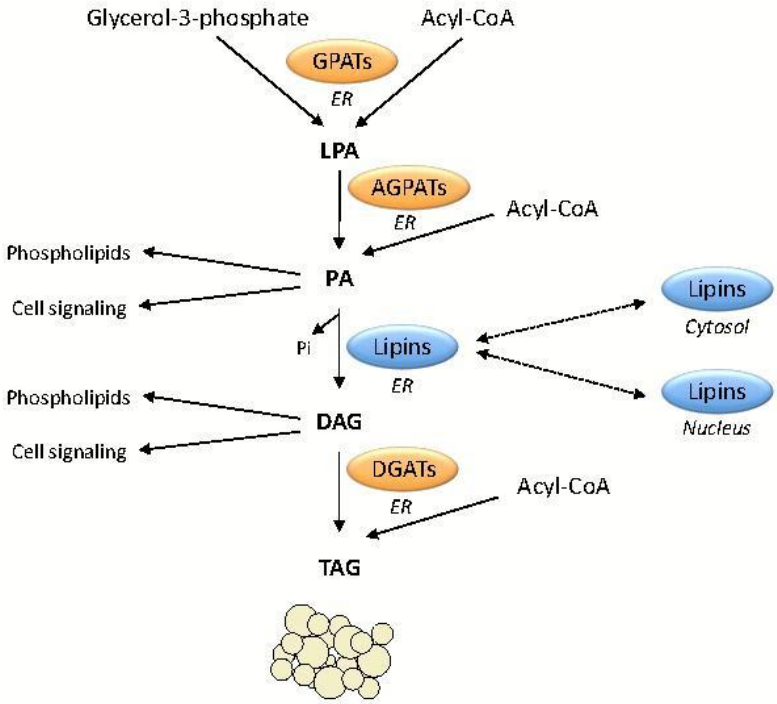

Fig 2. Lipins function as phosphatidic phosphatases in the Glycerol 3-phosphate pathway. Lipins function in the ER as a PAP enzymes and are responsible for the production of DAG. DAG is the precursor for TAG and phospholipid synthesis. Figure from adapted from Csaki et al., 2013.

1a. lipin gene family

i. *Drosophila* Lipin

The single Lipin ortholog in *Drosophila* (Péterfy et al. 2001) is essential for normal fat body (adipose tissue) development and TAG storage (Ugrankar et al., 2011). Loss of Lipin in *Drosophila* results in reductions of whole-animal TAG content, lipid droplet size, and larval fat body mass. Overall reduction in the fat body and ultrastructural defects of individual fat body cells in the autophagosomes, mitochondria, and cell nuclei have been observed in *Drosophila Lpin* mutants (Ugrankar et al., 2011). Defects displayed by Lipin mutants are associated with impairment of starvation resistance and reduced fertility and viability (Ugrankar et al., 2011).

ii. Mammalian Lipin

Studies done in mice have revealed three lipin paralogs in mammals (Péterfy et al., 2001). Lipin 1, is encoded in the *Lpin1* gene, where the other two paralogs, *Lpin2* and *Lpin3*, are encoded by different genes. Lipin 1 is most highly studied of the mammalian *Lpin* genes and is the most similar to *Drosophila Lpin* (Csaki et al., 2013). Mice with a lipin 1 deficiency experience a variety of metabolic disorders including lipodystrophy, insulin resistance, peripheral neuropathy, and neonatal fatty liver (Péterfy et al., 2001).

Independent physiological roles are expected for the three *Lpin* genes of mammals as they exhibit unique patterns of tissue expression (Reue, 2009). *Lpin1* is expressed predominantly in the muscle and adipose tissue, and has lower expression in bone, brain, kidney, and liver (Csaki et al., 2013). *Lpin2* expression extends to many tissues including lung, brain, kidney and liver. *Lpin3* has been detected at low levels in the liver and other visceral tissues (Reue, 2009).

iii. Additional homologs

Lipin is found in species well beyond mammals and *Drosophila*. Homologs of mouse lipin genes have been found in *Trypanosoma brucei, Plasmodium falsiparum, Shizosaccharomyces pombe, Caenorhabditis elegans* (*C. elegans*), *Arabidopsis thaliana, Saccaromyces cerevisa,* and *Homo sapiens* (Péterfy et al., 2001). Yeast as well as most invertebrates contain a single lipin ortholog, whereas plants and some worm species (excluding *C. elegans*) contain two lipin paralogs (Harris et al., 2011).

Loss of the single lipin ortholog in yeast results in increases in phosphatidic acid (PA) and decreases in TAG production. In *C. elegans*, loss of the single lipin homolog impacts the nuclear structure and morphology of the endoplasmic reticulum (ER). Loss of the lipin homologs in *Arabidopsis* increases PA levels but TAG content in the plant seeds remains unaltered (Harris et al., 2011).

2. Structure of Lipin

Both mammalian lipin1b and *Drosophila* Lipin proteins have conserved domains located in the NH_2- and COOH- terminal regions, known as the NLIP and CLIP domains (Fig. 3). Contained within the CLIP domain is the DXDXT motif which is responsible for the PAP activity of Lipin and the LXXIL motif, which is a transcriptional co-regulator motif (Finck, 2006). A comparison of the Lipin protein structure across species is depicted in Figure 3.

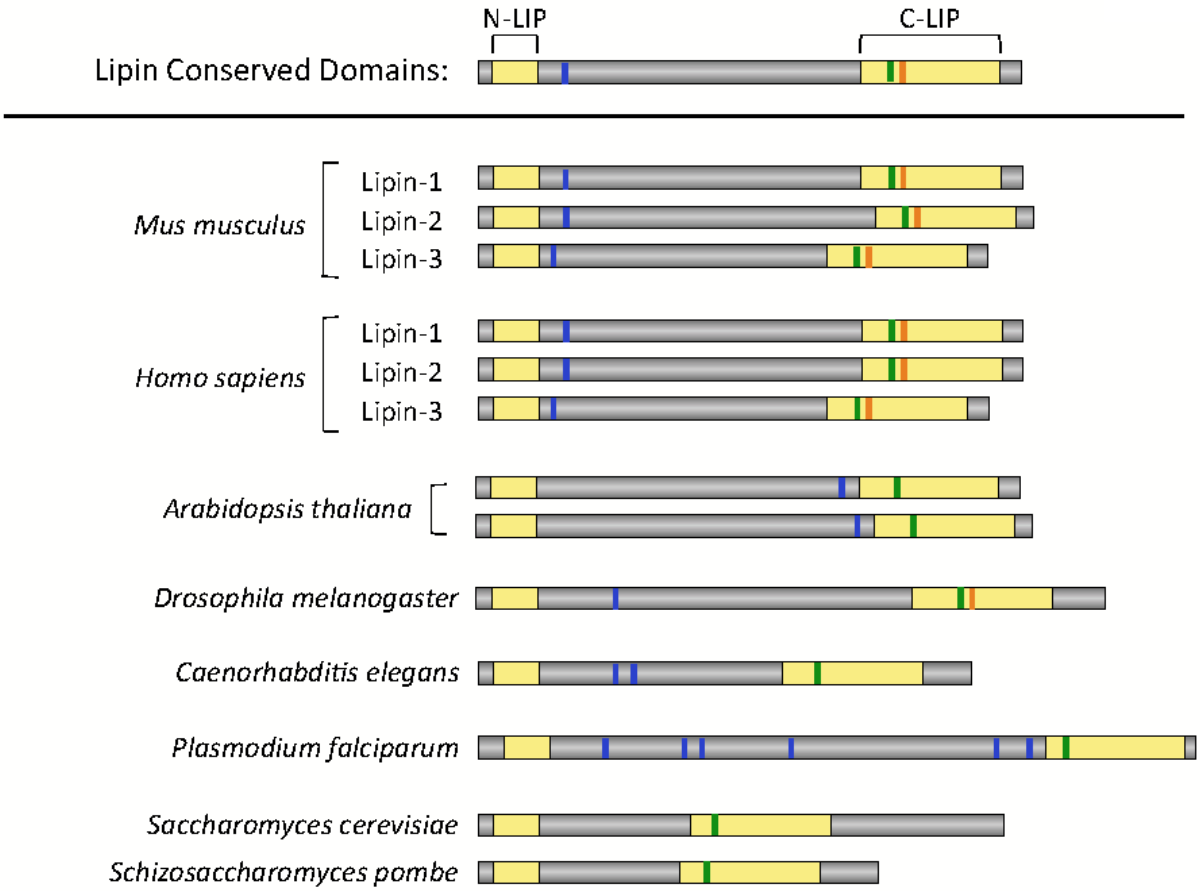

Fig 3. A cross-species comparison of Lipin protein structure reveals evolutionary conservation of protein domains. Homologs of Lipin show conservation of the NLIP and CLIP domains (yellow). Nuclear localization sequence (blue). The CLIP domain contains the catalytic motif, PAP (green) and transcriptional co-regulator motif (orange). Image adapted from Csaki et al., 2013.

3. Regulation of Lipin

3a. Regulation by phosphorylation

Phosphorylation of proteins is a highly dynamic and reversible modification that influences the function of the protein. There are several key differences between the post-translational modifications of lipins that exist between yeast and higher organisms (Harris et al., 2011). Phosphorylation is known to alter the intrinsic PAP activity in yeast but not in mammals (Harris et al., 2011). Rather, phosphorylation of lipins in vertebrates is suggested to control the activity of the protein by altering its subcellular localization (Reue, 2009). The activity of *Drosophila* Lipin is also predicted to be controlled by subcellular localization. Phosphorylation by protein kinases and removal of the phosphate groups by phosphatases is predicted to mediate the cellular location of Lipin (Harris et al., 2011).

One of the kinases suspected to be responsible for phosphorylation of lipins is Target of rapamycin (TOR). It has been directly shown that the mammalian paralog, lipin 1, is phosphorylated by TOR (Peterson et al., 2011). TOR kinase is also believed to be responsible for phosphorylation of *Drosophila* Lipin. During fed conditions, when TOR activity is high, Lipin is located in the cytosol in both mammals and *Drosophila* (Peterson et al., 2011; Schmitt et al., 2015).

How TOR kinase works to control the intracellular localization of *Drosophila* Lipin is only somewhat understood. During times of starvation or when TOR is knocked down by RNAi, Lipin translocates to the nucleus (Schmitt et al., 2015), suggesting that phosphorylation by TOR restricts nuclear import of Lipin. However, it is predicted that other kinases also contribute to the regulation of Lipin in *Drosophila* (Bodenmiller et al., 2008; Bridon et al., 2012). Serine and threonine residues are targets for other protein kinases and/or phosphatases

and may contribute to the regulation of lipins. Such kinases may include mitogen-activated protein kinases (MAPK) (Steinhauer, 2017) or kinases of the insulin/PI3K pathway (DiAngelo et al., 2009).

Phosphorylation of mammalian and *Drosophila* lipins has only ever been studied in cell culture lines. The cell lines used to study these phosphorylation events in *Drosophila*, Kc and S2 cells, are embryonic cell lines, and are not representative of different cell types (Bridon et al., 2012). Similarly, in mammals, these phosphorylation events were studied in NIH 3T3 cells, originating from mouse embryonic fibroblast, adipocyte-like cell derivatives of cultured 3T3-L1 fibroblasts, and HEK293T cells, originating from embryonic kidneys (Peterson et al., 2011). Since these studies were done in cell culture, the observed phosphorylation events may not be representative of all the kinases which are responsible for the phosphorylation of lipins. This idea is supported by the evidence that lipins are differentially regulated depending on the tissue type in which they reside (Reue, 2009). This is true for mammalian lipin (Reue, 2009) and it is therefore likely that additional kinases are responsible for the phosphorylation of lipins in a tissue-specific manner in other organisms, such as *Drosophila*.

3b. Comparison of putative phosphorylation sites

Amino acid residues that are targets of phosphorylation have previously been identified by mass spectrometry in two studies which used cultured *Drosophila* cells. Lipin was identified as one of the genes from the PhosphoPep project which mapped over 10,000 high-quality phosphorylation sites from roughly 3,500 *Drosophila* genes in Kc167 cells (Bodenmiller et al., 2008). *Drosophila* S2 cells were used in a different study where Lipin was identified as a phosphoprotein that is differentially regulated in response to stimulation by insulin (Bridon et al., 2012). The phosphosites identified from these two studies are illustrated in Figure 4 and are

compared to the distribution of phosphosites in mouse lipin1b. Most of the phosphorylation sites identified in both *Drosophila* Lipin and mouse lipin 1 are located between the conserved N-terminal NLIP and C-terminal CLIP domains. Clusters of phosphorylation sites are present in similar regions of the two proteins, suggesting that the sites and clusters are likely functionally conserved. Based on the distribution of the phosphosites, five clusters can be resolved (Fig. 4). Despite the presence of similar sites and clusters of phosphorylation sites in the two proteins, only two of these sites are conserved on the sequence level between *Drosophila* Lipin and mouse lipin1b, *Drosophila* S103, which corresponds to mouse S106, and *Drosophila* S820, which corresponds to mouse S720.

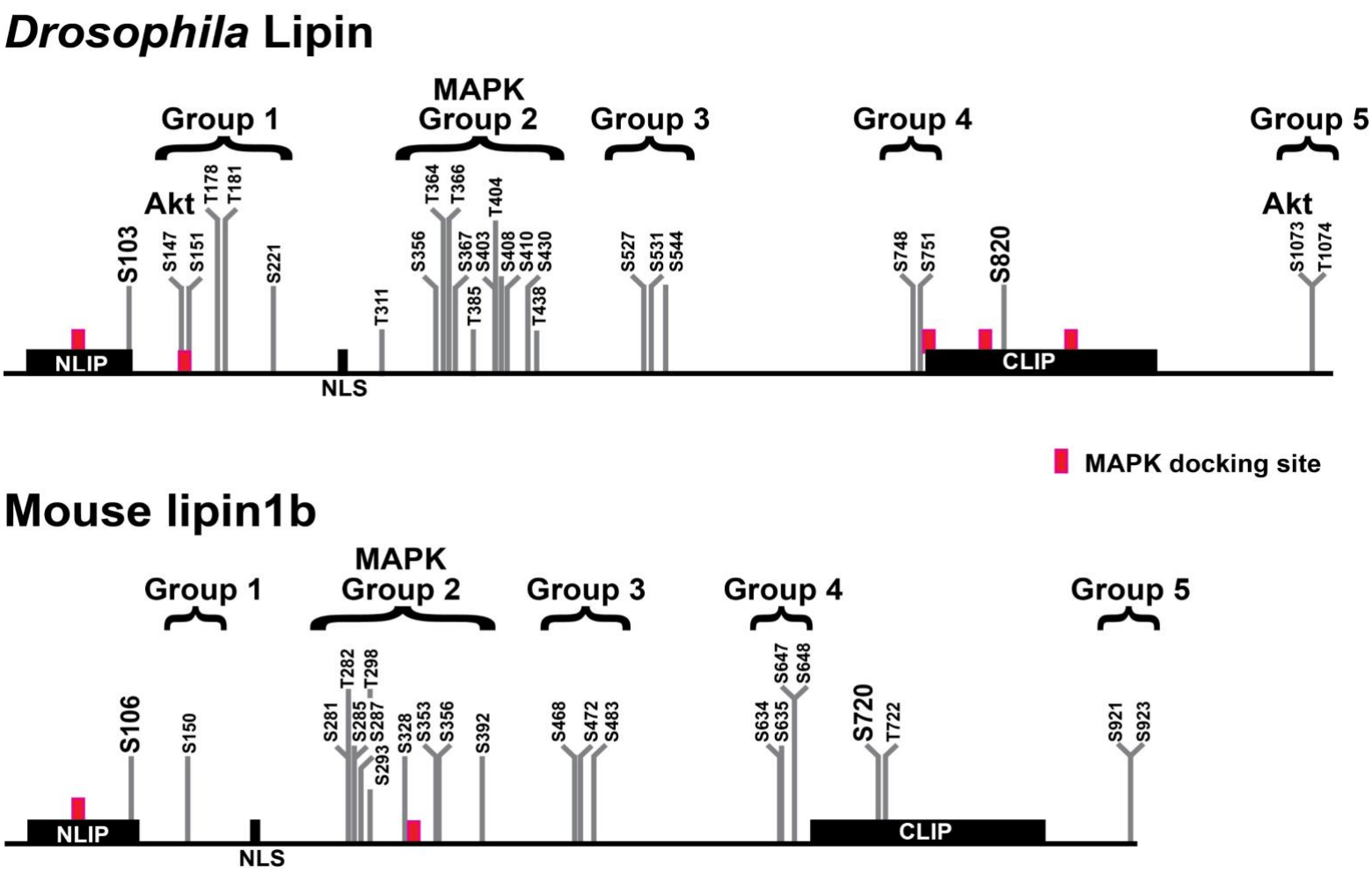

Fig 4. Comparison of mapped serine and threonine phosphorylation sites of *Drosophila* Lipin and mouse lipin1b. Distribution of phosphosites is similar between the two proteins. S103 and S820 in *Drosophila* Lipin correspond to sites S106 and S720, respectively, in mouse lipin1b. Homologous sites are found within the NLIP and CLIP regions whose sequences are conserved between species. PPSP (http://ppsp.biocuckoo.org) and ELM (http://elm.eu.org/index.html) where used to map the consensus sequences for MAPK phosphorylation and docking sites. NLS, nuclear localization sequence (Image adapted from: Lehmann, 2018).

4. Control of lipid metabolism in *D. melanogaster*

The *Drosophila* fat body has functions that are equivalent to the functions of both white adipose tissue and the liver in vertebrates (DiAngelo et al., 2009). Fat in *Drosophila* is stored in the form of lipid droplets. In addition to the fat body, oenocytes have been shown to aid in metabolic regulation and help in storage functions similar to the mammalian liver (Liu et al. 2013).

Basic metabolic and signaling pathways involved in lipid metabolism are also evolutionarily and functionally conserved between *Drosophila* and mammals (Liu et al., 2013). Such pathways include the glycerol-3-phosphate (Fig. 2) (Csaki et al., 2013), insulin (Fig. 5) (DiAngelo et al., 2009; Schmitt et al., 2015), and TOR (Fig. 5) (Zhang et al., 2000; Schmitt et al., 2015) pathways. In vivo studies of well-established biochemical pathways in the fly have revealed a striking similarity between fly and mammalian lipid metabolism while also revealing distinctive features of fly lipid metabolism (Kühnlein, 2012; Lehmann, 2018).

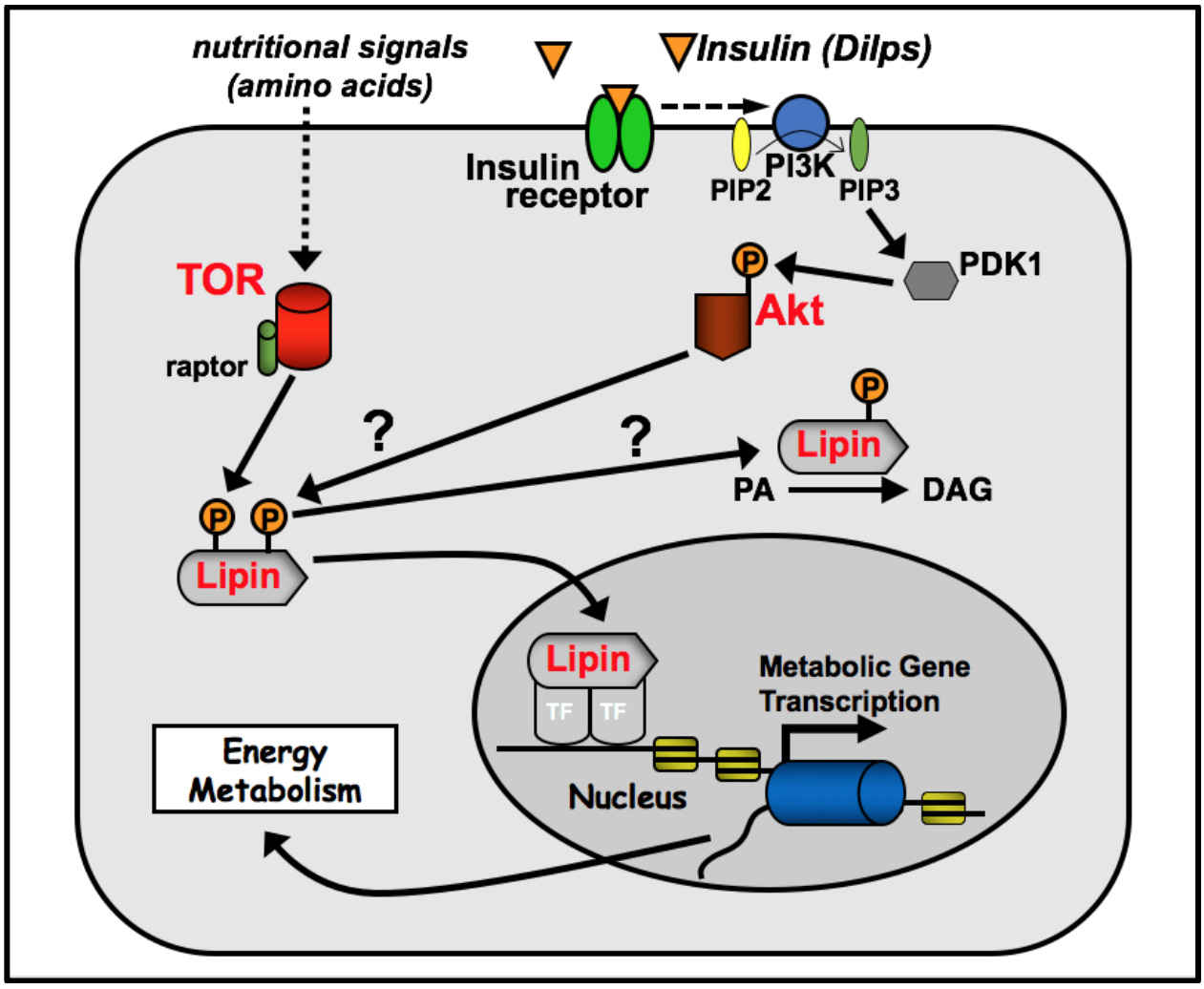

Fig 5. Lipin is regulated by TOR and insulin signaling. Nutrient sensing TOR kinase phosphorylates Lipin in the cytoplasm. *Drosophila* insulin-like peptides (Dilps) bind to the insulin receptor initiating the insulin/PI3K signaling cascade.

5. Functions of the Akt and MAPK pathways in lipid metabolism

Conserved amongst all metazoans, the insulin pathway is imperative for regulation of growth and development in *Drosophila melanogaster* and mammals alike. Insulin signaling mediates biological activities on a metabolic level aiding in lipid biosynthesis and glucose uptake; as well as on the level of energy expenditure and production where it plays a role in cell growth, proliferation, and survival. Examples of systematic disorders resulting from dysregulated insulin signaling include obesity, cancer, high cholesterol, and diabetes (Vinayagam et al., 2016).

Binding of insulin to a membrane bound insulin receptor results in activation of the receptor, triggering a cascade of phosphorylation events within the cell (Saltiel et al., 2001). The insulin receptor is then responsible for enlisting two major signaling pathways, the PI3K/Akt pathway and the MAPK pathway. The phosphatidylinositol 3-kinase (PI3K) pathway is responsible for mediating the metabolic effects of insulin, whereas the MAPK pathway facilitates the mitogenic effects of insulin acting jointly with the PI3K pathway (Vinayagam et al., 2016).

In *Drosophila*, insulin-like peptides, known as Dilps, enter the circulatory system following feeding and stimulate glucose uptake in the cell while also prompting the storage of excess energy as TAG (Saucedo et al., 2002; DiAngelo et al., 2009). Dilps bind to the insulin receptor (InR) activating the insulin pathway. Activation of this pathway stimulates fatty acid uptake, the import of glucose, and the synthesis of lipids, proteins and glycogen (Saucedo et al., 2002). Key regulators of TAG storage and the development of fat tissue in both *Drosophila* and mammals include lipin family proteins. Lipin deficient animals have higher levels of insulin (Reue et al., 2000) and experience insulin resistance in mammals as well as in *Drosophila* (DiAngelo et al., 2009). In fact, PI3K signaling in the fat body cells of *Drosophila* is reduced

when Lipin is deficient (Schmitt et al., 2015). *Drosophila* Lipin contains many serine/threonine phosphorylation sites, some of which are predicted to be regulated by kinases of the insulin pathway. Thus, it is possible that an insulin-sensitive kinase or phosphatases could aid in the regulation of Lipin (Fig. 4).

An insulin-kinase which is predicted to target Lipin is Akt (Bridon et al., 2012). Akt is the downstream intermediary or the insulin/PI3K pathway. In response to insulin, phosphorylation of FOXO by Akt causes the relocation of FOXO out of the nucleus, where it is then degraded (DiAngelo et al., 2009).

6. Functions of the TOR pathway in lipid metabolism

Target of Rapamycin (TOR) is an evolutionarily conserved serine/threonine kinase responsible for cell growth and proliferation (Peterson et al., 2011). TOR has the ability to sense nutrients and is responsible for maintaining a balance between protein synthesis and degradation (Schmelzle et al., 2000). Processes such as autophagy are downregulated when TOR is active and inactivation of TOR in both mammalian cell culture and yeast can lead to an increase in autophagy even in nutrient-rich medium (Schmelzle et al., 2000).

Drosophila TOR mutants experience reductions in cell size, cell proliferation, and have arrests or delays in development (Zhang et al., 2000). *Drosophila* TOR is required for proper animal development by coupling growth factor signaling to nutrient availability (Zhang et al., 2000).

7. Goals of Master's research

Goals: To determine the nuclear function(s) of Lipin and to identify signaling pathways that act on Lipin through functionally significant phosphorylation sites.

This study had two main goals. The first goal was to help in determining the nuclear function(s) of *Drosophila* Lipin by creating a form of Lipin that was constitutively nuclear. Having a form of Lipin which persisted in the nucleus would allow for subsequent experiments, such as RNA sequencing, which would help determine the genes in which Lipin acts as a transcription factor.

The second goal of this study was to examine the functional importance of specific serine/threonine phosphorylation sites by rendering these sites either non-phosphorylatable or by replacing them with phosphomimetic amino acid residues. The functional significance of these individual sites or groups of phosphorylation sites would help in better understanding the regulation of Lipin. Studying putative phosphorylation sites could potentially lead to the identification of additional kinases and/or phosphatases that aid in the regulation of the protein.

II. Materials and Methods

1. Fly stocks

Table 1. List of fly stocks. Fly stocks used in experiments. List includes a brief description of the fly stock as well as the source.

Simplified genotype	Genotype	Description	Source
w1118	*w^{1118}*	*white* mutant control stock in UAS-Lipin 20 S/T>A experiments	Bloomington *Drosophila* Stock Center (BDSC)
Injection stocks			
RFP.attP	*y[1] M{vas-int.Dm}ZH-2A w[*]; M{3xP3-RFP.attP}ZH-86Fb*	attP injection stock for construction of UAS lines	BDSC: 24749
vas-Cas9	*y[1]M{vas-Cas9}ZH-2A w[1118]/FM7c*	CRISPR injection stock	BDSC: 51323
nos-Cas9	*y[1] M{w[+mC]=nos-Cas9.P}ZH-2A w[*]*	CRISPR injection stock	BDSC: 54591
nos-Cas9(III-attp2)	*y1 w1118; attP2{nos-Cas9}/TM6C, Sb Tb*	CRISPR injection stock	Kondo Lab- Japan
Balancer Stocks			
Sp-1/CyO	*w[1118]; wg[Sp-1]/CyO*	2nd chromosome balancer stock	BDSC: 6326
w; Xa/CyO; Tm3, Sb	*w[*]; T(2,3)ap[Xa]; ap[Xa]/CyO; TM3, Sb[1]*	2nd & 3rd chromosome balancer stock	BDSC: 2475
w; Xa/SM5; TM6B, Tb	*w[*]; T(2,3)ap[Xa]; ap[Xa]/In(2L)Cy, In(2R)Cy, Doux[Cy];TM6B, Tb[1]; TM3, Sb[1]*	2nd & 3rd chromosome balancer stock	BDSC: 3234
UAS Responder Lines			
$Akt_{myrlacZ}$	*yw; UAS-Dakt[myr] UAS-lacZ; on 3rd*	UAS-Akt responder on 3rd chromosome	Tien Hsu
UAS Lipin 20	*UAS-Lipin 20 S/T>A*	UAS line where 20 of the putative serine/ threonine phosphorylation sites of Lipin have been rendered to alanine	Stephanie Hood

Table 1 (Cont.)

Simplified genotype	Genotype	Description	Source
GAL4 Driver Lines			
r[4]-GAL4	*yw; r[4]-GAL4 (III); on 3rd*	Strong fat body driver, active throughout development in fat body and saliv glands	BDSC: 33832
FB-GAL4	*w[1118]; P{w[+mC]=Cg-GAL4.A}2 On1;2*	Moderate fat body driver. Also expressed in hemocytes and lymph gland	BDSC: 7011
da-GAL4	*w[1118]; P{da-GAL4.w[-]}3 On1;3*	Ubiquitous GAL4 driver. Moderate strength driver	BDSC: 8641 (No longer carried)
Lsp-GAL4	*y[1] w[1118]; P{w[+mC]=Lsp2-GAL4.H}3*	Fat body driver activated in 3rd instar larvae	BDSC: 6357
Lipin Deficiency Stocks			
Df(2R)Exel7095/ CyO	*Df(2R)Exel7095/CyO*	Deficiency stock lacking chromosomal regions 44B3-44C2 which removes the entire *lipin* gene at 44B4-44B5	BDSC: 7860
Df(2R)Exel7095/ CyO-GFP	*Df(2R)Exel7095/CyO-GFP*		Bloom Stock 7890
CRISPR Mutant Stocks			
Lipin S147A	*Lipin Sl47A/Lipin S147A*	Lipin S147A mutant vas-Cas9 injection stock (BDSC: 51323)	Austin Morgan Stephanie Hood
Lipin S147E	*Lipin Sl47E/Lipin S147E*	Lipin S147E mutant vas-Cas9 injection stock (BDSC: 51323)	Austin Morgan Stephanie Hood

Table 1 (Cont.)

Simplified genotype	Genotype	Description	Source
CRISPR Mutant Stocks			
Lipin 5/CyO-GFP	*Lipin 5 S/T>A / CyO-GFP*	Lipin Group 1 mutant nos-Cas9 (III-attp2) injection stock	Heidi O'Dell Stephanie Hood
Lipin 9/CyO-GFP	*Lipin 9 S/T>A / CyO-GFP*	Lipin Group 2 mutant nos-Cas9 (III-attp2) injection stock	Hannah Davis Josephine Gottsponer Stephanie Hood
Lipin S820A	*Lipin S820A / CyO-GFP*	Lipin S820A mutant nos-Cas9 injection stock (BDSC: 54591)	Stephanie Hood

2. Plasmids

Table 2. List of plasmids. Plasmids used in experiments. List includes a brief description of the plasmid as well as the source.

Name	Description	Source
GH19076	*Lipin* cDNA in POT2 vector	Berkley Drosophila Genome Project -(BDGP)
pUASTattB	*Drosophila* transformation vector containing attB site	Basler Laboratory, University of Zurich
pBluescriptSKII	Cloning vector (used for ampicillin resistance)	Stratagene
pCFD3-dU6:3gRNA	Expresses a single gRNA under the control of the U6:3 *Drosophila* promoter	Addgene: 49410
pCFD4-U6:1_U6:3tandemgRNAs	Expresses two gRNAs under the control of the U6:1 and U6:3 *Drosophila* promoters	Addgene: 49411

3. Antibodies

Table 3. List of primary and secondary antibodies. Primary antibody list includes host, dilution used for experiments and source. Secondary antibody list includes host, conjugate, dilution used for experiments and source

Primary Antibodies

Name	Host	Dilution	Source
anti-Lipin	Rabbit	Immunohistochemistry 1:200	Lehmann Laboratory, Fayetteville AR

Secondary Antibodies

Name	Host	Conjugate	Dilution	Source
anti-rabbit	Donkey	Cy-3	1:1000	*Jackson ImmunoResearch*

4. Primers

Table 4. List of primers. Primers used in experiments. List includes sequence of the primers as well as how they were used.

Name	Sequence	Description
Generation of Lipin20 S/T>A cDNA plasmid		
Position_103 (F)	5'-[Phos]AACCTGGCCACCGCCCCCA TACCCAACAGC-3'	Primer used to generate S103A
Position 147 151 (R)	5'-[Phos]GGGCTCCTCCTTGGCGAA GTCAATGGCGTTGCGCCGCGG-3'	Primer used to generate S147A/S151A
Positions 178 181 (F)	5'-[Phos]CAGCGCAGGCACGCCGAC AACGCCCTGGAGCGTCGC-3'	Primer used to generate T178A/T181A
Positon_221 (R)	5'-[Phos]GCTTTGGTTGTCCAGGGC GTCCGAGTCCGC-3'	Primer used to generate S221A
Position_356 (F)	5'- [Phos]CTCGCACTGGGGACGATGCCC CGCTCAGCG-3'	Primer used to generate S356A
Pos_364_366_ 367 (F)	5'[Phos]AGATTCCCCACGCCCCCG CCGCCAATCCACGTCTGGATTTG-3'	Primer used to generate T364A/T366A/ S367A
Pos403404408 410 (R)	5'[Phos]GGTTTCCAGTTCGGCGTCGGCTT GGATGGGGGCGGCAGGTCGTCCGCC-3'	Primer used to generate S403A/T404A/ S408A/S410A
Position_430 (F)	5'-[Phos]GAAAGCACCGCAGCCTGGAA GTGGGGC-3'	Primer used to generate S430A

Table 4 (Cont.)

Name	Sequence	Description
Generation of Lipin20 S/T>A cDNA plasmid		
Position 527 531 (R)	5'-[Phos]CAGCGAGCTGGGGGCGT GAGGCAGGGCGGTGCCATTGCC-3'	Primer used to generate S527A/S531A
Position_544 (F)	5'-[Phos]CAGAAGAGTATTGACGCCG ACTTTGACGAGACCAAGC-3'	Primer used to generate S544A
Positions 748 751 (F)	5'-[Phos]GCTAACCATGGCCGCCAA CAAGGCCGACGAGCCCAAAGAGCG-3'	Primer used to generate S748A/S751A
PCR_7_F_Repair	5'-[Phos]TGCTACTTGTTCCGCTGGAAGC ACAAC-3'	Primer used to switch back AA changed accidently during site-directed mutagenesis R801R (different codon)
PCR_7_R_Repair	5'-[Phos]GTCCGTCCGGCAGCATC ACGTTGCCCTG-3'	Primer used to switch back AA changed accidently during site-directed mutagenesis V880A back to V880

Table 4 (Cont.)

Name	Sequence	Description
Generation of Lipin20 S/T>A cDNA plasmid		
K156_RepairNew (F)	5'-[Phos]CTTCGCCAAGGAGGAGC CCAAGGAAGCCGTTGTTGAGGGC-3'	Primer used to switch back AA changed accidently during site-directed mutagenesis K156E back to K156
NonMutant Reverse	5'- [Phos]GGCGGTCGAACTCCTCGT CCGAGGGTGGTGCTCCCTGCTCCG-3'	Non-mutant primer used for amplification of plasmid without introducing mutations
gRNA Sequencing Primers for CRIPSR		
pCDF3_gRNA_F	5'-ACCTACTCAGCCAAGAGGC-3'	Sequencing primer for pCFD3 plasmid
pCFD4_gRNA_F	5'-GACACAGCGCGTACGTCCTTCG-3'	Sequencing primer used for pCFD4 plasmid
Generation of gRNA plasmid for Lipin S147 Mutants		
ProtoS147-1	5'-GTCGATGGAGTTGCGCCGCGGCAA-3'	Protospacers annealed and used for gRNA insert into pCFD3 plasmid
ProtoS147-2	5'-AAACTTGCCGCGGCGCAACTCCAT-3'	
Screening Primers used to recover Lipin S147 Mutants		
S147PrimerPair2-F	5'-TCCTTCATTCAGGTGGACATTGA-3'	Sequencing primers to screen for S147 mutants
S147PrimerPair2-R	5'-CTTTGGTTGTCCAGCGAGTC-3'	

Table 4 (Cont.)

Name	Sequence	Description
Generation of gRNA plasmid for Lipin Group1 Mutant		
Lipin5_gRNA1	5'-TATATAGGAAAGATATCCGGGTGAACTTC GAAAATGGTTTCGCAAATGATGTTTTAGAGCT AGAAATAGCAAG-3'	Forward primer containing protospacer for gRNA plasmid
Lipin5_gRNA2	5'-ATTTTAACTTGCTATTTCTAGCTCTAAA ACGCGCAAGAACTCTTCAAGCACGACGTT AAATTGAAAATAGGTC-3'	Reverse primer containing protospacer for gRNA plasmid
Generation of Lipin5 S/T>A Donor Plasmid		
5'HR_Forward_ Lipin5	5'-CGAATTGGAGAAAGTACCGCCAAATA CGCC-3'	Used to amplify the 5'HR region of the donor plasmid
5'HR_Reverse_ Lipin 5	5'-GTTTCGCAAATGATAGAGTGAGACTGGTG GATC-3'	
Generation of Lipin5 S/T>A Donor Plasmid		
Group 1_Insert_ Forward_Lipin 5	5'- CTCACTCTATCATTTGCGAAACCATTTTAGA AACG-3'	Used to amplify the gBlock containing desired mutations
Group 1_Insert_ Reverse_Lipin 5	5'- GCTGAGCATTCTTCTTCATTTGCGACTT CTTG -3'	
3'HR_Forward_ Lipin5	5'- GCAAATGAAGAAGAATGCTCAGCGCAA GAAC-3'	Used to amplify the 3'HR region of the donor plasmid
3'HR_Reverse_ Lipin 5	5'- AAGCTGGGTTGGGCCATTTGAACAATACT CACG -3'	
Vector_Forward_ Lipin5	5'- AAATGGCCCAACCCAGCTTTTGTTCCCTTTA GTGAG -3'	Used to amplify the pBSK backbone of the donor plasmid
Vector_Reverse_ Lipin5	5'- GCGGTACTTTCTCCAATTCGCCCTATAGTG AGTCGTATTACGC -3'	

Table 4 (Cont.)

Name	Sequence	Description
Screening Primers used to recover Lipin Group1 Mutant		
Oligo710_PP4_F	5'-AGATGAAGCTGGGCGATTCT-3'	Sequencing primer to screen for Group1 mutant
Oligo710_PP4_R	5'-TTGTGACCGTGGTGAGGTTA-3'	
Generation of Lipin9 S/T>A cDNA		
Lipin_T438A_ Fwd	5'-[Phos]GCCTGGAAGTGGGGCGAGTTG CCCGCCCCGGAGCAGGCCAAG-3'	In-vitro mutagenesis primer for T438A substitution
LipinT385A_Rev	5'-[Phos]GCACCACCGCCACCCAC GGGGGCGGTGATCTCCGTGTCGCTG-3'	In-vitro mutagenesis primer for T385A substitution
Lipin11_cDNA_F OR	5'-AGACGCCATCACTGGGAG-3'	Sequencing Primer to detect in-vitro substitutions
Generation of Lipin9 S/T>A Donor Plasmid		
5'HR_FOR_ Lipin11	5'- CGAATTGGGTGTGCTCAGGAGTC-3'	Used to amplify the 5'HR region of the donor plasmid
5'HR_REV_ Lipin11	5'- TCGCTGGTTGTGACGGTGGTGAGG-3'	
Group2_FOR_ Lipin11	5- CTCACCACCGTCACAACCAGCGAAGCC-3'	Used to amplify the cDNA region of the donor plasmid
Group2_REV_ Lipin11	5- GGGAAGTAGAGGGCGGCCATCTCGG-3'	
3'HR_FOR_ Lipin11	5'- CCGAGATGGCCGCCCT CTACTTCCCTAGTC-3'	Used to amplify the 3'HR region of the donor plasmid
3'HR_REV_ Lipin11	5'- CAAAAGCTGGAGGTCGGGCGAGG-3'	

Table 4 (Cont.)

Name	Sequence	Description
Generation of Lipin9 S/T>A Donor Plasmid		
pBSK_FOR_ Lipin11	5'- CCTCGCCCGACCTCCAGCTTTTG-3'	Used to amplify the pBSK backbone of the donor plasmid
pBSK_REV_ Lipin11	5'- TCCTGAGCACACCCAATTCGCCC-3'	
Generation of gRNA plasmid for Lipin Group2 Mutant		
Lipin11 fwdprimer	5'-TATATAGGAAAGATATCCGGGTGAA CTTCGACCAGACGTTAACCTCACCA GTTTTAGAGCTAGAAATAGCAAG-3'	Forward primer containing protospacer for gRNA plasmid
Lipin11 revprimer	5'_ATTTTAACTTGCTATTTCTAGCTCTA AAACCCATCTCGGGGTCCATGCTGCGA CGTTAAATTGAAAATAGGTC-3'	Reverse primer containing protospacer for gRNA plasmid
Screening Primers used to recover Lipin Group2 Mutant		
Lipin11_SCR_F	5'-GATGCCCCCATATCCAGTGCC-3'	Sequencing primer to screen for Group2 mutant
Lipin11_SCR_R	5'-GGCCTCATTCTTGGCCTGCTC-3'	
Group2_Seq_For	5'- GCAAGAAGTCGCAAATGAAGAAG-3'	New sequencing primer to screen for Group2 mutant
Group2_Seq_Rev	5'- GGCATCCAGATCAGACAGGTAG-3'	
Lipin11_3HR_ REV	5'-GTCGCTCTTGCTCAGCGTGG-3'	Primer outside cDNA donor plasmid
Generation of gRNA plasmid for Lipin S820A Mutant		
S820_FWD_ Primer	5'-TATATAGGAAAGATATCCGGGTGAACTT CGCTGGAAGCACAACGACAAGGGTTTTAGAG CTAGAAATAGCAAG-3'	Forward primer containing protospacer for gRNA plasmid
S820_REV_ Primer	5'-ATTTTAACTTGCTATTTCTAGCTCTAAA ACAGATCACCACCTTGTCGTTGCGACGTTAA ATTGAAAATAGGTC-3'	Reverse primer containing protospacer for gRNA plasmid

Table 4 (Cont.)

Name	Sequence	Description
Screening Primers used to recover Lipin S820A Mutant		
S820PrimerPair1 F	5'- GCGTTACAAGAAGTCGCTGC-3'	Sequencing primers to screen for S820A mutant
S820PrimerPair1 R	5'- GAAGGCCGATATCAGGGACG-3'	

5. Guide RNAs

Table 5. List of guide RNAs. Guide RNAs used in experiments. List includes targeted regions as well as the gRNA sequence and PAM.

Targeted Residue(s)/Region	gRNA Sequence + PAM
S147	5'-ATGGAGTTGCGCCGCGGCAA TGG-3'
Group1_gRNA_1	5'-AAAATGGTTTCGCAAATGAT AGG-3'
Group1_gRNA_2	5'-TGCTTGAAGAGTTCTTGCGC TGG-3'
Group2_gRNA_1	5'-ACCAGACGTTAACCTCACCA CGG-3'
Group2_gRNA_2	5'-CAGCATGGACCCCGAGATGG CGG-3'
S820_gRNA_1	5'-CTGGAAGCACAACGACAAGG TGG-3'
S820_gRNA_2	5'-CAACGACAAGGTGGTGATCT CGG-3'

6. Single-stranded oligonucleotide donors

Table 6. List of single-stranded oligonucleotide donors. Single-stranded oligonucleotides used in experiments. List includes targeted residues as well as sequences.

Targeted Residue	ssOligo Sequence
S147A	5'-ATCATTTGCGAAACCATTTTAGAAACGCTAGCGAGGAGCTGCTTC TGCCACTGCCATTGCCGCGGCGCAACGCCATTGACTTCTCCAAGGAGG AGCCCAAGGAAGCCGTTGTTGAGGGCAGCAAG-3'
S147E	5'-ATCATTTGCGAAACCATTTTAGAAACGCTAGCGAGGAGCTGCTTC TGCCACTGCCATTGCCGCGGCGCAACGAGATTGACTTCTCCAAGGAGG AGCCCAAGGAAGCCGTTGTTGAGGGCAGCAAG-3'
S820A	5'-GCCACACCGAGTTGCGCCCAATCCTTGCCCACCATGGGTAAAATG TGGCCCAGCACGTCGGCCTTGGTGATGGTGCCGTCAATGTCCGAGATC ACCACCTTGTCGTTGTGCTTCCAGCGGAACAAGTAGCA -3'

7. Double-stranded DNA templates

Table 7. Sequences of double-stranded templates. Double-stranded DNA templates used for construction of donor plasmids which contains base exchanges for S/T>A substitutions.

Mutant Template	**gBlock DNA Sequence for CRIPSR/Cas9 Donor Plasmid**
Lipin Group 1	5'-ATTTGCGAAACCATTTTAGAAACGCTAGCGAGGAGCTGCTTC TGCCACTGCCATTGCCGCGGCGCAACGCCATTGACTTCGCCAAGGAGG AGCCCAAGGAAGCCGTTGTTGAGGGCAGCAAGTTCGAGAATCAAGTC TCGGACTACACGCAGCGCAGGTACATAATGCCTTTTCATGCTCCTCAA ACGAAGGACAAAGTTAGCTAACATCATCCTTGACCCAAACAGGCACG CCGACAACGCCCTGGAGCGTCGCAACCTAAGCGAAAAGCTCAAGGAG TTCACCACGCAGAAGATCCGGCAGGAGTGGGCCGAGCACGAAGAGCT GTTTCAGGGCGAGAAGAAGCCGGCGGACTCGGACGCCCTGGACAACC AAAGCAAAGCTTCAAACGAAGCTGAGACGGAGAAGGCAATTCCGGCG GTCATTGAAGACACGGAAAAAGAAAAGGATCAGATCAAACCAGACGT TAACCTCACCACGGTCACAACCAGCGAAGCCACCAAGGAGGTGTCCA AGAGCAAAACCAAGAAGCGGCGCAAGAAGTCGCAAATGAAGAA-3'
	Lipin cDNA Sequence for CRISPR/Cas9 Donor Plasmid
Lipin Group 2	5'-CAACCAGCGAAGCCACCAAGGAGGTGTCCAAGAGCAAAACCAA GAAGCGGCGCAAGAAGTCGCAAATGAAGAAGAATGCCCAGCGCAAG AACTCTTCAAGCAGCTCATTGGGCAGCGCCGGCGGCGGTGATTTGCCT TCGGCGGAGACGCCATCACTGGGAGTGAGCAACATCGATGAAGGAGA TGCCCCCATATCCAGTGCCACAAACAACAACAACACCTCGTCGTCGAA CGATGAACAGCTATCCGCTCCCCTGGTGACAGCTCGCACTGGGGACGA TGCCCCGCTCAGCGAGATTCCCCACGCCCCCGCCGCCAATCCACGTCT GGATTTGGACATTCACTTCTTCAGCGACACGGAGATCACCGCCCCCGT GGGTGGCGGTGGTGCTGGGTCAGGTCGTGCCGCCGGCGGACGACCTG CCGCCCCGATCCAAGCCGACGCCGAACTGGAAACCACCATGCGAGAC AACCGTCACGTGGTGACTGAAGAAAGCACCGCAGCCTGGAAGTGGGG CGAGTTGCCCGCCCCGGAGCAGGCCAAGAATGAGGCCATGAGCGCCG CCCAGGTGCAGCAAAGCGAGCACCAATCGATGCTCAGCAACATGTTC AGCTTCATGAAGAGGGCAAATCGGCTACGCAAAGAGAAGGGCGTCGG CGAAGTGGGTGACATCTACCTGTCTGATCTGGATGCCGGCAGCATGGA CCCCGAGATGGCGGCCC-3'

8. Fly Husbandry

Flies were kept on standard fly food for all experiments. Fly food contained 8.2% malt extract, 1.1% agar, 1.3% corn syrup, 6.1% cornmeal and 1.8% yeast in tap water. To prevent bacterial or fungal growth, 0.75% propionic acid and 1% Tegosept were added. Unless otherwise stated, flies were kept at 25^{o}C for all experiments.

9. Media

Lysogeny broth (LB) was prepared using LB Broth MILLER (EMD:1.10285.0500). LB broth was used to grow overnight bacterial cultures. To prepare 1 L, 25 g of the LB Broth MILLER was re-suspend in 800 mL of ddH_2O on a hot plate set to 100^{o}C, stirring. Once the powder was dissolved, the broth was measures in a 1 L graduated cylinder and the volume was brought up to 1 L. Media was then poured into respective glassware before sterilization by autoclave. Autoclave was used on the 30-minute liquid cycle setting. For LB plates, LB agar MILLER (EMD:1.10283.0500) was prepared using the same method as the LB broth, using 37 g/L. LB agar was cooled to 55^{o}C before antibiotics were added. Antibiotic working concentrations were as follows: Ampicillin (100 μg/mL): and Chloramphenicol (34 μg/mL).

10. Transformation of competent cells

Competent cells used for transformations, unless otherwise stated, were NEB 5-alpha Competent *E. coli* (High Efficiency) purchased from New England BioLabs$_{inc.}$ (NEB-C2987H). Cells were stored at -80^{o}C until needed.

Competent cells were thawed on ice for 10 minutes. 2-5ul of chilled ligation/assembly product was added to the cells. Components were mixed gently by pipetting up and down or swirling with the pipette tip. Do not vortex the mixture. Mixture was placed on ice for 30 minutes. Tube was then heat-shocked at 42^{o}C for 30 seconds, being careful not to mix. Tube was

transferred back to ice for 2-5 minutes. 950 μL of room temperature SOC media (Super Optimal Broth with Catabolite repression: (NEB-B9020S)) was then added to the cells. Reaction was incubated in a 37$_o$C incubator for 60 minutes. Shaker on incubator was set for 250 rpm. While the cell mixture was allowed to shake, the selection plates were warmed to 37$_o$C. Spread 100-200 μL of the cells onto the selection plate. If transformation rate was known to be low, remaining cells were spun-down at 3800 RCF for 5 minutes. Supernatant was decanted to 100-200 μL and cells were resuspended in the remaining volume and plated on an additional selection plate. Plates were incubated at 37$_o$C overnight; agar side up.

11. Ligation

Plasmid ligations were done using T4 DNA ligase (NEB-M0202S) following the recommendations of the manufacturer. Reactions were kept at room-temperature for a minimum of 2 hours before heat inactivation of the ligase at 65$_o$C for 10 minutes. Transformations of ligations were done using 4 μL of the ligation mixture in 50 μL of competent cells.

12. Site-directed mutagenesis and generation of *Lipin20S/T>A* construct

Putative phosphorylation sites were selected for site-directed mutagenesis (Fig. 4). Base pair exchanges were introduced to replace the codons for serine and threonine of *Lipin* to those coding for alanine using a USB Change-IT Multiple Mutation Site Directed Mutagenesis Kit (Affymetrix-78480) following the protocol described by the manufacturer. The Lipin cDNA GH19076 plasmid (cloned into vector *pOT2*) served as the DNA template. Plasmid GH19076 was grown on an LB plate with chloramphenicol as the selective marker. Individual colonies were selected and grown up overnight in liquid culture, LB broth + chloramphenicol at 37$_o$C in 3-5 mL. Plasmid DNA was extracted from overnight cultures using a QiaPrep Spin Miniprep Kit (Qiagen-27106) and concentration was checked on an agarose gel.

To create the *Lipin20S/T>A* cDNA, phosphorylated mutagenic primers were designed to contain 1-4 codon substitutions where the selected serine or threonine codon was exchanged with the preferential codon for alanine used in *Drosophila*, GCC (Table 4 Primers: Generation of Lipin20 S/T>A cDNA plasmid/ Fig. 6). Nine subsequent rounds of PCR were done to introduce the 20-desired substitutions. Between each round of mutagenesis, clones were screened by sequencing (Eurofins Genomics) for the presence of the intended mutations for that round. If clones only contained some of the intended residue substitutions, the same primer was used in a repeat reaction in an attempt to incorporate all desired exchanges. Unintended codon mutations were switched back to the endogenous codon using the same technique.

Position	Amino Acid
103	S
147	S
151	S
178	T
181	T
221	S
356	S
364	T
366	T
367	S
403	S
404	T
408	S
410	S
430	S
527	S
531	S
544	S
748	S
751	S

Fig 6. List of amino acid residues changed from S/T>A in *UAS Lipin20* transgenic line.

Once all the mutations were introduced to the Lipin cDNA, the cDNA portion of the *pOT2* vector was removed and incorporated into the pUASattB plasmid by restriction enzyme digest. XhoI and Eco53KI were used to cut the *pOT2* vector overnight at 37$_{o}$C. Enzymes were

heat inactivated at 65oC for 20 minutes and the reaction was kept at -20oC until an agarose gel was run for gel extraction of the cDNA insert (3.8 kb).

The pUASattB plasmid was linearized using XbaI in an overnight digest at 37oC. XbaI was heat inactivated at 65oC for 20 minutes before adding dNTPs, followed by Klenow enzyme to fill the 5'overhangs created by the digestion. The reaction mixture was incubated at 25oC for 15 minutes and 5.5 μL of 100 mM EDTA was added to the reaction. A 30-minute heat inactivation was done at 75oC and the reaction was cleaned up using a Qiaquick PCR Purification Kit (Qiagen-28104). Concentration and size of the linear pUASattB plasmid were verified on an agarose gel.

A subsequent overnight digestion was then done at 37oC with Xho1. The linear pUASattB plasmid was treated with 1 μL of Shrimp Alkaline Phosphatase (NEB-M0371S) to prevent re-ligation, 37oC for 30 minutes. Enzyme and phosphatase were heat inactivated at 65oC for 5 minutes. An agarose gel was run to confirm the size and concentration of the dual digested pUASattB plasmid (8.5 kb).

Ligation of the cDNA insert and the pUASattB plasmid was done using T4 DNA ligase (NEB-M0202S) with a 3:1 ratio of insert to vector. After the overnight ligation, the ligase was heat inactivated at 65oC for 10 minutes. Transformation into competent cells was done using 5 μL of the ligation reaction. Cells were plates on LB-AMP and allowed to grow overnight at 37oC. Individual colonies were selected and grown overnight at 37oC in 3-5 mL LB-AMP. Plasmid DNA was extracted from overnight cultures using a QiaPrep Spin Miniprep Kit (Qiagen-27106)

Analytical digests of the overnight cultures were done to verify that the plasmids were the correct size. A single digest was done with AflII, and two double digests were done with HindIII

+ AflII, and HindIII + NcoI-HF to be sure that the clones were correct. Reactions were incubated for 90 minutes at 37^{o}C and run on an agarose gel to analyze. Positive clones were sent off to the BestGene Inc. where they a received Service Z1, regular plasmid DNA Midiprep, which guaranteed the DNA quality for injection before into *Drosophila* embryos containing attP sites (Bloomington Stock- 24749) to create the *UAS-Lipin20S/T>A* fly stock.

PhiC31 integrase-mediated transgenesis was employed to produce the *UAS-Lipin20S/T>A* stock. The site-specific bacteriophage PhiC31 integrase was used to mediate sequence-directed, highly efficient, and irreversible integration between a phage attachment site, *attP,* and a bacterial attachment site, *attB.* Embryos from a fly line containing an *attP* docking site were injected with an *attB*-containing plasmid, pUASTattB, which contained a Lipin cDNA where 20 of the codons for the putative serine/threonine phosphorylation sites that were rendered to the codon coding for alanine via site-directed mutagenesis. Injections were done by the BestGene, Inc. (Chino Hills, CA, USA). Injected animals were then crossed with fly stock *w1118*, a w^{-} (white eyed) fly stock, and successful transformants were selected based on the w^{+} screening marker (red eyes) in the F1 progeny and were used to establish the *UAS-Lipin20S/T>A* stock.

13. Fat droplet staining

Bodipy 493/503 (Invitrogen #D2191) was used to stain fat droplets. Routine staining was done using 3rd instar wandering larvae. Larvae were transferred to depression slides where they were dissected in cold 0.1M phosphate buffered saline (1XPBS). Fat body was separated from the other tissues and placed in a depression well containing freshly prepared cold 3.7% formaldehyde, making sure that all tissue was submerged to ensure even fixation. Alternatively, the fixation process was done using a 1.5 mL micro-Eppendorf tube to maximize likelihood of

homogeneous fixation. Samples were placed on shaker and allowed to fix for 30-60 minutes at room temperature (RT). (Longer fixation seemed to help with eliminating uneven staining). Tissue was then transferred to a depression well or 1.5 mL micro-Eppendorf tube containing a 1:1000 dilution of Bodipy in 1XPBS. Samples were placed back on the shaker/mixer and allowed to stain for 40-60 minutes, covered, at RT. Fat body was mounted using a mounting media containing DAPI (EMS Shield Mounting Medium with DAPI & DABCO (EMS:17989-20) or ProLong Gold Antifade Mountant with DAPI (ThermoFisher Scientific-P36931)), sealed with clear nail polish and imaged using a Zeiss Axio or Nikon fluorescence microscope.

14. Lipin antibody staining

Affinity purified anti-Lipin antibody created by the Lehmann Laboratory was used to stain for presence, concentration, and intracellular location of the Lipin protein. Before starting the protocol, freshly prepared 3.7% formaldehyde in 0.1M phosphate buffered saline (1XPBS) was prepared and kept on ice. Tissue was dissected in cold (4$_o$C) 1XPBS (pH 7.4) in depression slides. Samples were fixed in 3.7% formaldehyde in PBS for 60 minutes in a 1.5 mL Eppendorf tube on a nutating mixture to ensure that all tissue would be evenly fixed. Samples were then transferred to large depression wells and washed in cold 1XPBST (0.1M PBS + 0.2% Tween20) 4X10 minutes, shaking lightly. 995 μL of cold blocking buffer, 1XPBST/1% Normal Donkey Serum (NDS), was added to a 1.5 mL micro-Eppendorf tube. Samples were transferred to the tubes and kept at room temperature (RT) for 2 hours, shaking gently. To achieve a 1:200 dilution of primary antibody, 5 μL of affinity purified Lipin antibody was added to the tube containing the blocking buffer and tissue. Tubes were place on a shaker at 4$_o$C overnight, shaking gently.

Following primary antibody incubation, tissue was washed as stated above, 4X10 minutes in cold PBST. While samples were washing, a 1:1000 dilution of secondary antibody

was prepared, 1ul of donkey anti-Rabbit IgG (*Jackson ImmunoResearch*:711-165-152) in 999 μL of cold 1XPBST. Amber 1.5 mL micro-Eppendorf tubes were used for the secondary antibody staining to help protect the samples against light. Samples were transferred to the tubes containing the secondary antibody and stained at RT for 2 hours, shaking gently, covered. 1X cold PBST was used to wash the samples, 4X10 minutes, following secondary antibody incubation. Samples were mounted using ProLong Gold Antifade Mountant with DAPI (ThermoFisher Scientific-P36931) or EMS Shield Mounting Medium with DAPI & DABCO (EMS:17989-20), sealed with clear nail polish and allowed to dry before imaging. Imaging was done using a Zeiss Axio or Nikon fluorescence microscope.

15. Single Fly Genomic Preparation

Genomic DNA used for experiments was obtained by extracting DNA from single flies. Squishing buffer (SB) was prepared fresh and kept on ice using the following components per 1 mL: 965 μL of ddH_2O, 10 μL of 1M Tris-CL pH 8.0, 10 μL of 100 mM EDTA, 5 μL of 5M NaCl and 10 μL of 20 mg/mL proteinase K (NEB-P8107S). Each single fly genomic preparation used 50 μL of SB. For genotyping purposes, flies could also be pooled; and volumes of squish buffer are added proportionally (ex. 3 flies= 150 μL SB).

Single adult flies were anesthetized with CO_2 and transferred to empty 1.5 mL micro-Eppendorf tubes. Tubes containing flies were placed on ice to assure that flies remained knocked out. 50 μL of SB was then aspirated into a 200 μL pipette tip and the fly was squished using the tip without expelling the SB. Once the fly was completely homogenized, the remainder of the SB was expelled. When all flies were squished, a timer was set for 20 minutes and samples were kept at room temperature (RT) for incubation. At the end of the RT incubation, the sample were

transferred to a 95^{o}C hot block for 5 minutes. Samples were then transferred to ice for 2-5 minutes and then spun down at max speed at RT in a table top centrifuge for 5 minutes.

Genomic DNA preps were used for subsequent polymerase chain reactions (PCR) and stored at 4^{o}C for up to 6 weeks. Routinely, 2.5 μL of genomic DNA is used as a template in a 25 μL PCR reaction.

16. Gibson/HiFi Assembly

Gibson Assembly or HiFi DNA Assembly cloning kits were obtained from New England BioLabs (NEB-E2611S/E5520S). Optimal quantity guidelines were followed per the recommendation of the manufacturer. Assembly reactions were prepared on ice, following the recommended DNA molar ratios. (Half-reaction yielded the same success rate and were used when applicable). All assembly reactions, regardless of number of fragments were incubated at 50^{o}C for 60 minutes in a thermal cycler to help improve assembly efficiency. Samples were either put on ice for immediate transformation (2 μL of assembly reaction used in 50 μL competent cells (provided with kit)) or stored at -20^{o}C until used for subsequent transformation.

17. CRISPR/Cas-9

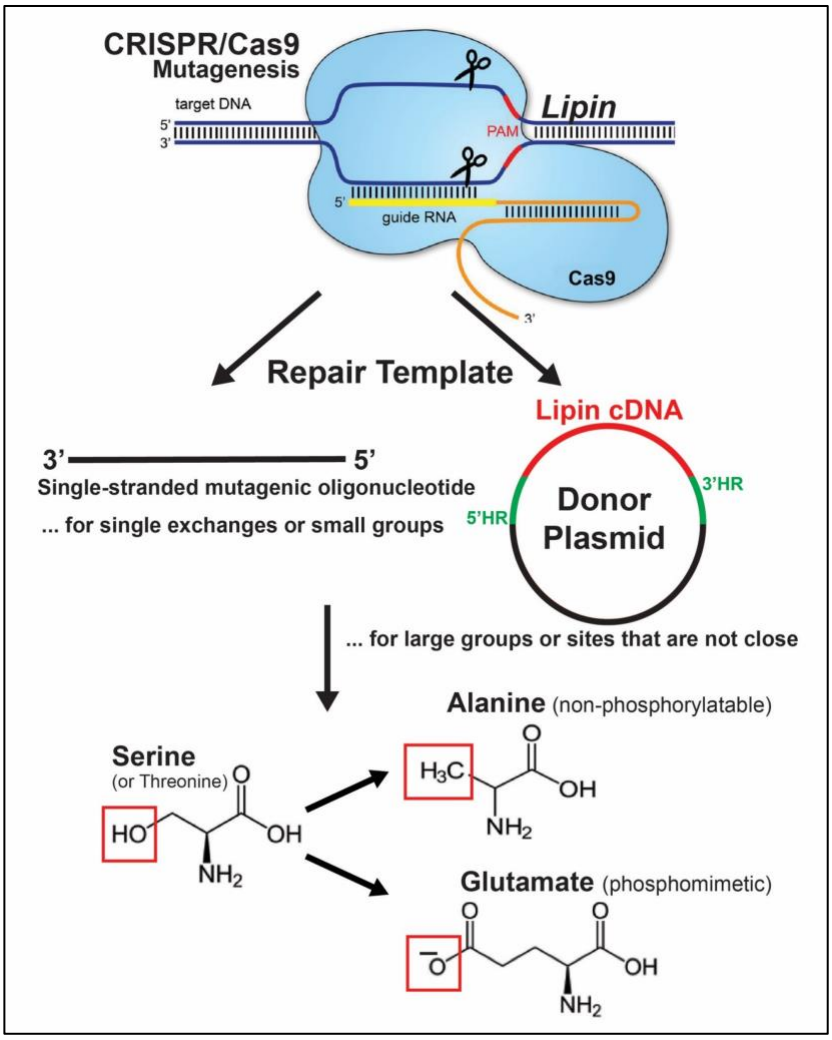

Fig 7. Schematic of approaches used to induce mutations by CRISPR-Cas9 mutagenesis. CRISPR-Cas9 mutagenesis was used to create phosphosite mutants. A guide RNA plasmid was co-injected with a repair template: either a single-stranded mutagenic oligonucleotide or a donor plasmid. Repair templates rendered phosphosite(s) either non-phosphorylatable by replacement with alanine or phosphomimetic by substitution with glutamate. Figure modified from Redman 2016.

17a. Selection of guide RNAs

Guide RNAs (gRNAs) were chosen using the online tool CRISPR Optimal Target Finder (http://targetfinder.flycrispr.neuro.brown.edu). *Drosophila melanogaster* (r_6) was used as the genome, and guide length was set to 20 nt.

While ideal to limit the number of off-target regions when selecting a gRNA, proximity to the location of interest often took precedence. Therefore, the stringency selected was "High" not "Maximum" as not to narrow the selection of gRNAs too far. PAM was restricted to "NGG only". If gRNAs contained off-target region(s) on a different chromosome, then they still were considered.

17b. pCFD3

If the intended mutations were close in the genome or a single amino acid was to be substituted, one gRNA can be used to direct the Cas-9 endonuclease to cut at a location upstream of the desired mutation(s). The pCFD3 gRNA plasmid (Addgene:49410) was used in these circumstances. The following protocol taken from www.crisprflydesign.org was followed to generate the pCFD3 gRNA plasmid targeting the region of interest.

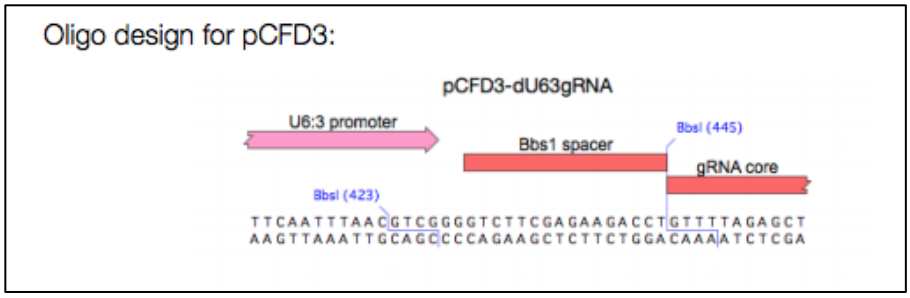

Fig 8. Schematic for protospacer design for use with pCFD3 plasmid.
Sense and anti-sense protospacers were designed with the appropriate overlaps. (Image: www.crisprflydesign.org)
Sense: 5'-GTC**G**-N19/20
Anti-sense: 5'-AAAC-N19/20 reverse compliment

The protospacers were designed based on the selected gRNA. Protospacers do not include the PAM sequence but do include sticky ends for ligation back into the pCFD3 plasmid (see Fig. 8 above). The sense strand contains the selected gRNA, where the anti-sense strain is the reverse complement. Single stranded oligos were purchased (Eurofins Genomics, Louisville KY) and resuspended to 100uM concentration. Oligos were used in a phosphorylation and annealing reaction and incubated at 37^{o}C for 30 minutes, brought to 95^{o}C for 5 minutes and ramped down to 25^{o}C at 5^{o}C/minute as described at: http://www.crisprflydesign.org/wp-content/uploads/2014/05/Cloning-with-pCFD3.pdf.

A ligation reaction was then setup using linear pCFD3 plasmid which had been digested by the BbsI enzyme (NEB-R0539S). Annealed oligos were diluted in ddH_2O to a 1:50, 1:100, or 1:200 dilution. Ligation was done at room temperature for 30 minutes or overnight at 16^{o}C (longer ligation increased transformation efficiency).

Transformations were set up using 4 μL of ligation reaction in 50 μL of competent cells and plated on Ampicillin plates. Individual colonies were screened for the presence of the protospacer. 3-5 mL LB-AMP cultures were set up overnight and grown to saturation (16-20 hours), shaking at 250-300 RPM. The QIAprep Spin Miniprep Kit (Qiagen-27106) protocol was followed to isolate plasmid DNA. After confirming DNA concentration on an agarose gel, clones were sent for sequencing (Eurofins Genomics) to identify successful transformants.

17c. pCFD4

In cases where two gRNA were needed, whether it where to increase the likelihood that a gRNA would cut the target region or because two gRNAs where required based on the template used for repair, the pCFD4 gRNA plasmid was used. Like the pCFD3 plasmid, single stranded

oligonucleotides where purchased. However, in this case, the two protospacers were incorporated into primers used for PCR to amplify the gRNA insert region.

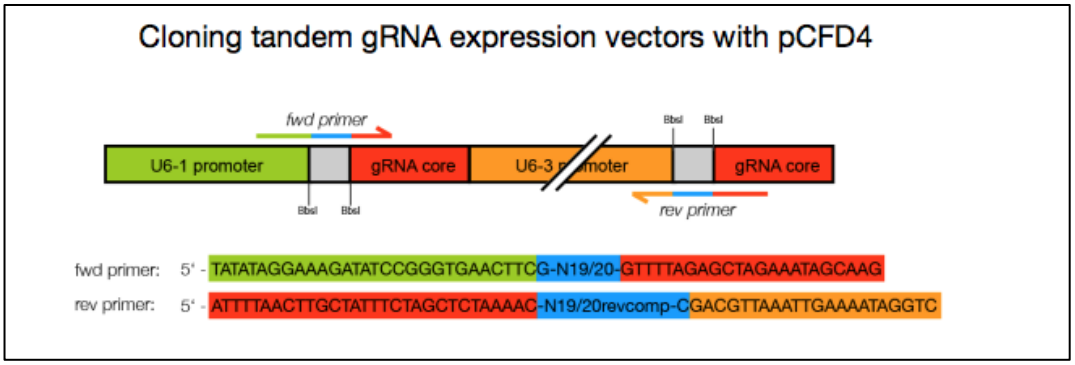

Fig 9. Schematic for protospacer design for use with pCFD4 plasmid.
Protospacers are introduced into the pCFD4 vector by PCR and are located downstream of two separate U6 promoters. (Image: www.crisprflydesign.org)

A high-fidelity DNA polymerase (Phusion Flash, Thermo Scientific-F548L) was used to amplify the target region of the pCFD4 plasmid using the primer design indicated in Figure 9. Circular pCFD4 plasmid (10 ng total) was used as the DNA template and the annealing temperature was set to 60ₒC. Following the PCR reaction, 1 µL DPN1 (NEB-R0176S) was added to the reaction and incubated at 37ₒC for 2-4 hours to ensure the DNA template used for the reaction was removed. The PCR reaction (600 bp) was cleaned up using a PCR purification kit rather than being gel extracted to prevent product loss (Zymo-D4013).

Following the recommendations of the manufacturer, BbsI-HF (NEB-R3539S) was used to linearize the pCFD4 plasmid. The restriction enzyme digest was extended to 1-2 hours to ensure total digestion of the plasmid. A Qiagen QIAquick Gel Extraction Kit (Qiagen-28704) was used to gel extract the linear plasmid backbone (6.4 kb) on a 1% agarose gel.

Once the linear plasmid backbone and PCR insert were recovered, the gRNA plasmid was assembled. Plasmid was created using Gibson or HiFi assembly (NEB-E2611S/E5520S)

following the manufacturer's instructions and 2 μL of the reaction assembly was used for subsequent transformation into competent cells and plated on Ampicillin plates. Single colonies were chosen, as they were for the pCFD3 gRNA plasmid (see section II.17c: pCFD3) and screened for the presence of the gRNA insert.

17d. Single-stranded oligonucleotide donor templates

Single-stranded oligonucleotides (ssOligos) were used as donor templates when only one codon was to be exchanged or if the cluster of putative phosphorylation sites targeted were grouped close together. Single-stranded donor templates where purchased from Integrated DNA technologies. The upper length limit of ssOligos was 200 nucleotides. Desired point mutations were introduced to the donor template and co-injected into *Drosophila* embryos containing a Cas-9 endonuclease.

Design of ssOligos was closely modeled after the method described in Richardson et al., 2016, choosing a template that was the reverse complement of the DNA strand which contained the PAM sequence. Further specifications on how ssOligos were designed are described in their manuscript.

17e. Donor plasmids

Donor plasmids were used when multiple sites were targeted and arranged over a larger genomic region (Fig. 10). Plasmid design was done using SnapGene. To create the donor plasmid, the pBluescript KS(-) backbone (pBSK) was used and the multiple-cloning site was removed. Genomic DNA from the would-be injection stock was chosen to create homology arms on the 5' and 3' ends. The Lipin cDNA or a synthetic double-stranded DNA was used (Integrated DNA technologies) to integrate the desired mutations. For information of the specifics of the donor plasmid used, see Table 8.

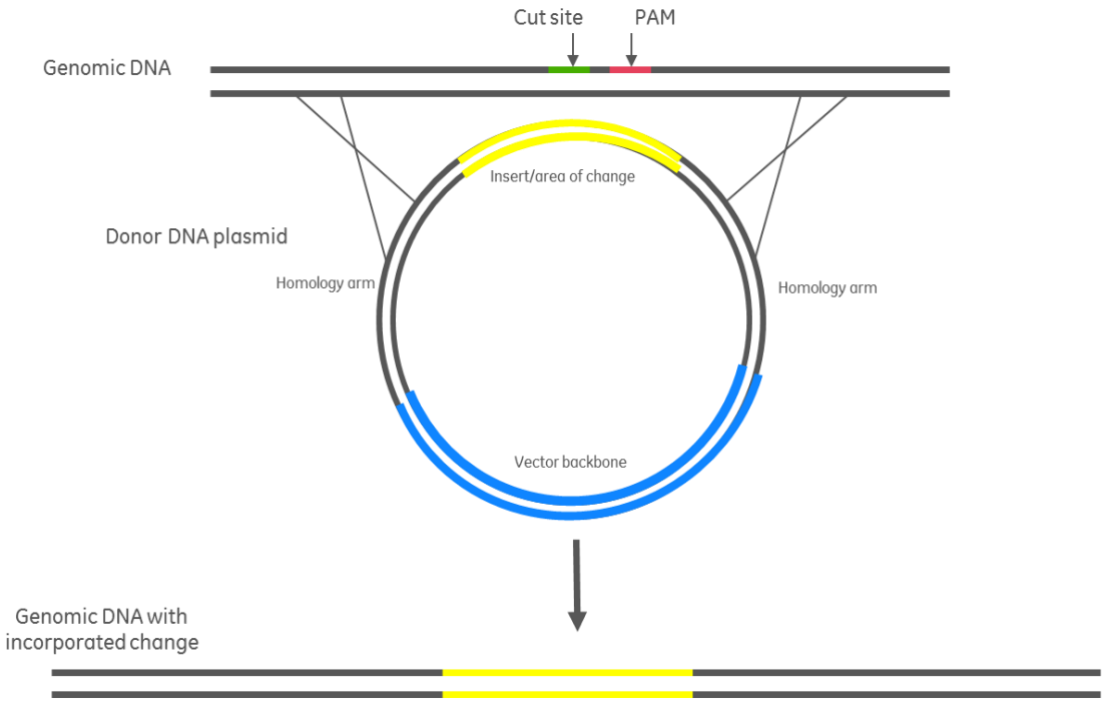

Fig 10. Diagram of donor plasmid design for CRISPR/Cas9 mutagenesis. Region of interest (cDNA or gBlock) is flanked by 5' and 3' homology arms from genomic DNA

Primer design for the amplification of the fragments for the donor plasmid was done using SnapGene. As a general rule, primers were designed to have no fewer than a 12 bp overlap with the adjacent fragments.

Once primers were chosen, PCRs were done using a high-fidelity DNA polymerase (Phusion Flash, Thermo Scientific-F548L). In some cases, genomic DNA reactions failed using Phusion Flash polymerase and therefore were amplified using a Taq polymerase (One*Taq* 2X Master Mix with Standard Buffer, NEB-M0482L). When plasmids were used as DNA templates, following the PCR reactions, 1 µL DPN1 (NEB-R0176S) was added directly to the reaction and incubated at 37ₒC for 2-4 hours to remove any starting template. Reactions were then cleaned up using a PCR purification kit (Zymo-D4013) and fragment sizes were verified on a gel.

Before the assembly reaction, concentrations were verified using a NanoDrop spectrophotometer and the components of the reaction were calculated based on the concentrations of the purified PCR products (see manufacturer's instructions: Gibson Assembly / HiFi DNA Assembly cloning kits, New England BioLabs (NEB-E2611S/E5520S)). Manufacturer's instructions were followed very closely as assembly of the plasmid was highly dependent on the correct of insert: vector ratios. Transformation of the assembly reactions were done using 2 μL of the assembled product on ampicillin plates. Individual colonies were selected and grown in 3-5 mL of LB-AMP overnight at 250-300 RPM at 37 ^{o}C. A QiaPrep Spin Miniprep Kit (Qiagen-27106) was used to isolate plasmid DNA and concentrations and size were verified on an agarose gel. Clones were sent to Eurofins Genomics, were the entire insert regions (excluding the pBSK backbone) were sequenced.

17f. Preparing injection mixtures

Individual components, repair template(s) and guide RNA plasmids were sent to BestGene Inc., (Chino Hills, CA, USA), or Rainbow Transgenic Flies, Inc. (Camarilla, CA, USA) for injection. Plasmids sent off for injection to BestGene Inc. received Service Z1, a regular plasmid DNA Midiprep, which ensured the DNA quality and plan RG was used CRISPR injections.

18. Screening for CRISPR Induced Mutations

Transgenic *Drosophila* lines containing a Cas-9 endonuclease were used for CRISPR injections. Injection stocks used for each of the mutant stocks are listed in Table 8. Bloomington stock #54591 is non-isogenic and results in homozygous lethality for the second chromosome. Because of this, stock *y1 w1118; attP2{nos-Cas9}/TM6C, Sb Tb,* was used to create subsequent

mutants. Injected animals were shipped back by the injection company as larvae and allowed to pupariate before being separated into individual vials.

18a. Crossing scheme and identification of mutations by sequencing

Injected animals were independently crossed with animals containing a CyO balancer. F1 animals containing the CyO balancer were selected for initial screening. Single fly genomic preps were completed as described above and the genomic DNA was used as a template for PCR. PCR reactions of the targeted region(s) were done for each mutant. In cases where point mutations were made, screening was only possible by sequencing. PCR products were purified (Zymo-D4013) and sequenced at Eurofins Genomics (Louisville, KY, USA). (Fig. 12)

The F1 screening identified "founder stocks" derived from animals in which the gRNA had led the Cas9 endonuclease to cut. Individual F1 males were then used to set up crosses with virgins from a balancer stock containing CyO-GFP. Once there were larvae visible on the food, the F1 male was sacrificed and screened for the presence of the intended mutation. GFP pupae were selected for crosses that contained the correct mutation(s) and mated together to test if the mutation was homozygous viable (indicated by the presence of non-GFP animals) (Fig. 11).

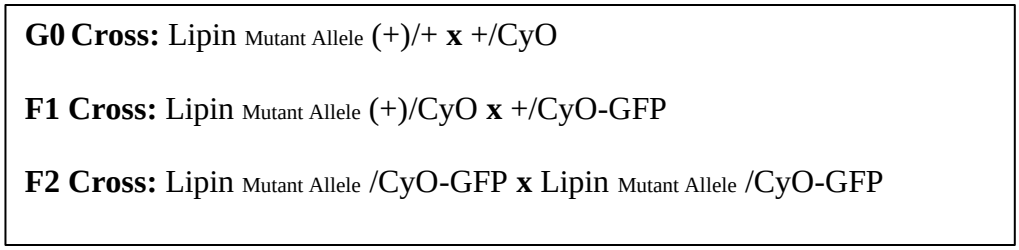

Fig 11. Crossing scheme used to recover CRISPR mutant stocks. Injected animals were individually crossed to a stock containing the CyO balancer. F1 animals balanced over CyO were screened to identify founder stocks. F1 males were crossed with virgins from a stock containing the CyO-GFP balancer. F1 males were screened for the intended mutation once larvae were visible in the food. GFP pupae were selected from positive stocks to establish mutant lines.

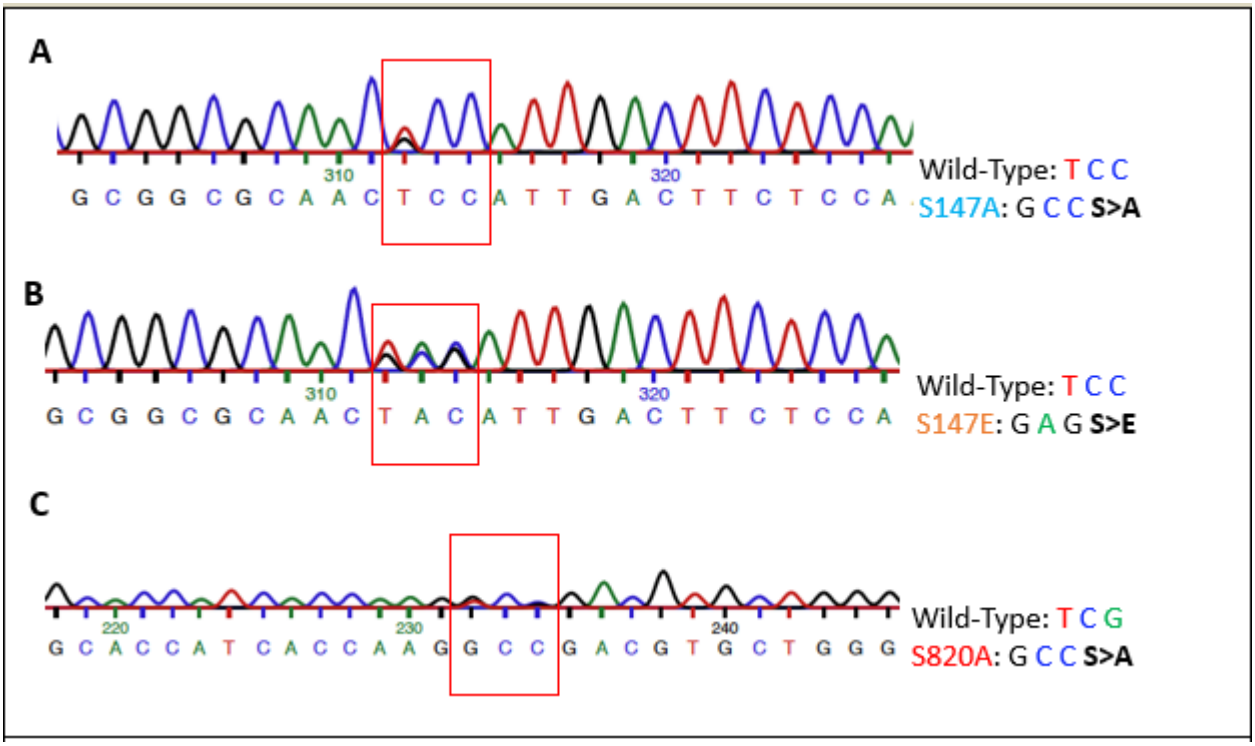

Fig 12. Identification of amino acid substitutions by Sanger sequencing. CRISPR/Cas9 mutagenesis was used to introduce base pair exchange into the *Lipin* gene that replaced serine/threonine phosphorylation residues with either alanine (GCC) or glutamic acid (GAG). A partial sequence for mutations where a single codon had been targeted are shown.

Table 8. Construction and Recovery of CRISPR Phosphosite Mutants. List of gRNA plasmids, donor templates used for repair, Cas9 injection stocks, companies used for CRISPR injections, total number embryos injected, larvae received and number of adult animals. In cases where more than one attempt was made to recover the mutant the data is separated as follows: first attempt/second attempt.

Mutant	gRNA Plasmid	Donor Template	Injection Stock	Injection Company	Embryos Injected	Larvae Received	Adult Animals
Lipin S147A	pCFD3	ssOligo	*y[1]M{vas-Cas9}ZH-2A w[1118]/FM7c* BDSC: 51323	Rainbow Transgenic Flies, Inc. Camarilla, CA USA	240	80	14
Lipin S147E	pCFD3	ssOligo	*y[1]M{vas-Cas9}ZH-2A w[1118]/FM7c* BDSC: 51323	Rainbow Transgenic Flies, Inc. Camarilla, CA USA	250	40	12
Lipin Group 1	pCFD4	Donor Plasmid	*y1 w1118; attP2{nos-Cas9}/TM6C, Sb Tb*	BestGene, Inc. Chino Hills, CA USA	~300/150	110/70	55/5
Lipin Group 2	pCFD4	Donor Plasmid	*y1 w1118; attP2{nos-Cas9}/TM6C, Sb Tb*	BestGene, Inc. Chino Hills, CA USA	~300	~100	55
Lipin S820A	pCFD3/ pCFD4	ssOligo	*y[1] M{w[+mC]=nos-Cas9.P}ZH-2A w[*]* BDSC: 54591	BestGene, Inc. Chino Hills, CA USA	>300/>300	86/~90	76/52

19. Determining viability of CRISPR Mutants

CRISPR mutant stocks were balanced over the balancer chromosome CyO-GFP. To determine if these stocks were homozygous viable, heterozygous mutants were mated: Lipin $_{\text{mutant allele}}$/CyO-GFP x Lipin$_{\text{mutant allele}}$/CyO-GFP. If non-GFP progeny were observed, then the introduced mutation(s) were non-lethal and homozygous mutant stocks were established.

Additionally, the CRISPR mutants were crossed to a stock containing a Lipin deficiency chromosome which lacks the entire *lipin* gene. Heterozygotes of the mutant stocks: Lipin $_{\text{mutant allele}}$/CyO-GFP were crossed to the Lipin deficiency stock: Df(2R)Exel7095/ CyO-GFP and crosses were observed for the presence of non-GFP, non-CyO animals: Lipin$_{\text{mutant allele}}$/ Df(2R)Exel7095. These transheterozygous animals contain one chromosome with the Lipin mutant allele and one chromosome with a Lipin deficiency. Transheterozygous animals were used as the experimental animals in all assays. Use of transheterozygotes in the experiments is important as it prevents any experimental artifacts that may result from using homozygous animals. Animals homozygous for the same mutagenized chromosome could contain addition unintended mutations at different loci that may result in phenotypes when homozygous for the mutation(s).

20. Developmental Timing Experiments

CRISPR mutants were tested for developmental delays using the following crossing scheme: Lipin$_{\text{mutant allele}}$(males)/CyO-GFP x Df(2R)Exel7095/CyO-GFP (females). Crosses were set up in biological triplicates on regular food and kept at 25^{o}C for 24 hours. Control crosses were also set up, injection stock (Cas9 stock used for injection (males)) x Df(2R)Exel7095/CyO-GFP(females). Following the initial 24-hour incubation, the flies were transferred to new food and allowed to mate until the following morning at 25^{o}C.

On the morning of the third day (Experimental day 1), the flies were transferred to new food and allowed to lay 6-8 hours at 25^{o}C. This was done for three consecutive days, where the egg laying occurred at the same time/duration each day and the overnight vials were discarded. Each following day, the vials were checked for prepupae and pupae. Number of pupae/prepupae were counted once or twice a day making note of the number of GFP and non-GFP animals pupariating. Recordings were made at the same time of day. Vials were observed until all animals in all vials had pupariated.

Some of the pupae (~20 for each genotype) were selected to monitor the time until eclosion to examine possible pupal lethality and delays in eclosion.

The total number of GFP and non-GFP pupae was calculated for each of the experimental replicates. The ratio of GFP vs. non-GFP pupae was then compared to the expected number of animals.

For example, consider the following cross:

- Lipin$_{\text{mutant allele}}$/CyO-GFP x Df(2R)Exel7095/CyO-GFP

The possible genotypes from this cross include:

- Lipin$_{\text{mutant allele}}$/CyO-GFP
- Df(2R)Exel7095/CyO-GFP
- Lipin$_{\text{mutant allele}}$/Df(2R)Exel7095

CyO-GFP/CyO-GFP is not viable.

Thus, the expected ratio of GFP to non-GFP animals would be 66.66% to 33.33%. A clear and reproducible reduction in the expected number of non-GFP animals indicates larval lethality of the mutant animals.

Graphs were generated to depict the mean percent pupariation of each of the genotypes over time (Y-axis: percent pupariation of a certain genotype; X-axis: time in days).

21. Triglyceride Assays

For this assay, 0.05% Tween 20 in 0.1 M Phosphate buffered saline was used for all steps where PBST is denoted.

21a. Triglyceride assays procedure

To measure the TAG levels of the prepared samples, samples were thawed, if applicable, and well vortexed. For each sample, 2 tubes were prepared. One consisted of the sample and PBST, to measure free cholesterol, and the other was for the sample and Triglyceride Reagent (Sigma: T2449). 80 μL of the sample was used for each of those reactions and 120 μL of either reagent was used. Samples were mixed by pipetting and placed in a 37$_{o}$C water bath for 60 minutes, allowing lipases to release glycerol from TAGs. Additionally, two control reactions were also processed in the same conditions, 80 μL PBST in 120 μL PBST and 80 μL PBST in 120 μL Triglyceride reagent. These measurements were crucial as they determine the background absorption from the reagents.

Male experimental and male control animals were processed all at once and then subsequently female samples were prepared or vice-versa.

Once samples were done incubating, they were transferred to a table-top centrifuge and spun at max speed (14,000 RPM) to 3 minutes at room temperature. 150 μL of the sample was then transferred into a 1.5 mL Eppendorf tube and 600 μL of Free Glycerol Reagent (Sigma: F6428) was added and mixed well by pipetting up and down. Samples were incubated at 37$_{o}$C in a water bath for 5 minutes and then spun down briefly in a table-top centrifuge (30 seconds at 14,000 RPM). The entire sample (750 μL) was then used to determine the absorbance readings.

Before taking sample readings the photometer was calibrated with PBST to an absorbance reading of 0 at 540 nm. Samples readings were taken at 540 nm in disposable polystyrene cuvettes (VWR: 97000-586).

21b. Sample Preparation

Freshly eclosed adults of the desired genotype were collected over ~24 hours or, if sufficient numbers of animals could not be obtained, collection time was extended to 48 hours. Males and females were separated into vials containing comparable amounts of animals to ensure all animals had adequate access to food (~30 animals per vial). 7 females and 10 males were used for each individual sample. Each genotype was done in biological triplicates. Animals were aged 3 days at 25^{o}C on standard food.

1.5 mL Eppendorf Safe-Lock tubes were used for TAG measurements. Tubes obtained from VWR (Cat. No. 20170-038) contained a contaminant that led to high background readings. The weight of each cohort of flies was recorded before the flies were frozen either on ice or by shock freezing using liquid nitrogen. Shock freezing was done in cases where eyes contained red pigment as the red eye pigment interferes with absorbance readings. Shock frozen animals were vigorously vortexed (~15 sec), to ensure the heads were removed. Wings and legs were also removed as a result of the vortexing. If samples contained animals with white eyes, this step was omitted as long as animals of all genotypes that were compared had white eyes.

Truncated animals were transferred to a new 1.5 mL microcentrifuge tube. Samples were homogenized in 300 μL ice-cold PBST using a micropestle. The pestle was rinsed with an additional 200 μL ice-cold PBST to remove any debris and the sample was then vortexed briefly. At this time, 100 μL of the homogenate was separated into a 1.5 mL Eppendorf tube for protein measurements to be done at a later time. The aliquots were shock frozen and stored at -80^{o}C until

needed for the protein assays. The remaining 400 µL of homogenate was heated at 70$_o$C for 10 min to inactivate enzymes. These samples were then shock frozen and kept at -80$_o$C until the triglyceride assays were performed. For performance of the assays, the samples were thawed and from then on handled at room temperature.

21c. Glycerol standard curve

In order to determine the unknown glycerol concentration of the samples, a glycerol standard curve was prepared using the following serial dilution (100 µL of higher concentration solution +100 µL PBST).

Table 9. Dilution scheme for glycerol standards. Used to generate the glycerol standard curve. Measurements were taken at 540 nm and ODs were plotted on a scatter plot.

1	**1 mg/mL** (120 µL glycerol standard solution (Sigma: G7793) + 180 µL PBST)
2	**0.5 mg/mL** (100 µL 1 mg/mL + 100 µL PBST)
3	**0.25 mg/mL** (100 µL 0.5 mg/mL + 100 µL PBST)
4	**0.125 mg/mL** (100 µL 0.25 mg/mL + 100 µL PBST)
5	**0.0625 mg/mL** (100 µL 0.125 mg/mL + 100 µL PBST)
6	**0.03125 mg/mL** (100 µL 0.0625 mg/mL + 100 µL PBST)

Prepared glycerol standards were stored at 4 °C but can also be kept at -20°C. Samples were spun down for 3 minutes at max speed in a table-top centrifuge if liquid had accumulated on the sides of the tubes.

To measure the glycerol standards, 80 µL of the sample was added to 120 µL of PBST and mixed well by pipetting. 150 µL of this mixture was then added to 600 µL Free Glycerol Reagent (Sigma: F6428) and mixed by pipetting. Samples were incubated for 5 minutes at 37$_o$C in a water bath. Before the absorbance readings were conducted, the standards were centrifuged at 14,000 RPM for 30 seconds in a table-top centrifuge. Before taking any measurements, the photometer was calibrated with PBST to 0 absorbance at 540 nm. Absorbance reading were taken for the entire sample (750 µL) at a wavelength of 540 nm in disposable polystyrene cuvettes (VWR: 97000-586).

Given the values generated by the standard curve, these numbers were used to generate a scatter plot in Excel. The plot was fitted with a linear trendline and the equation generated by this line was then used to determine the unknown concentrations of the samples based on the ODs measured.

22. Bradford Assays

To conduct the Bradford Assays, a Bradford Assay Kit (Thermo Scientific: 23200) was used. Before beginning the assays, the bottle containing the Coomassie Reagent was inverted several times (NOT shaken) and the volume needed for the assays was transferred to a Falcon tube and allowed to equilibrate to room temperature. Each sample required 1 mL of Coomassie Reagent, and an additional 9 mL of reagent was needed for the BSA Standard Curve. Protein samples used for these assays were prepared as instructed above (see section II.21b: Triglyceride Assays- Sample Preparation).

22a. Bradford Assay Procedure

Thawed protein samples were centrifuged at max-speed (14,000 RPM) in a table-top centrifuge for 3 minutes. 20 µL of supernatant was transferred to a new 1.5 mL Eppendorf tube (Eppendorf: 022364111). 1 mL of the Coomassie Reagent was added to the sample and mixed well by pipetting. Samples were incubated at room temperature for 10 minutes. A photometer was set to 595 nm and blanked using a cuvette filled with 1 mL ddH_2O. Samples readings were taken at 595 nm in disposable polystyrene cuvettes (VWR: 97000-586).

22b. BSA Standard Curve

To determine the unknown protein concentrations of the samples, a BSA standard curve was generated using the dilution scheme below. Stock solution (2 mg/mL BSA) was included in the Bradford Assay kit. Prepared standards were kept at 4_oC until use.

Table 10. Dilution scheme used to generate the BSA Standard Curve. Used to determine the unknown sample protein concentrations. A polynomial equation generated from the curve was used to solve for the unknowns.

Vial	Volume of PBST	Volume and Source of BSA	Final BSA Concentration
1	0	300µL of Stock	2000µg/mL
2	125µL	375µL of Stock	1500µg/mL
3	325µL	325µL of Stock	1000µg/mL
4	175µL	175µL of vial 2 dilution	750µg/mL
5	325µL	325µL of vial 3 dilution	500µg/mL
6	325µL	325µL of vial 5 dilution	250µg/mL
7	325µL	325µL of vial 6 dilution	125µg/mL
8	400µL	100µl of vial 7 dilution	25µg/mL
9	400µL	0	0 µg/mL = Blank

Standards were centrifuged at max-speed for 3 minutes at room temperature. 20 μL of supernatant for each of the standards was added to 1 mL room temperature Coomassie Reagent and incubated to 10 minutes at room temperature. Photometer was set to 595 nm and blanked with 1 mL ddH_2O. Measurements for the standard curve were done using standard cuvettes (VWR: 97000-586) and plotted in excel to generate a polynomial equation used to determine the unknown protein sample concentrations.

To generate a graph in Excel, the OD measurements were plotted on the Y-axis and the protein concentrations were plotted on the X-axis. However, to determine the polynomial equation, the inverse was plotted, protein concentration on the Y-axis and OD on the X-axis. An XY scatter plot was generated and a polynomial trendline was added where the best fit (either 2,3, or 4) was chosen. The equation generated by the polynomial trendline was then used to plug in the sample ODs to determine the unknown protein concentrations of each sample.

23. Starvation Assays with Adult Flies

Recently eclosed adult flies of the desired genotype were collected over a ~24-hour time window and transferred to vials with standard food. Each vial contained similar numbers of animals (~30) containing both males and females of the desired genotypes. Animals were aged for 3 days, transferring to fresh food after 2 days. Experiments were done in biological triplicates, each vial containing 25 animals (3 x 25 males and 3 x 25 females).

On the third day, animals were separated by sex and transferred to starvation vials. Starvation vials consisted of Flugs (hard cotton plugs) which were cut in half and were pushed to the bottom of an empty fly vial. Flugs were saturated with tap water, vials were decanted of excess water and flies were transferred into the vials. Vials were then plugged with cotton balls.

Dead flies were counted every day at the same time and removed to prevent surviving animals from feeding on dead animals. Every 2 or 3 days, about 200 μL of tap water was added to the vial to prevent dehydration of the flies. Females were transferred frequently to prevent them from feeding on eggs they have laid (days 2,4,7,10, etc.). Males were transferred once every 5 days as they feed on mold that may form in the vials. Animals were transferred to new vials as needed until all animals from all replicates had died.

Survival fit plots of these data were then generated in Excel where the Y-axis depicts % survival and the X-axis is the time in days. Total number of animals for each genotype were pooled to generate the graphs.

24. Statistical Analysis

Log-rank tests were done for both the developmental timing and starvation assays. These tests were done to determine if there was a statistically significant difference between the experimental and control animals considering all data points. Numbers of animals for each time point for each of the biological replicates and technical replicates were pooled and the tests were done online here: http://bioinf.wehi.edu.au/software/russell/logrank/. For the developmental timing assays, graphs depict means derived from 3 biological replicates.

Student's t-test were done to determine differences seen in the triglyceride and protein assays. Means and standard deviations for each of the biological replicates were calculated and unpaired t-test were done in Microsoft Excel. The standard deviations were used to generate error bars.

III. Results

1. Recovery and characterization of the UAS-Lipin20S/T>A transgenic line

The motivation for this experiment was to create a form of Lipin that constitutively localized to the nucleus. Previously published work done on lipin 1 in mammalian cell culture helped in the design of this project (Peterson et al., 2011). Here, the authors created a mutant version of Lipin where 17 of the phosphorylation sites of mammalian lipin 1 were converted from serine or threonine to alanine. This Lipin17 S/T>A mutant displayed robust nuclear translocation in cell culture. Additionally, a lipin 1 mutant where only 6 of the putative phosphorylation sites were rendered non-phosphorylatable showed partial nuclear translocation. This nuclear localization phenotype mimicked the effects seen when there is an inactivation of mTORC1 by the TOR inhibitor Torin1 (Peterson et al., 2011). Like mammalian lipin 1, *Drosophila* Lipin has also been shown to translocate into the nucleus when TORC1 is knocked down. TORC1 knockdown in the fat body of *Drosophila melanogaster* by RNAi leads a strong translocation of Lipin into the nucleus (Schmitt at al., 2015). Thus, it was hypothesized that nuclear translocation of Lipin would also occur in *Drosophila* if putative phosphorylation sites were rendered non-phosphorylatable. Here, in an effort to test this hypothesis, I created a UAS transgenic line, *Lipin20S/T>A,* where I replaced 20 of the predicted serine/threonine phosphorylation sites of *Drosophila* Lipin with alanine, rendering these sites non-phosphorylatable.

1a. Developmental timing experiments

Utilizing the GAL4/UAS system, tissue specific expression of *Lipin20S/T>A* was accomplished in the fat body of *Drosophila melanogaster* using *Cg-GAL4*, which is a fat body

driver of moderate strength (Lee et al., 2004). For simplicity, *Cg-GAL4* will be referred to as *FB-GAL4* (fat body GAL4).

Animals that expressed *UAS-Lipin20S/T>A* ectopically in the fat body displayed a severe developmental delay and began pupariating three days later than the wild-type control animals (Fig. 13). Larvae collected at the same time points for both *FB-GAL4 >UAS-Lipin20S/T>A* and *w1118>UAS-Lipin20S/T>A,* a control cross without GAL4 driver, were compared to observe differences in animal size and fat body content (Fig. 14). Transgenic larvae had a dramatic reduction in size and contained almost no fat body, thus appearing nearly transparent as seen in Lipin loss-of-function mutants (Ugrankar et al., 2011).

1b. Fat droplet staining

Fat droplets of animals with ectopic expression of *UAS-Lipin20S/T>A* appeared to show increased size variability compared to the control animals (Fig. 15). Animals expressing the transgene also showed increased variability in cell size and shape, which is seen more clearly when stained with Lipin antibody (Fig. 16). Cells appeared rounded and enlarged compared to cells of control animals and the fat body cells were less uniform in size.

1c. Lipin antibody staining

Lipin protein antibody staining revealed a significant decrease in the levels of Lipin in animals which ectopically expressed the *Lipin20S/T>A* transgene in the fat body. Small surrounding fat body cells appear to contain large amounts of Lipin protein, while the enlarged fat body cells contained almost none. Control animals had a more uniform distribution of Lipin throughout the tissue (Fig. 16).

Decrease in Lipin antibody staining was not due to the inability of the anti-Lipin antibody to recognize the mutant protein. *Lipin20 S/T>A* expressed in the salivary glands (Sgs-GAL4

>UAS- Lipin20 S/T>A), which do not normally express Lipin (Ugrankar et al., 2011), was detected by the Lipin antibody (Fig. 16).

1d. Ubiquitous and transient expression of Lipin20S/T>A

Expression of *Lipin20S/T>A* driven by *FB-GAL4* did not result in nuclear translocation of the protein as seen in mammalian cell culture (Peterson et al., 2011). Therefore, subsequent experimentation was done to reveal if expression under different GAL4 drivers would alter the result seen here. The *da-GAL4* driver is a weak ubiquitous driver that was chosen to express the transgene ubiquitously at low levels. In addition, the *Lsp-GAL4* driver, a transient fat body driver, which is only active in 3rd instar wandering larvae, was selected.

When expression of the *Lipin20S/T>A* transgene was driven by these additional GAL4 drivers, the loss-of-function phenotype seen with the *FB-GAL4* driver was no longer observed. Lipin antibody staining was completed for these crosses and not only were the levels of antibody staining for these genotypes similar to those for the control animals, but the cell morphology showed no apparent differences (Fig. 17). Animals appeared to have no significant differences in the amount of fat body as was seen when expression of the transgene was driven by the *FB-GAL4* driver.

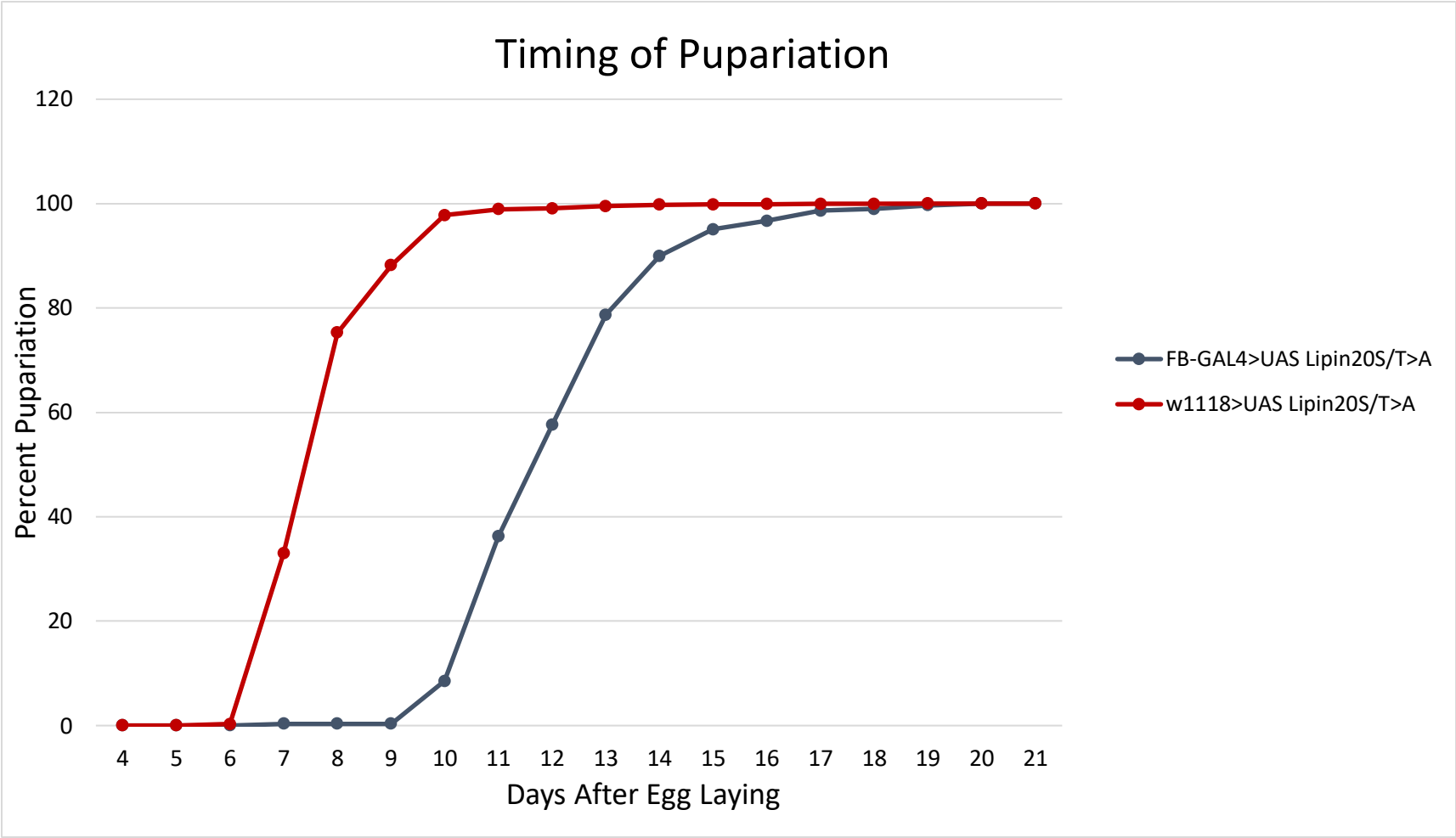

Fig 13. Timing of pupariation in animals expressing *Lipin20S/T>A* in the fat body. Control (red) animals began pupariating 7 days after egg laying, compared to the animals with ectopic expression of *Lipin 20S/T>A* (gray), where pupae began to form on day 10. Data is statistically significant. Log-rank, $p < 0.0001$.

Fig 14. Expression of *Lipin20S/T>A* in *Drosophila* fat body dramatically decreases fat body content and animal size. Images of *Lipin20S/T>A* (left) and wild-type Lipin (right) larvae that were collected the same day. Ectopic expression of the transgene exclusively in the fat body results in a severe growth phenotype. Experimental animals are dramatically reduced in both body size and fat body content. Scale bar (red) = 1 cm.

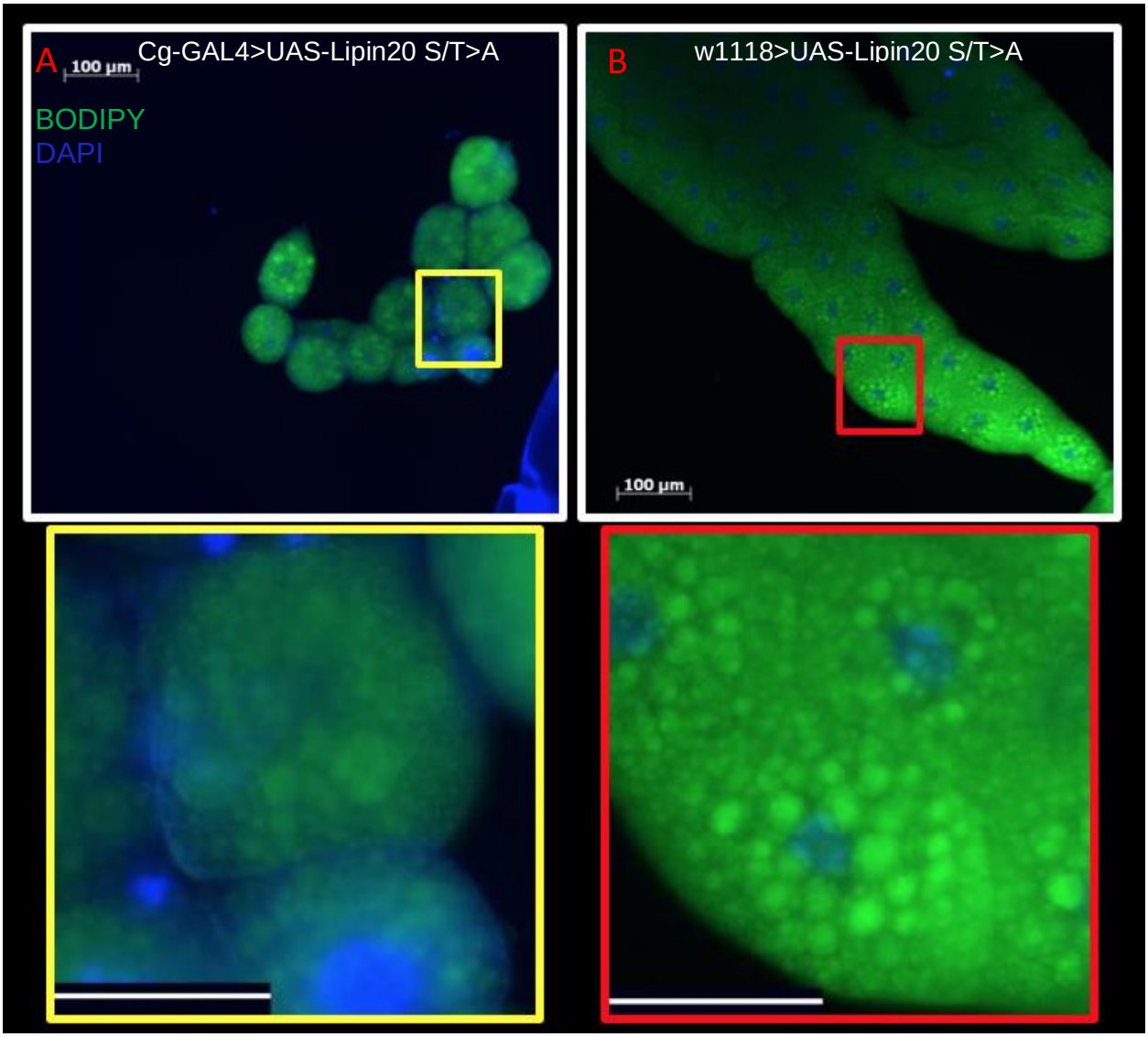

Fig 15. BODIPY 493/503 staining of larval fat body expressing *Lipin20S/T>A*. Fat body expression of the *Lipin20 S/T>A* (A), shows enlarged cell nuclei and increased variability in cell size control (B). Colored boxes indicate zoomed images. Scale bar zoomed images = 50 µm.

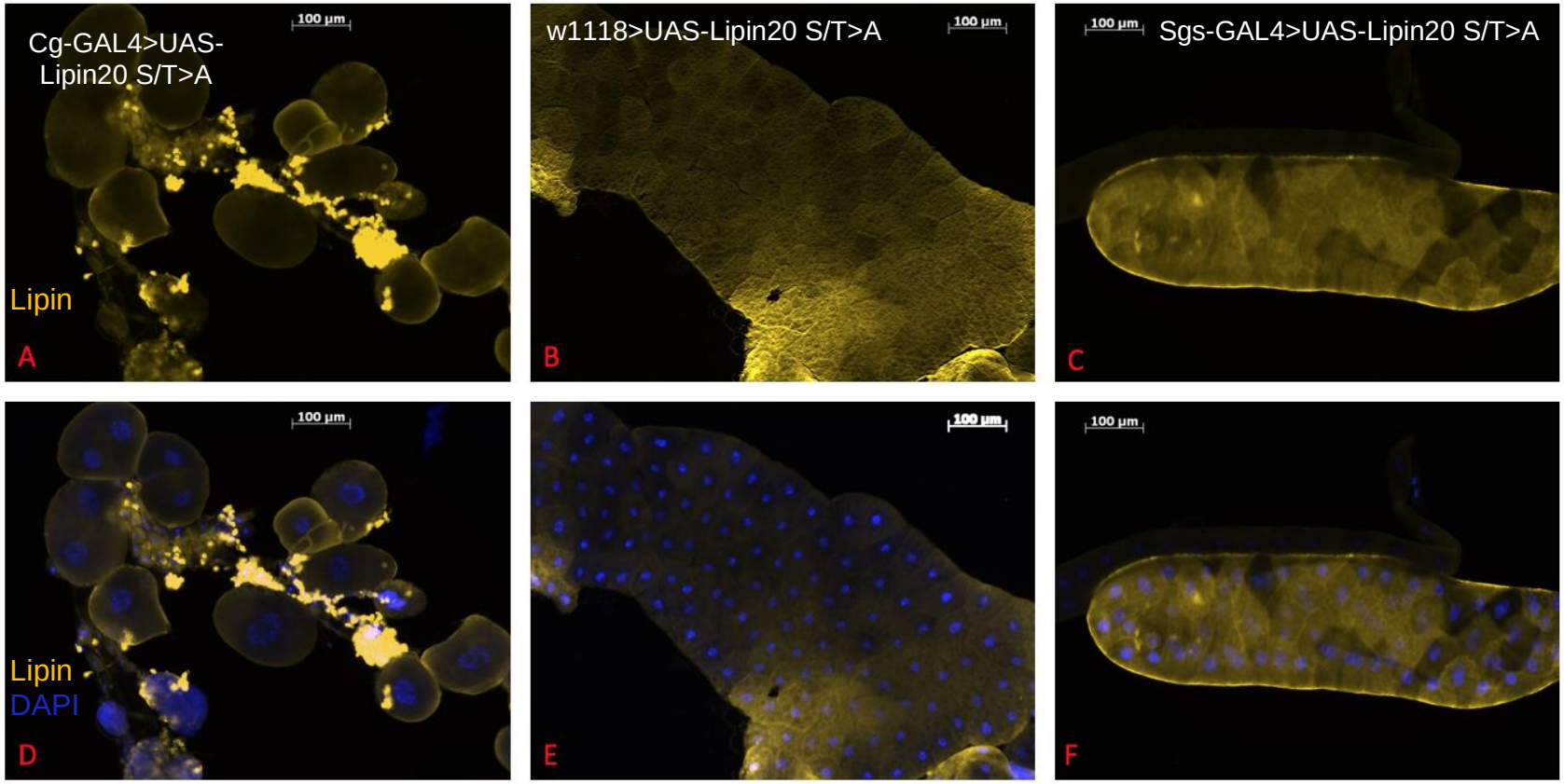

Fig 16. Lipin antibody staining of larvae expressing *Lipin20S/T>A*. (A and D) Fat body expressing *Lipin20S/T>A*. (B and E) Control fat body of larvae carrying the *UAS-Lipin20S/T>A* responder but not the *FB-GAL4* driver (from cross with w^{1118} flies). (C and F) Salivary gland driven expression of *Lipin20S/T>A*. Scale bar = 100 µm.

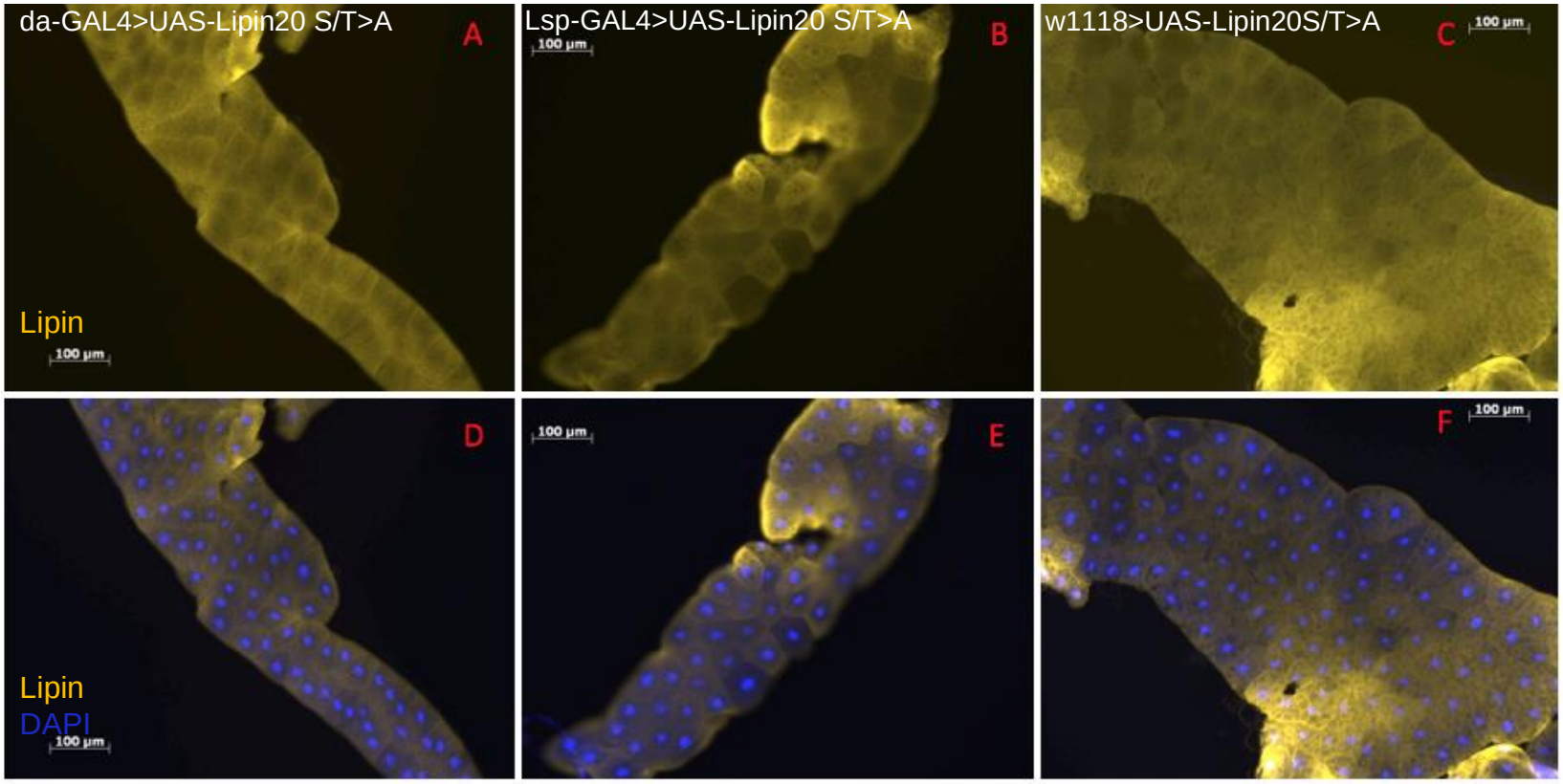

Fig 17. Lipin antibody staining of larval fat body expressing *Lipin20S/T>A* under the control of various GAL4 drivers. Ubiquitous driver (*da-GAL4*: A and D), transient fat body driver (*Lsp-GAL4*: B and E), control (*w1118*: C and F). Scale bar = 100 µm.

2. Recovery and Characterization of Lipin phosphosite mutants created by CRISPR/Cas9 mutagenesis

As suggested by the effects of *Lipin20 S/T>A* expression in the fat body, phosphorylation of Lipin may be important for the growth and development of *Drosophila melanogaster*. *Drosophila* Lipin, like mammalian lipin, has clusters of phosphorylation sites that are thought to have functional importance for the regulation of the protein and that are potential target sites for the insulin PI3K/Akt and MAP-kinase pathways. Here, a subset of mutants was created using CRISPR/Cas9 mutagenesis. These mutants targeted these putative phosphorylation sites and clusters of sites to determine their functional importance.

Most of the Lipin phosphosite mutants characterized here were generated by undergraduate students as part of their Honors Thesis projects. I aided in the project design and supervised the undergraduates in the laboratory. Unless otherwise noted, I carried out characterization of the mutants and helped the students in establishing mutant fly stocks.

Four of the five mutants discussed here were recovered by undergraduates, who also determined whether the mutants were homozygous viable and/or viable when the mutant allele was placed over a Lipin deficiency, Df(2R)Exel7095. The names of the students are listed in Table 11.

Once the viability of the mutant animals was determined, each of the mutants was subjected to phenotypic characterization. Listed below are the assays which I carried out to aid in better understanding the functional importance of the mutated residues.

1. **Developmental timing assays:** to observe for any developmental delays in either pupariation or eclosion.
2. **Fat droplet staining with BODIPY 493/503:** to observe fat body cell morphology and fat droplet content.
3. **Lipin antibody staining:** to determine subcellular localization and intensity of the mutant protein expression.
4. **Triglyceride and protein assays:** to determine if the phosphosite mutations affected the TAG and/or total protein production of the animals.
5. **Starvation assays:** to detect differences in the ability for the mutant animals to tolerate nutrient deprivation.

Phenotypic characterization of the mutants was done with animals of the genotype $Lipin_{mutant\ allele}$/ Df(2R)Exel7095. These animals will simply be referred to as Lipin mutants in the descriptions that follow. Control animals were of the genotype LipinWT/ Df(2R)Exel7095, carrying the wild-type allele of the injection stock used for CRISPR mutagenesis. An exception were the developmental timing experiments where internal control animals were used that developed in the same vials as the Lipin mutants ($Lipin_{mutant\ allele}$ or Df(2R)Exel7095/LipinWT).

Table 11. Summary table for phenotypic characterization of CRISPR mutants. Overview of results obtained for the characterization of the indicated Lipin phosphosite mutant.

Mutant	Recovered by:	Homozygous Viable	Viable over Lipin Deficiency	Development Timing	Fat Droplet Morphology	Lipin Staining	TAG/ Protein Ratio	Starvation Assays
Lipin S147A	Austin Morgan	Yes	Yes	No delays	No differences	Increased Lipin staining in mutant	No differences	Females have higher starvation resistance
Lipin S147E	Austin Morgan	Yes	Yes	No delays	No differences	Increased Lipin staining in mutant	No differences	Males have less tolerance to starvation
Lipin Group 1 S/T>A	Heidi O'Dell	Yes	Yes	Mutants show increased rate of pupariation	Mutants show increased staining	Increased Lipin staining in mutant	Mutant males have higher TAG production	No differences
Lipin Group 2 S/T>A	Hannah Davis + Josephine Gottsponer	Yes	Yes	No delays	Mutants show increased staining	Increased Lipin staining in mutant	No differences	Males have less tolerance to starvation
Lipin S820A	Stephanie Hood	No	Yes	Mutants show decreased rate of pupariation	No differences	Increased Lipin staining in mutant	Mutant females have a lower TAG production	Males and females have less tolerance to starvation

2a. Lipin S147A / Lipin S147E

The PI3K/Akt pathway is responsible for the metabolic effects of insulin. Insulin-sensitive kinases are predicted to aid in the regulation of Lipin. One site which has been predicted to be a target of Akt is the serine at position S147 of *Drosophila* Lipin (Bodenmiller et al., 2008). Mutants where the single putative phosphorylation site, S147, was rendered either non-phosphorylatable or phosphomimetic were used to study the functional importance of this residue.

Mutants where the serine residue at position S147 has been exchanged to alanine or glutamic acid are referred to as Lipin S147A and Lipin S147E, respectively. Both Lipin S147 mutants are homozygous viable and viable over a Lipin deficiency.

i. Developmental timing experiments

Developmental timing experiments revealed no significant differences in development when compared to the internal controls. Neither Lipin S147A or Lipin S147E showed a delay in pupariation (Fig. 18 + Fig. 19). No delay in eclosion or significant pupal lethality could be observed for either mutant. Sample size: n (Sl47A) = 33; n (control) =35 and n (S147E) =31; n (control)=31.

ii. Fat droplet staining

Fat droplet staining revealed no substantial differences in the fat body morphology of either Lipin S147 mutant when compared to the wild-type control. Cell shape and size as well as fat droplet number and fat droplet size were comparable to the control (Fig. 20).

iii. Lipin antibody staining

Lipin antibody staining unveiled that both Lipin S147A and Lipin S147E indicate an increase in staining intensity compared to the control (Fig. 21). Additionally, Lipin staining revealed that both forms of the mutant protein were present predominantly in the cytoplasm.

iv. Triglyceride and Protein assays

There were no statistically significant differences in the TAG/protein ratio between the experimental and control animals for either Lipin S147 mutant (Fig. 22).

However, despite there being no indication that residue S147 is essential for the activity of Lipin in TAG synthesis during normal fed conditions, it is possible that this site is only sensitive to high levels of PI3K/Akt activity. Additional experiments were conducted to test if this site would respond to increased activity of Akt. To carry out this experiment, fly lines which expressed constitutively active Akt in both a Lipin S147A and Lipin wild-type background were generated. Implementing the GAL4/UAS system the following genotypes were created: Lipin S147A/Df(2R)Exel7095; *r[4]-GAL4/UAS-Dakt[myr]* and LipinWT/Df(2R)Exel7095; *r[4]-GAL4/UAS-Dakt[myr]*. The *r[4]-GAL4* driver is a fat body driver which is expressed in both larval and adult fat body and the *UAS-Dakt[myr]* responder expresses constitutively active Akt (Cavaliere et al., 2005).

Constitutively active Akt in the fat body of Lipin S147A males led to a statistically significant increase in TAG/protein ratios as compared to mutant males with normal Akt expression (Fig. 23). Lipin S147A females with constitutively active Akt showed no statistically significant differences in TAG/protein ratios when compared to mutant females with normal Akt expression (Fig. 23). Control animals of either sex with constitutively active Akt showed no

statistically significant increases in TAG/protein ratios compared to controls with normal Akt expression (Fig. 23).

v. Starvation assays

Lipin S147A males showed a comparable resistance to starvation as the males of the control group. However, Lipin S147E males displayed a highly significantly reduced starvation resistance (Fig. 24). Females from the Lipin S147A stock reveal a statistically significant increase in starvation resistance, whereas Lipin S147E females showed no significant difference in starvation tolerance (Fig. 25).

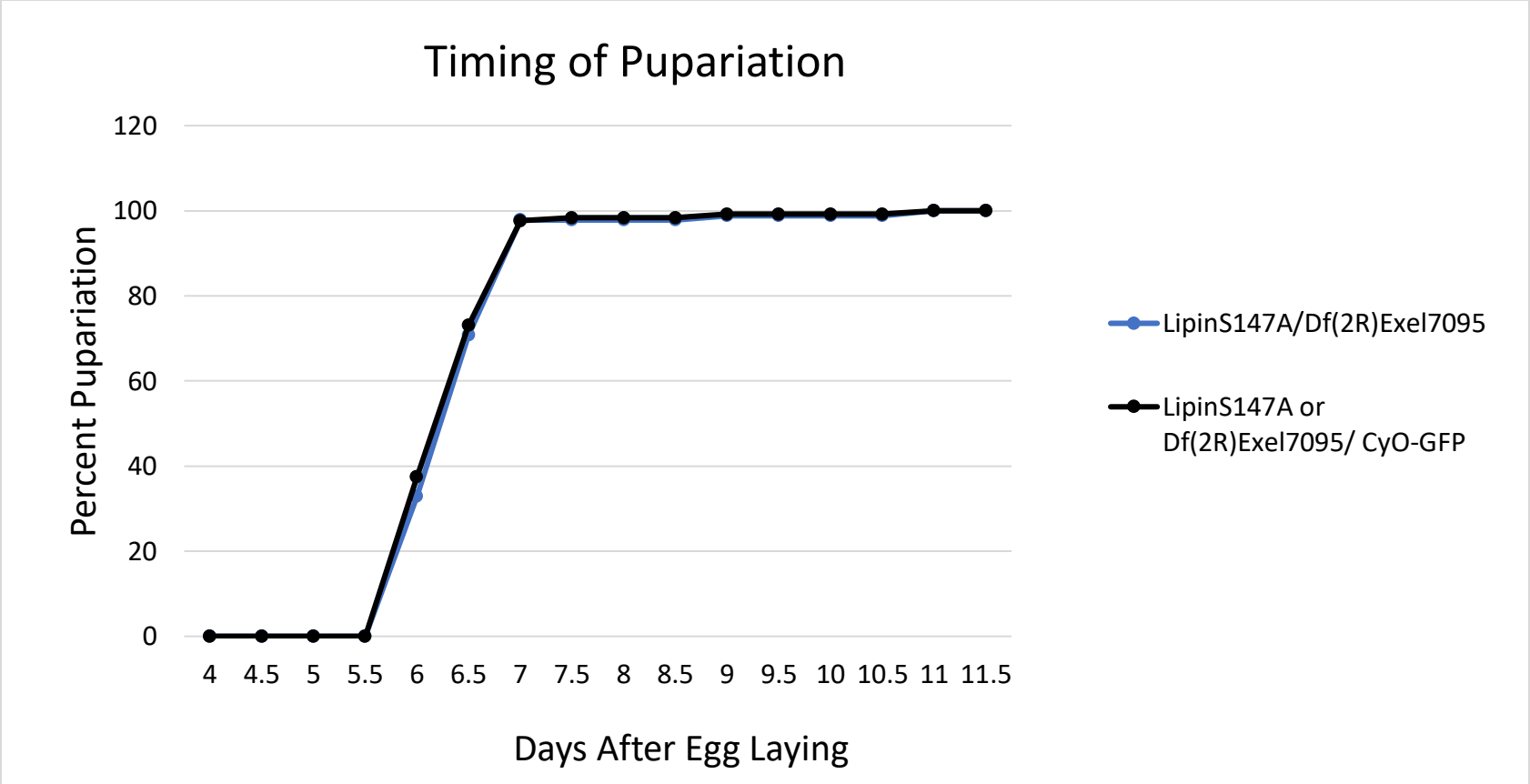

Fig 18. Timing of pupariation for Lipin S147A mutants. Lipin S147A animals pupariate at similar times as the internal controls. Differences are not statistically significant.

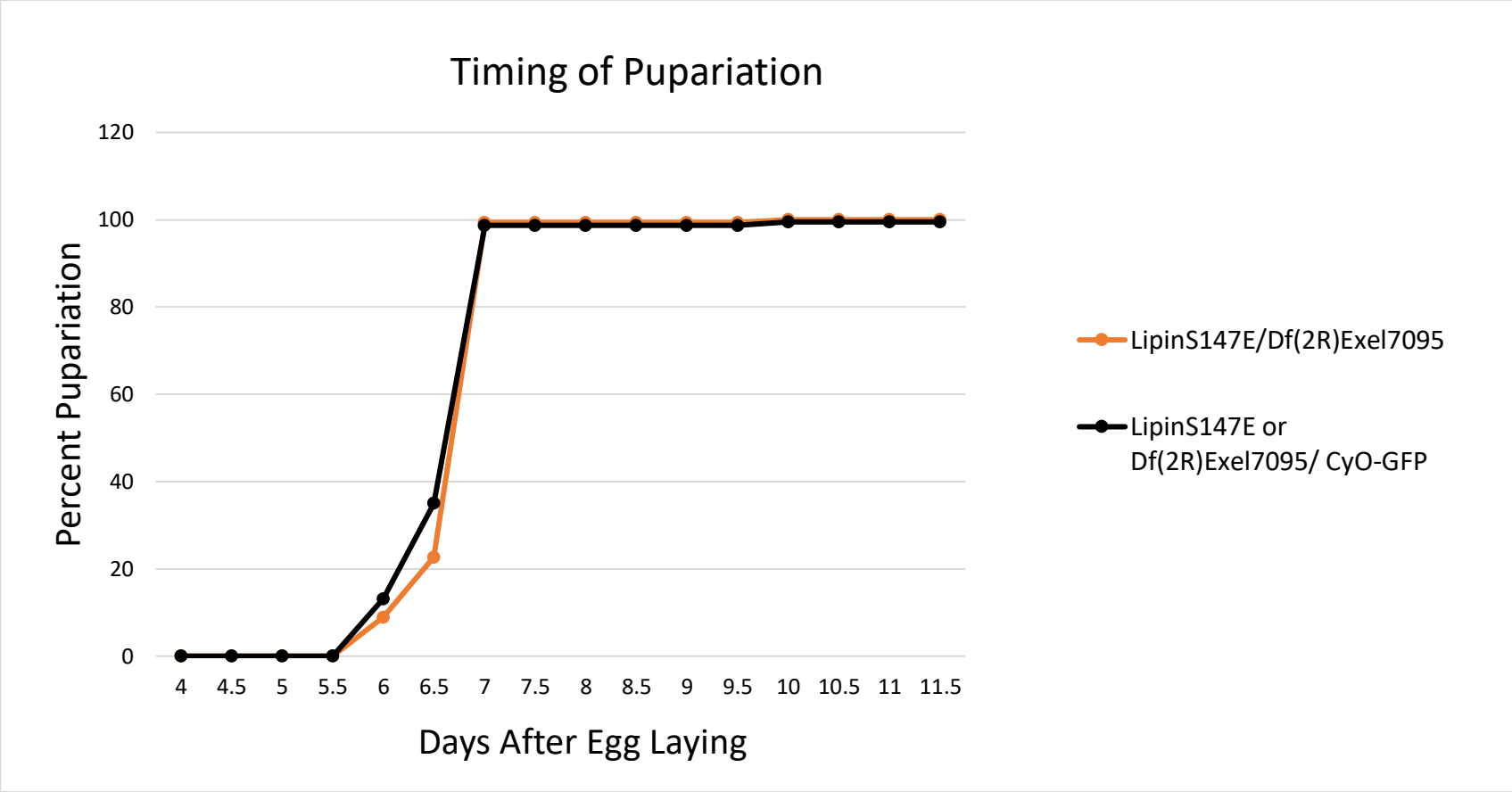

Fig 19. Timing of pupariation for Lipin S147E mutants. Lipin S147E animals pupariate at similar rates as the internal controls. Differences are not statistically significant.

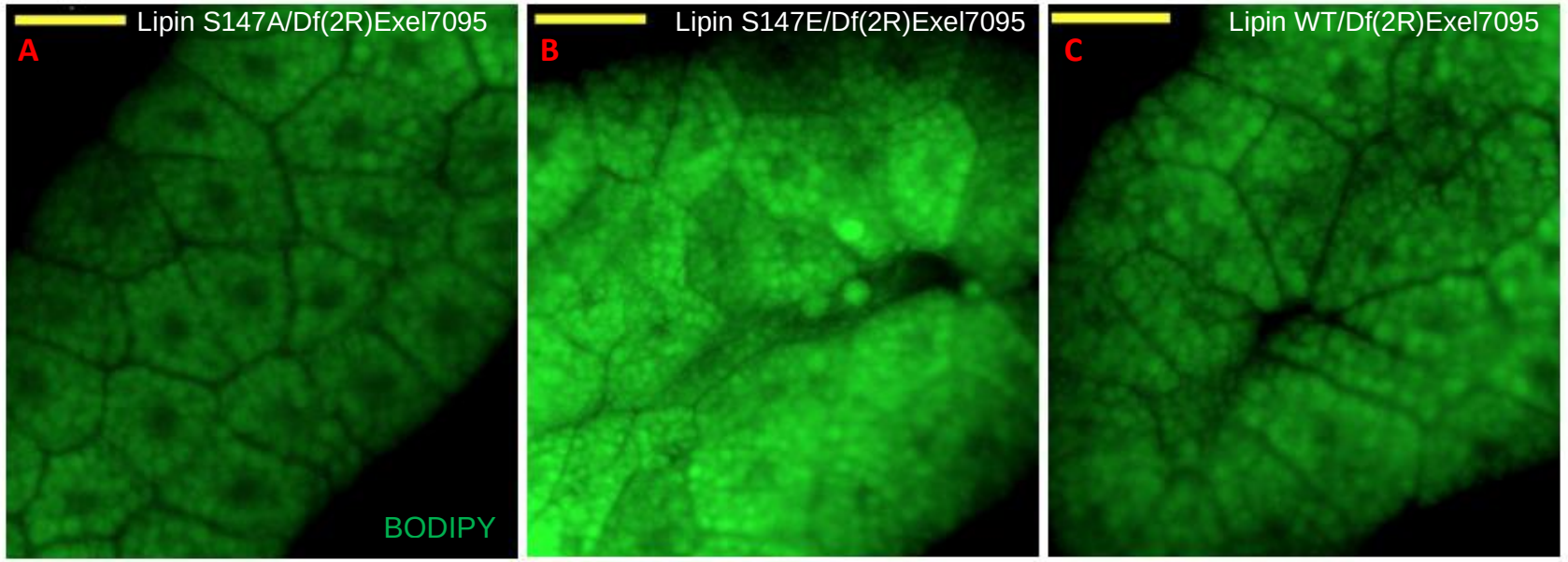

Fig 20. BODIPY 493/503 staining of Lipin S147 mutant fat body. Lipin S147A (A) and Lipin S147E (B) mutants have apparently similar fat body morphology when compared to the wild-type control (C). Animals have similar amounts of fat body and fat droplets and comparable cell size. Fat droplet size in both mutants is similar to fat droplet size in the control. Scale bar = 50 μm.

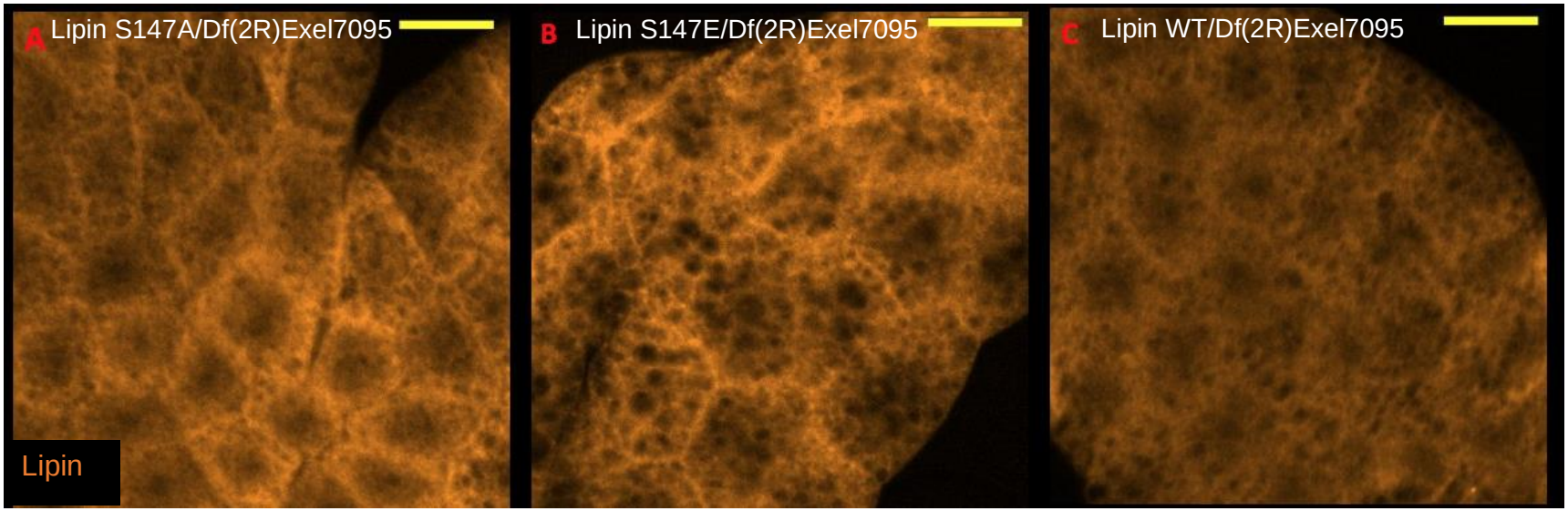

Fig 21. Lipin Antibody Staining of Lipin S147 mutant fat body. Lipin S147A (A) and Lipin S147E (B) mutants suggest higher expression levels of Lipin as compared to the control (C). Protein expression for all animals is predominantly cytoplasmic. Scale bar = 50 μm.

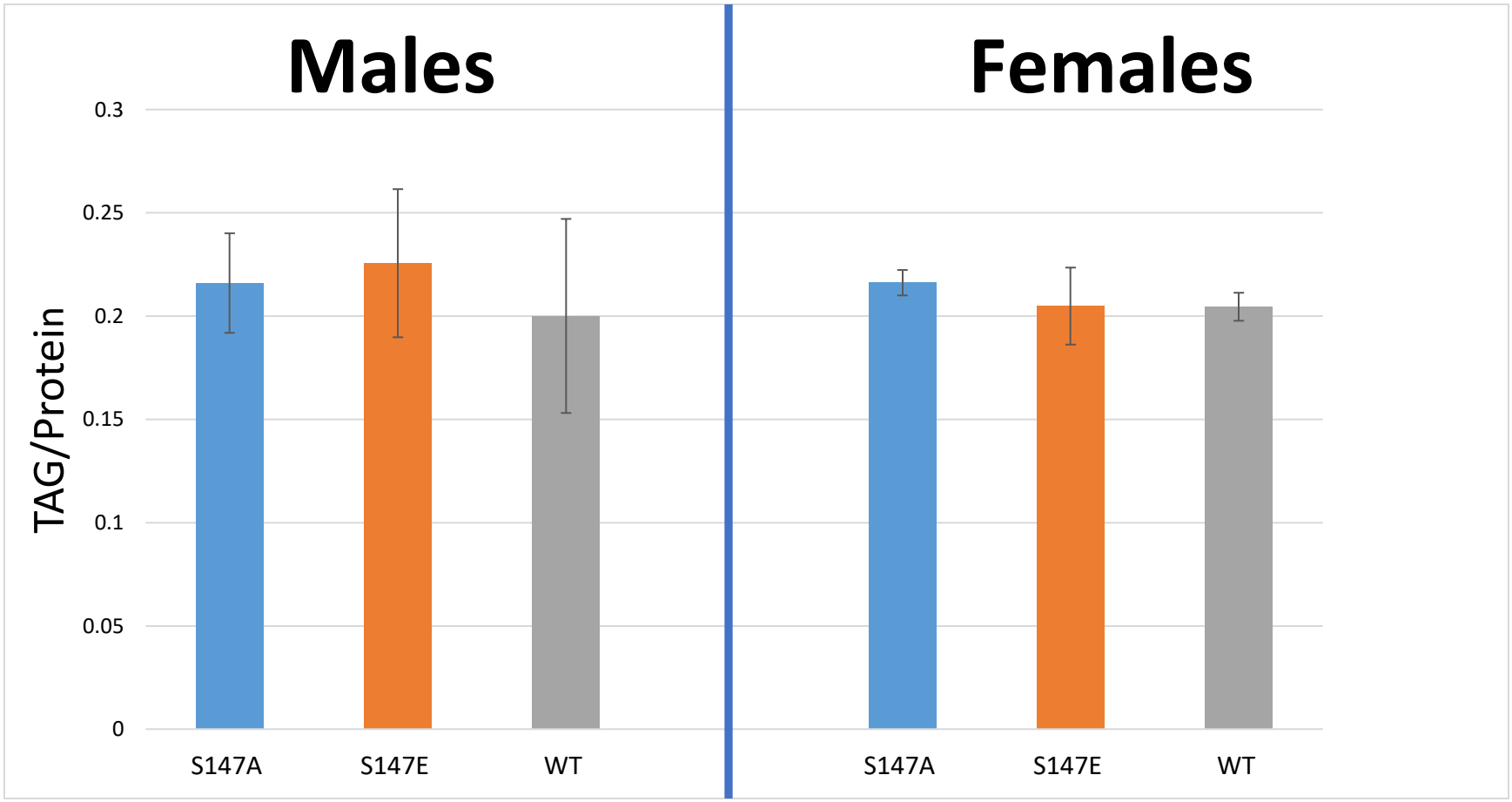

Fig 22. Triglyceride/protein ratio of Lipin S147 mutants. Lipin S147A(blue) and Lipin S147E (orange) mutants show comparable TAG/protein ratios when compared to the control (gray). Error bars: SD.

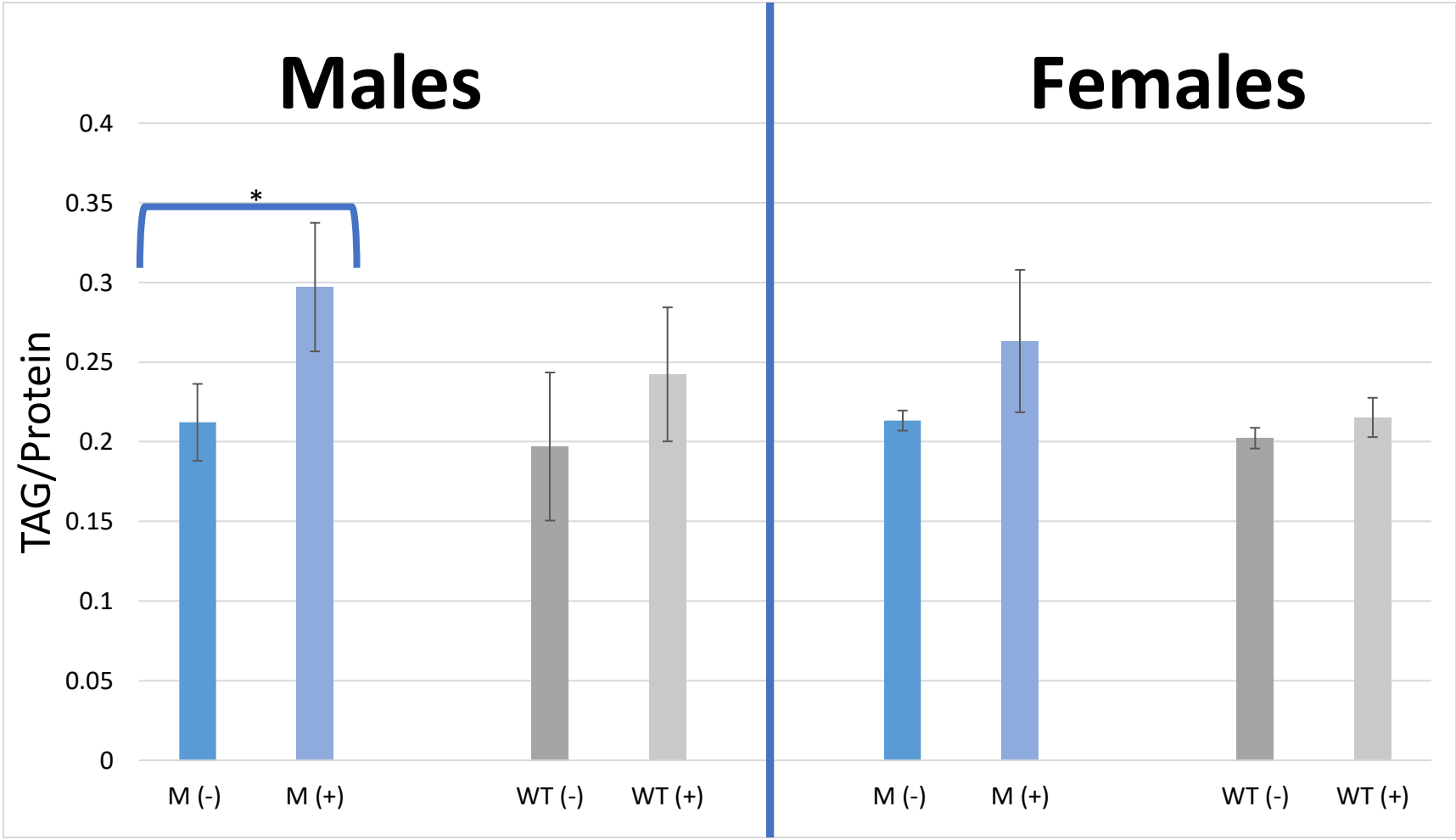

Fig 23. Triglyceride/total protein ratio of Lipin S147A mutants vs. Lipin S147A mutants expressing constitutively active Akt. Lipin S147A/Df(2R)Exel7095; r[4]-GAL4/ UAS-Dakt[myr] (light blue; (+)) mutant males but not females have a statistically significant increase in TAG/protein ratios as compared to animals where Akt is not constitutively active, Lipin S147A/Df(2R)Exel7095 (blue, (-)). Student's t-test, p = 0.035. Control animals, LipinWT/Df(2R)Exel7095; r[4]-GAL4/ UAS-Dakt[myr] (light gray) with constitutively active Akt (+) suggest a trend in the increase of TAG/protein ratios as compared to genotypes without active Akt (-); however, these data are not statistically significant. Error bars: SD.

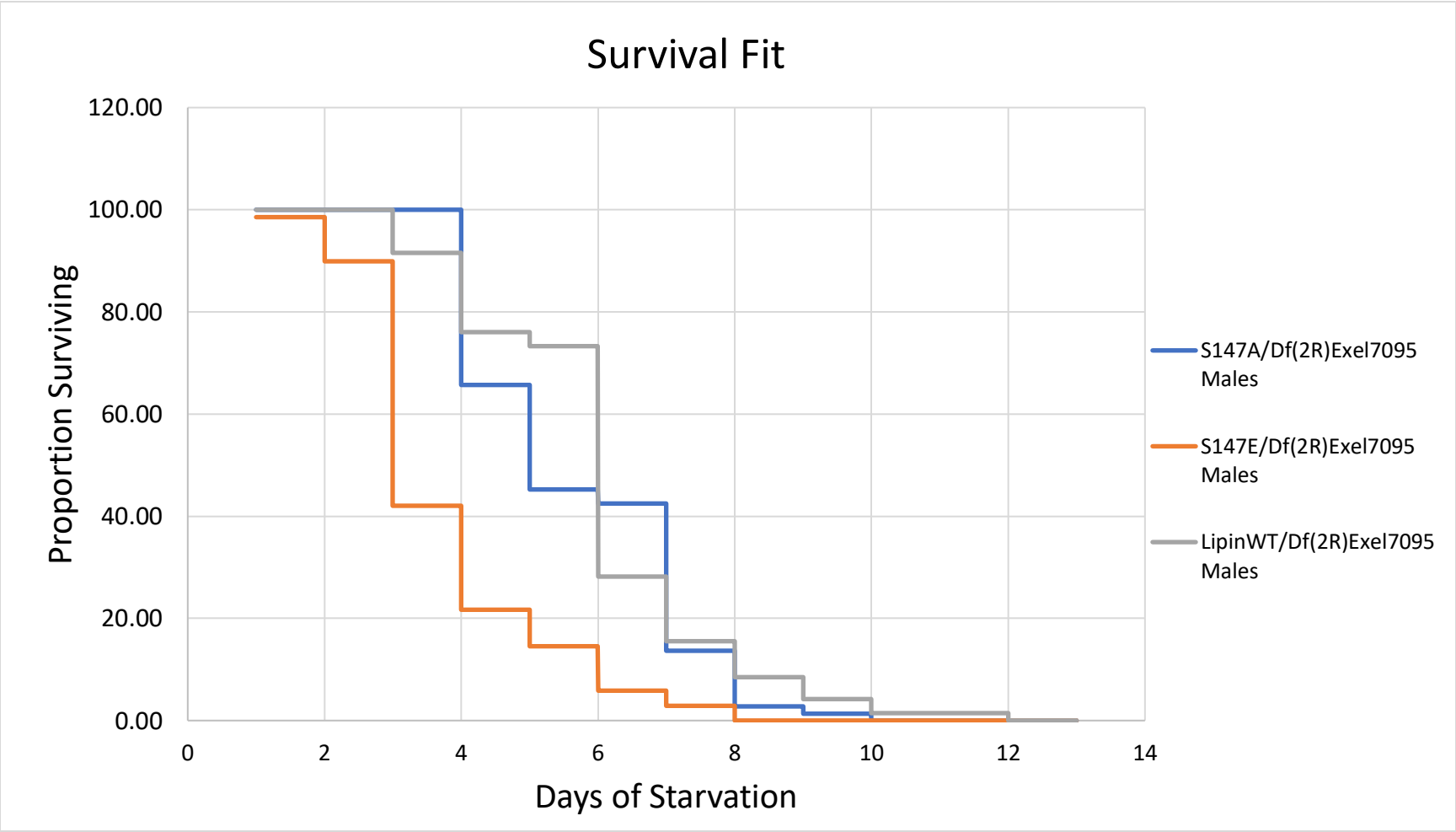

Fig. 24. Starvation resistance of Lipin S147 mutant males. Lipin S147E (orange) but not Lipin S147A (blue) flies have less resistance to starvation than control males, LipinWT (gray). Differences are highly significant. Log-rank, $p < 0.0001$.

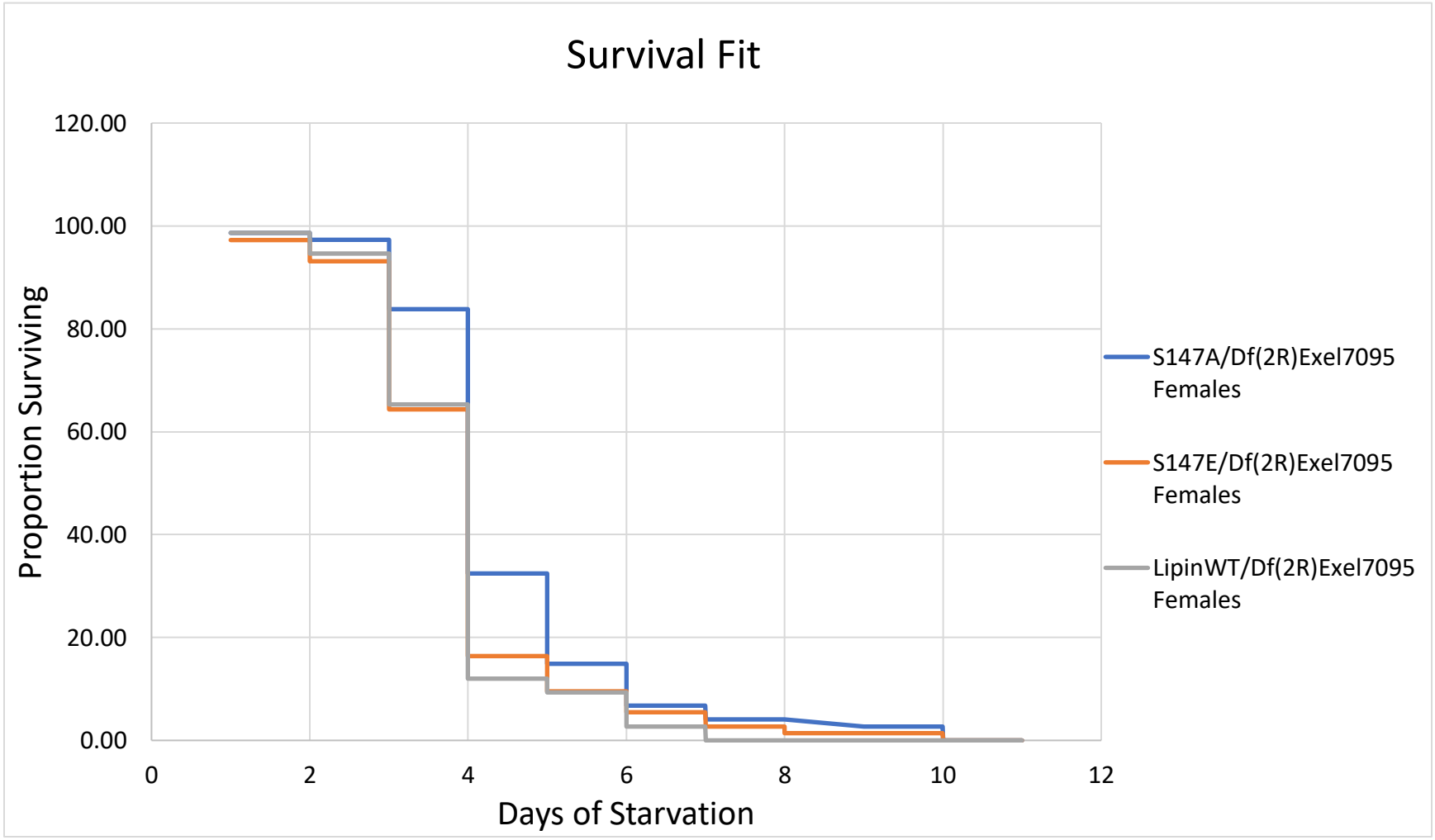

Fig 25. Starvation resistance of Lipin S147 mutant females. Lipin S147A (blue) but not Lipin S147E (orange) flies have a higher resistance to starvation than control females, LipinWT (gray). Differences are statistically significant. Log-rank, p = 0.0029.

2b. Lipin Group 1 S/T>A

Lipin Group 1 contains the putative Akt phosphorylation site, S147, as well as an additional 4 serine/threonine phosphorylation sites, S151, T178, T181, and S221. Interestingly, this cluster of putative phosphorylation sites is found in *Drosophila* Lipin but not mouse lipin1b (Fig. 4).

A mutant where the serine/threonine residues of Lipin Group 1 were rendered non-phosphorylatable was created. The Lipin Group 1 mutant is homozygous viable and viable over the Lipin deficiency.

i. Developmental timing experiments

When compared to the control animals, Lipin Group 1 animals experienced a small but statistically significant increase in pupariation rate (Fig. 26). No delay in eclosion or significant pupal lethality could be observed. Sample size: n (Group 1) = 151; n (control) =151.

ii. Fat droplet staining

BODIPY 493/503 staining of the mutant fat body showed no apparent differences in cell size compared to the control. However, the intensity of the staining for the Lipin Group 1 mutants appears stronger when compared to the control animals (Fig. 27).

iii. Lipin antibody staining

Immunostaining of Lipin Group 1 third instar wandering larvae with an anti-Lipin antibody indicated an increase in Lipin expression in the Lipin Group 1 mutants as compared to the control animals (Fig. 28). Mutant and control protein resided in the cytoplasm.

iv. Triglyceride and Protein assays

Mutant Lipin Group 1 males had an elevated TAG/protein ratio. Mutant females showed no significant difference in TAG/protein ratio compared to the control (Fig. 29).

v. Starvation assays

Lipin Group 1 mutant males and females appear to have a similar resistance to starvation as the control animals (Fig. 30 + Fig. 31).

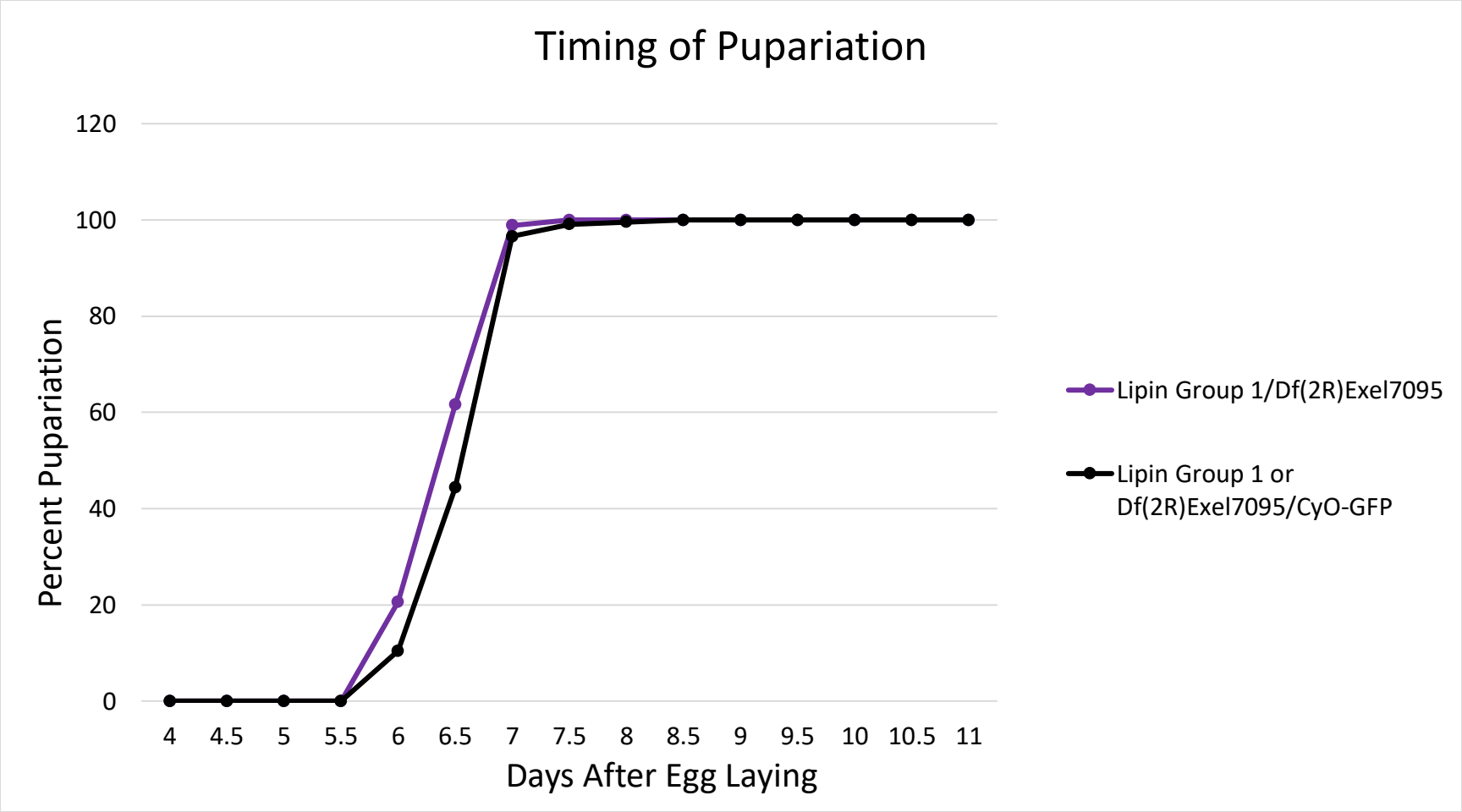

Fig 26. Timing of pupariation for Lipin Group 1 mutants. Lipin Group 1 (purple) animals appear to pupariate at slightly elevated rate compared to the internal control (black). Log-rank, p = 0.0011.

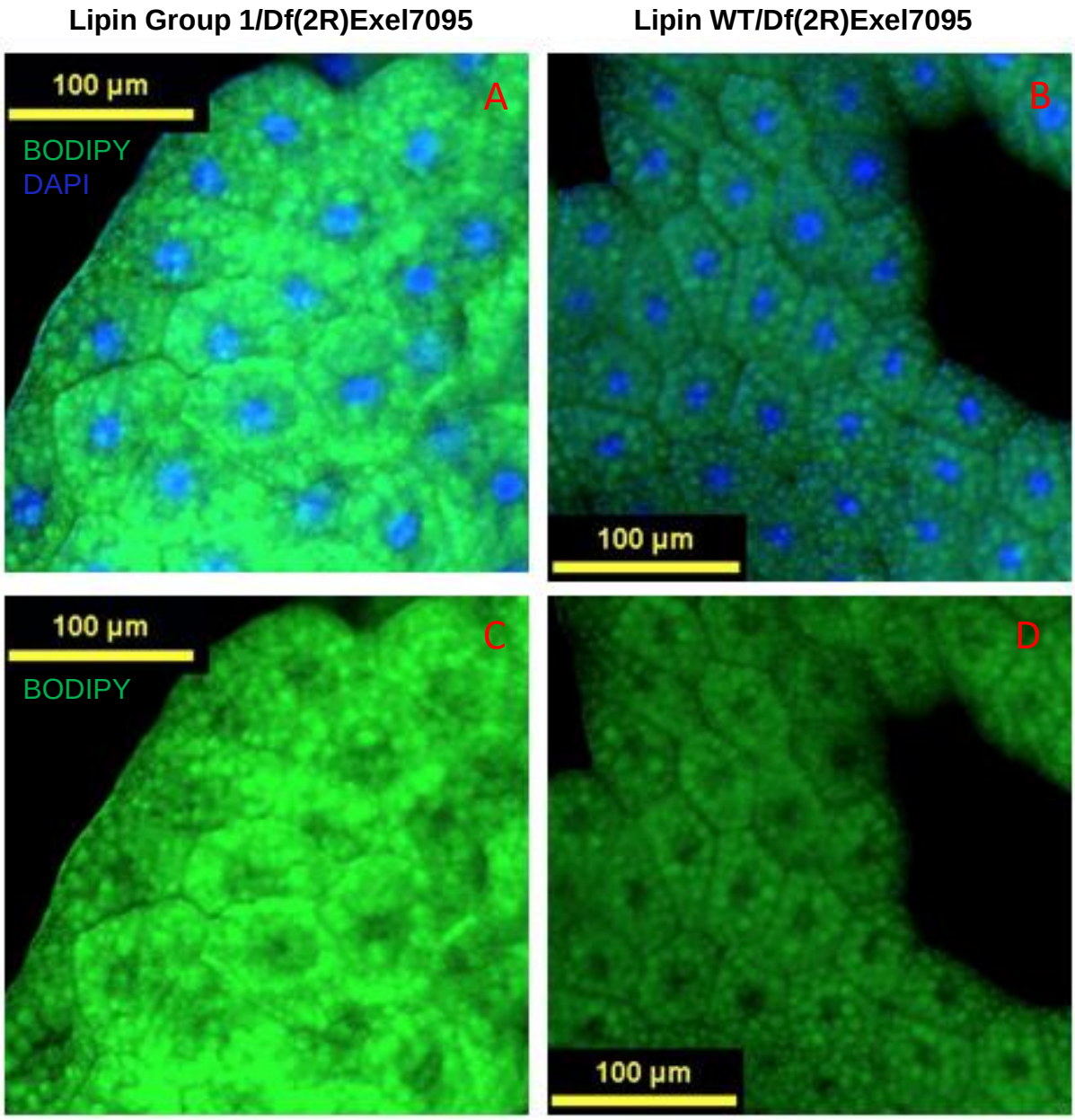

Fig 27. BODIPY 493/503 staining of Lipin Group 1 mutant fat body. Lipin Group 1 mutants (A and C) have similar fat body cell size when compared to the control (B and D). Animals have comparable amounts of fat body. Intensity of staining appears stronger in the Lipin Group 1 mutants. Nuclear staining (A and B): DAPI (Blue). Scale bar: 100 µm.

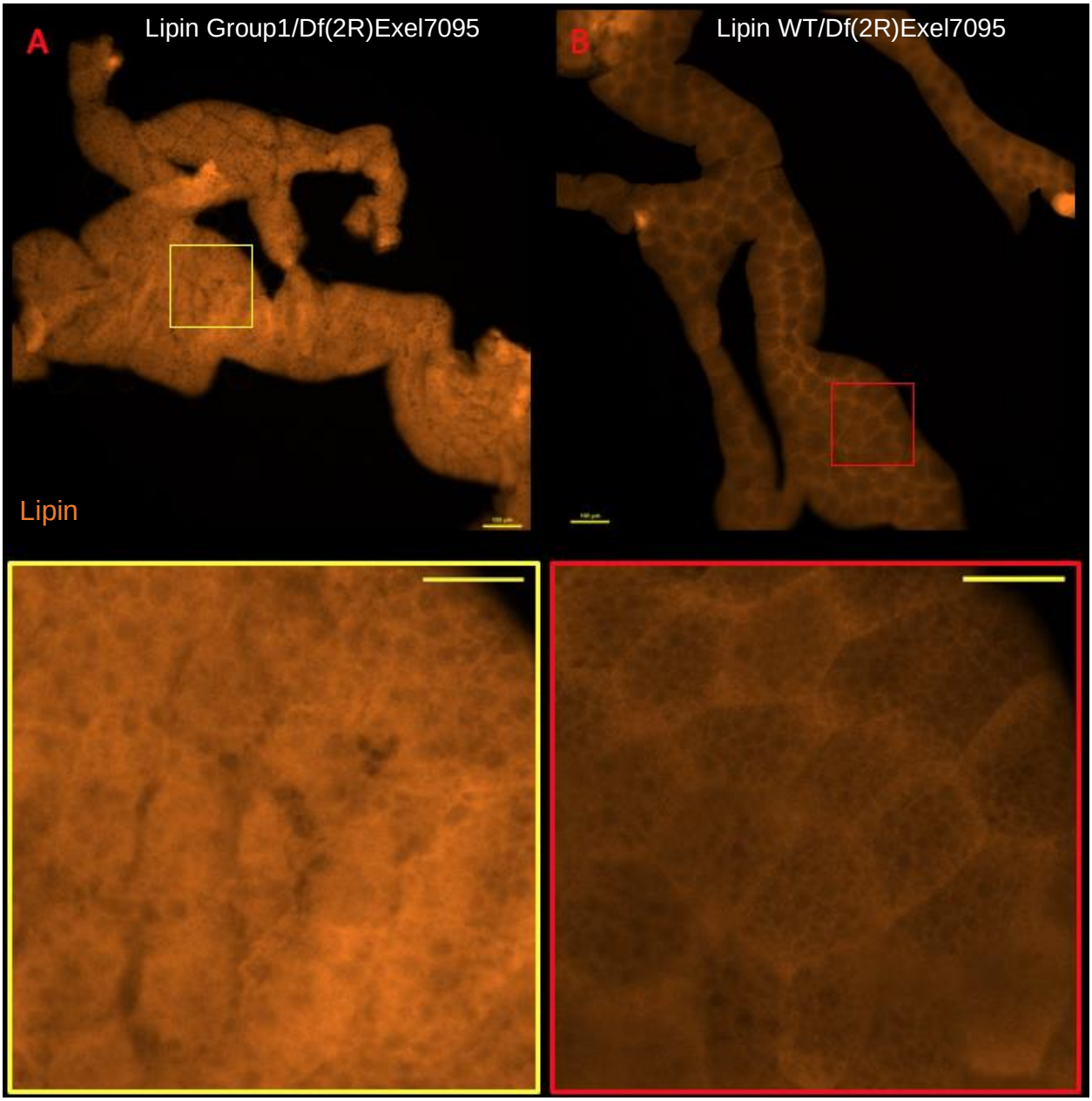

Fig 28. Lipin Antibody Staining of Lipin Group 1 mutant fat body. Lipin Group 1 mutants (A) appear to have an increase in expression of Lipin compared to the control (B). Protein expression for all animals is predominantly cytoplasmic. Colored boxes indicate zoomed images. Scale bar zoomed images = 50 μm.

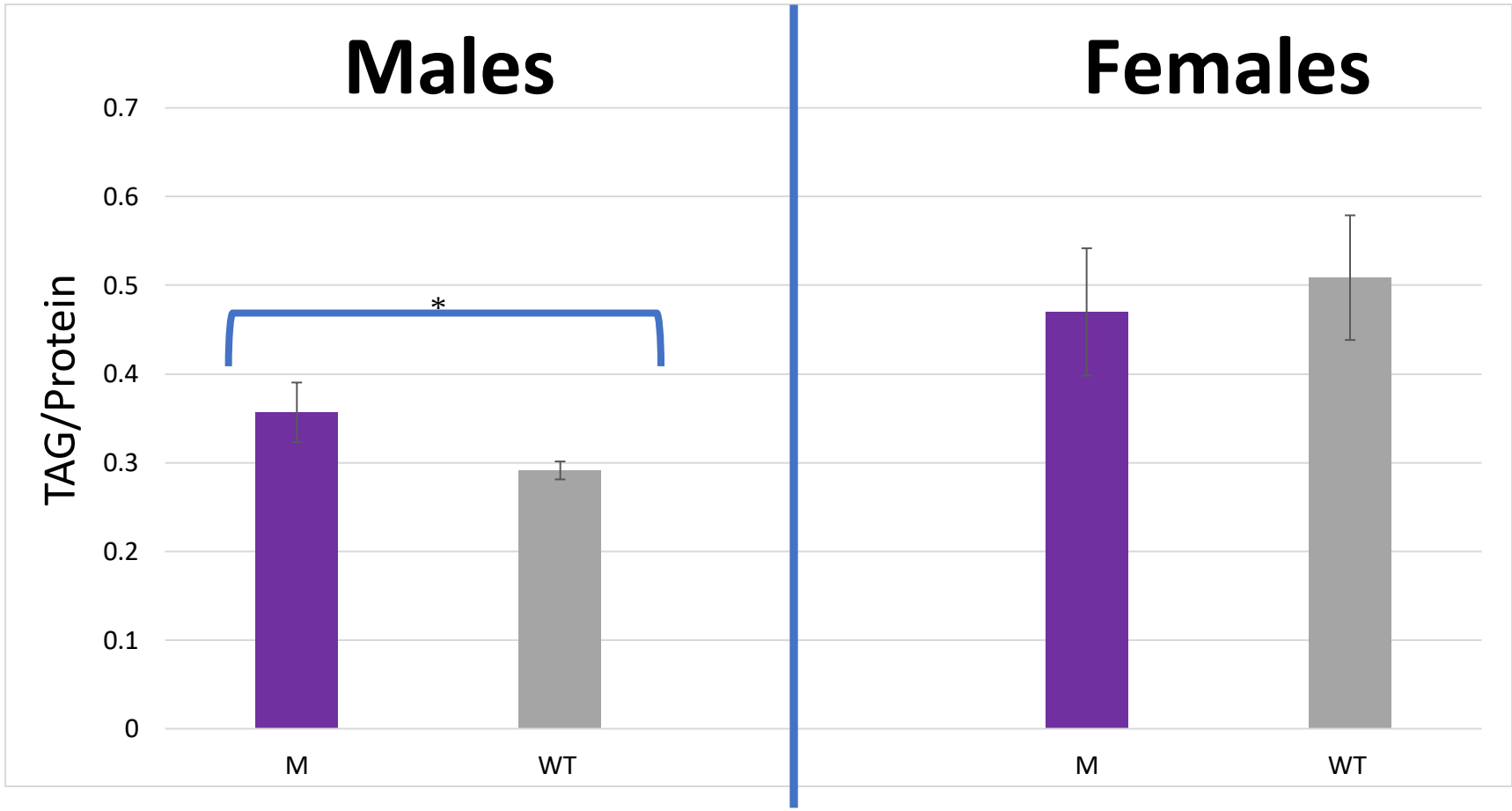

Fig 29. Triglyceride/total protein ratio of Lipin Group 1 mutants. Lipin Group 1 (purple) males have an elevated TAG/protein ratio compared to control (gray) males. Student's t-test, p = 0.032. Lipin Group 1 and control females have similar TAG/protein ratios. Error bars: SD.

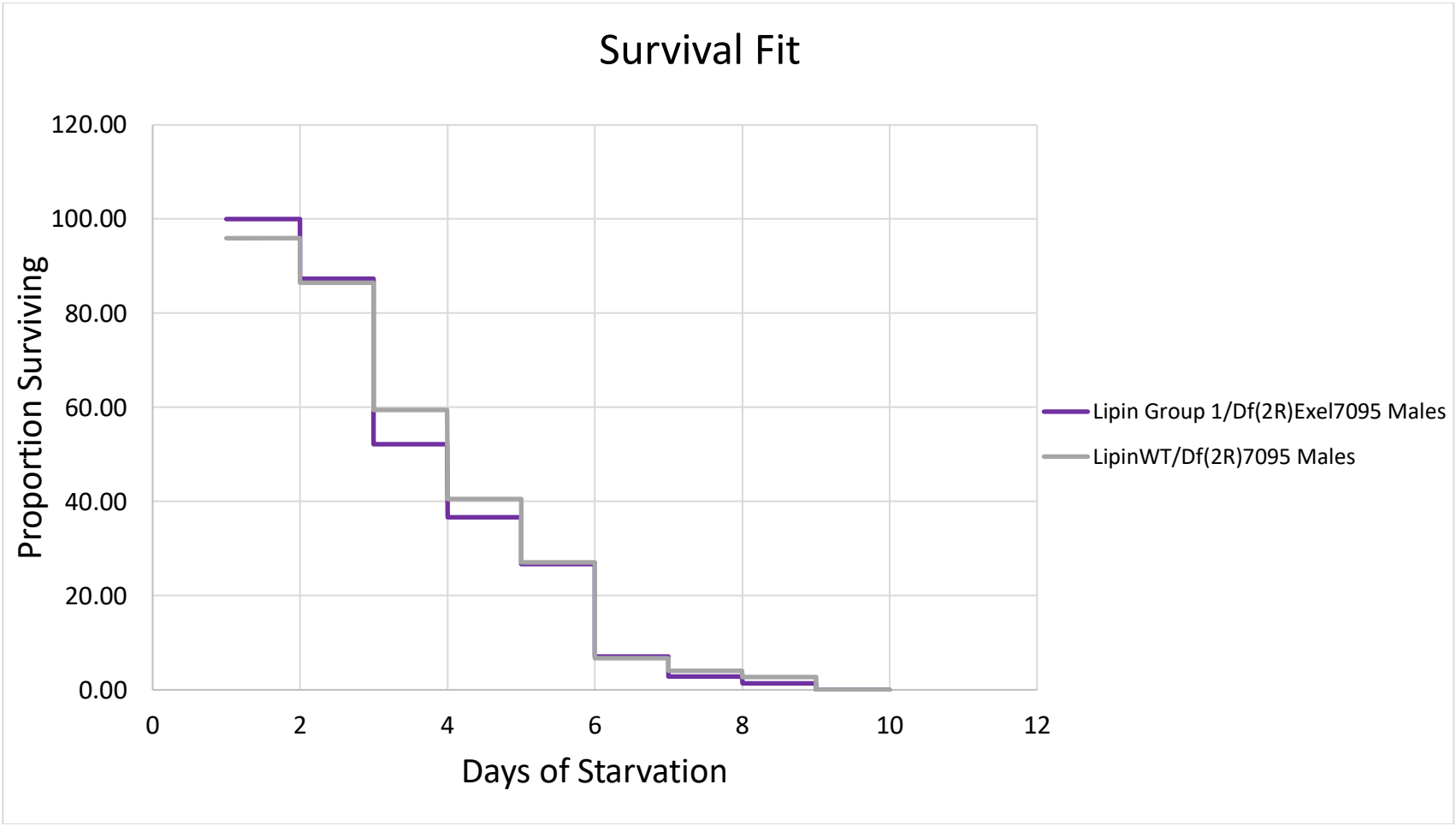

Fig 30. Starvation resistance of Lipin Group 1 mutant males. Lipin Group 1 (purple) flies have a similar resistance to starvation as control flies (gray). Differences are not statistically significant.

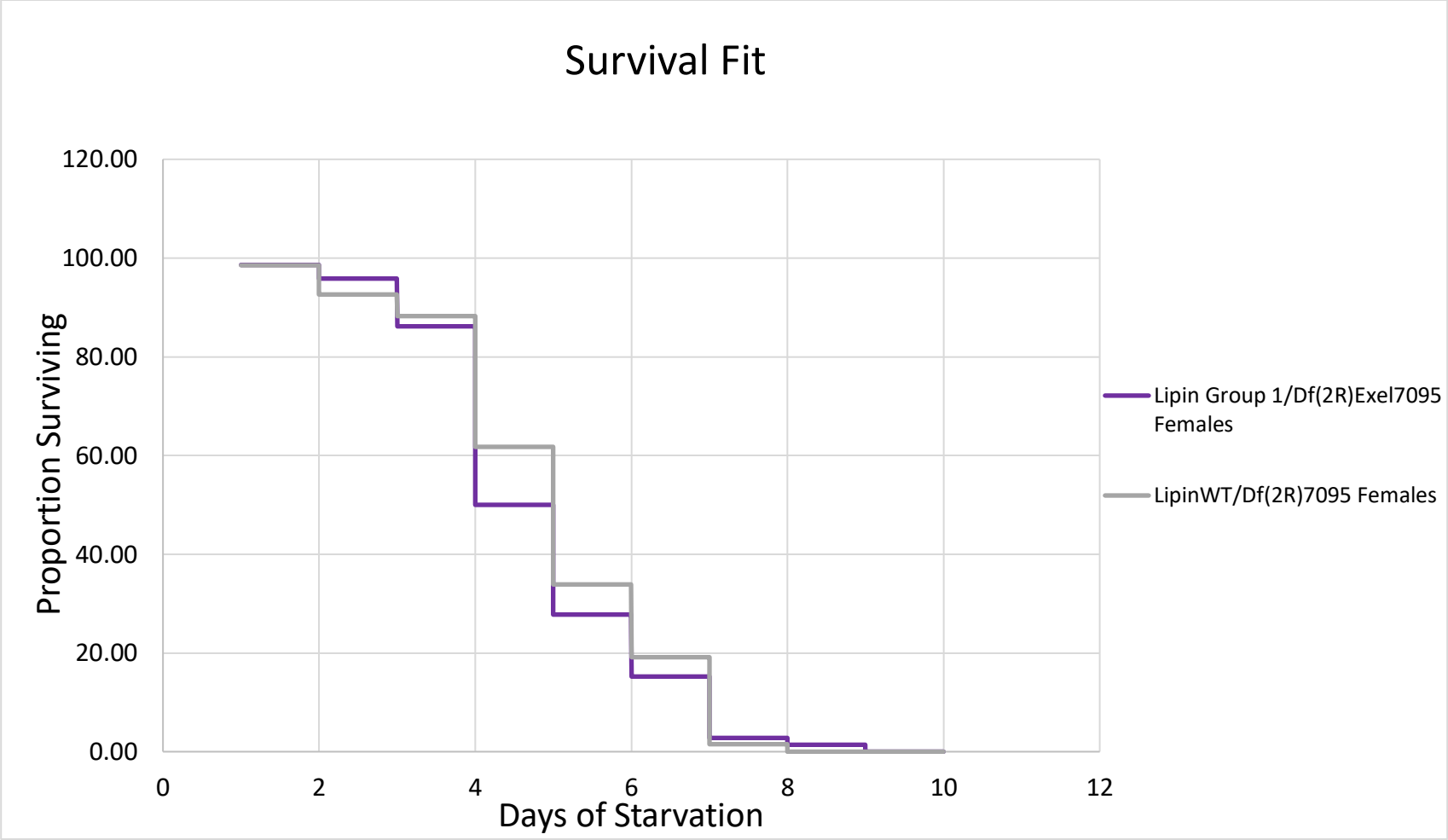

Fig 31. Starvation resistance of Lipin Group 1 mutant females. Lipin Group 1 (purple) flies have a similar resistance to starvation as control flies (gray). Differences are not statistically significant.

2c. Lipin Group 2 S/T>A mutant

The putative phosphosites of Lipin Group 2 are predicted to be phosphorylated by MAP kinases (Fig. 4). MAP kinases mediate mitogenic effects and are key regulators in cell growth and proliferation (Vinayagam et al., 2016). These serine/threonine residues, therefore, may have functional importance for the regulation of Lipin.

A mutant containing amino acid substitutions at all but the last 2 putative serine/threonine phosphorylation sites of *Drosophila* Lipin Group 2 was generated. Serine and threonine residues target here included: S356, T364, T366, S367, T385, S403, T404, S408, and S410. The Lipin Group 2 mutant is both homozygous viable and viable over the Lipin deficiency.

i. Developmental timing experiments

Lipin Group 2 mutants show no delays in development timing. Pupariation rates show no significant differences to the control (Fig. 32). No delay in eclosion or significant pupal lethality could be observed. Sample size: n (Group 2) = 20; n (control) = 20.

ii. Fat droplet staining

Cell size and shape were similar between the control and experimental animals (Fig. 33). However, BODIPY 493/503 staining appeared stronger in the Lipin Group 2 mutant.

iii. Lipin antibody staining

Lipin Group 2 mutant fat body showed a higher level of antibody staining than the control fat body (Fig. 34). Lipin staining was cytoplasmic in both the experimental and control animals.

iv. Triglyceride and Protein assays

Analysis of Lipin Group 2 mutants revealed no significant differences in the TAG/protein ratios for either male or female animals compared to the control (Fig. 35).

v. Starvation assays

Males of the mutant background displayed a statistically significant decrease in starvation resistance compared to the control animals (Fig. 36). Lipin Group 2 mutant and control females, however, showed no statistically significant differences in starvation resistance (Fig. 37).

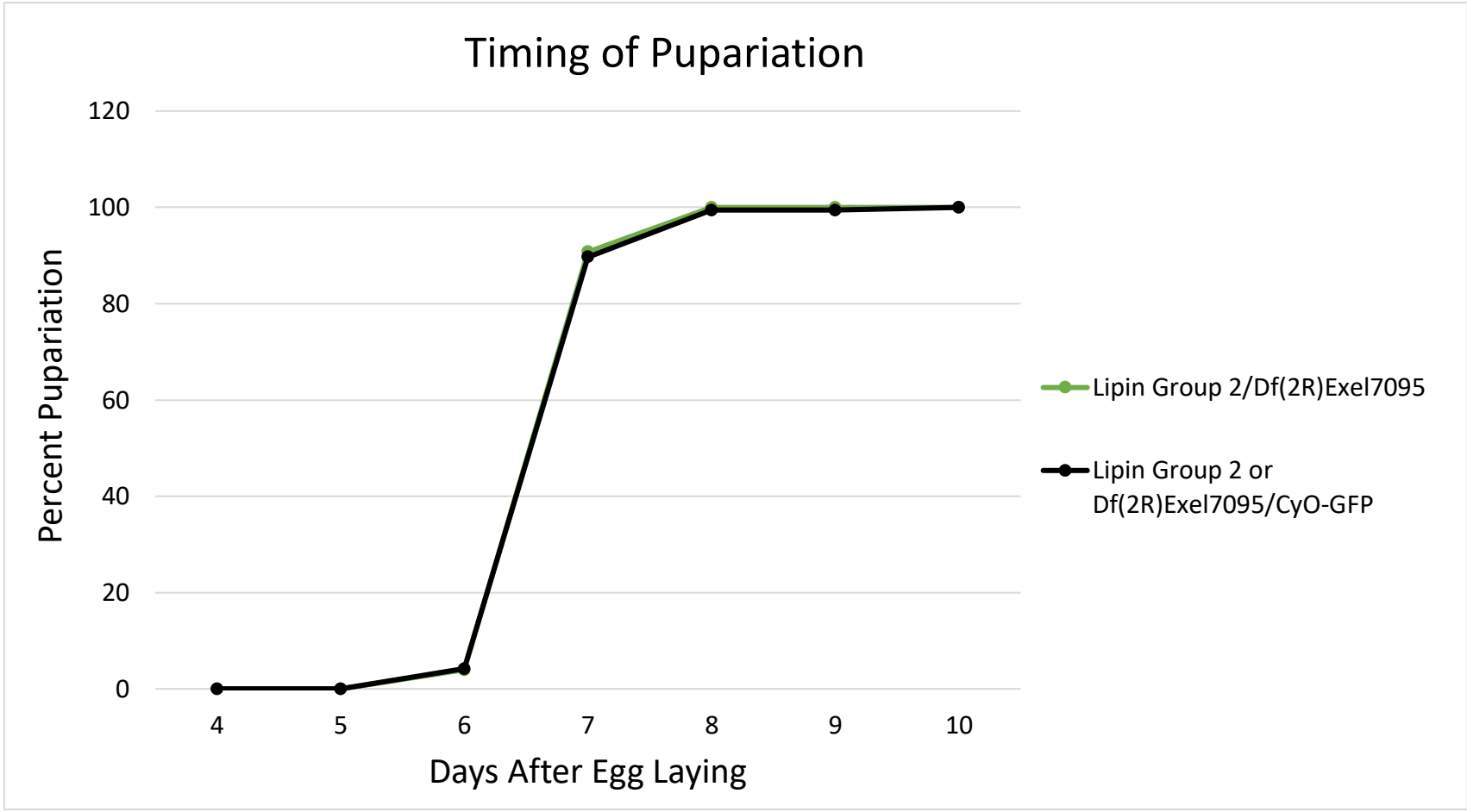

Fig 32. Timing of pupariation for Lipin Group 2 mutants. Lipin Group 2 (green) animals pupariate at the same rate as the internal control (black). Differences are not statistically significant.

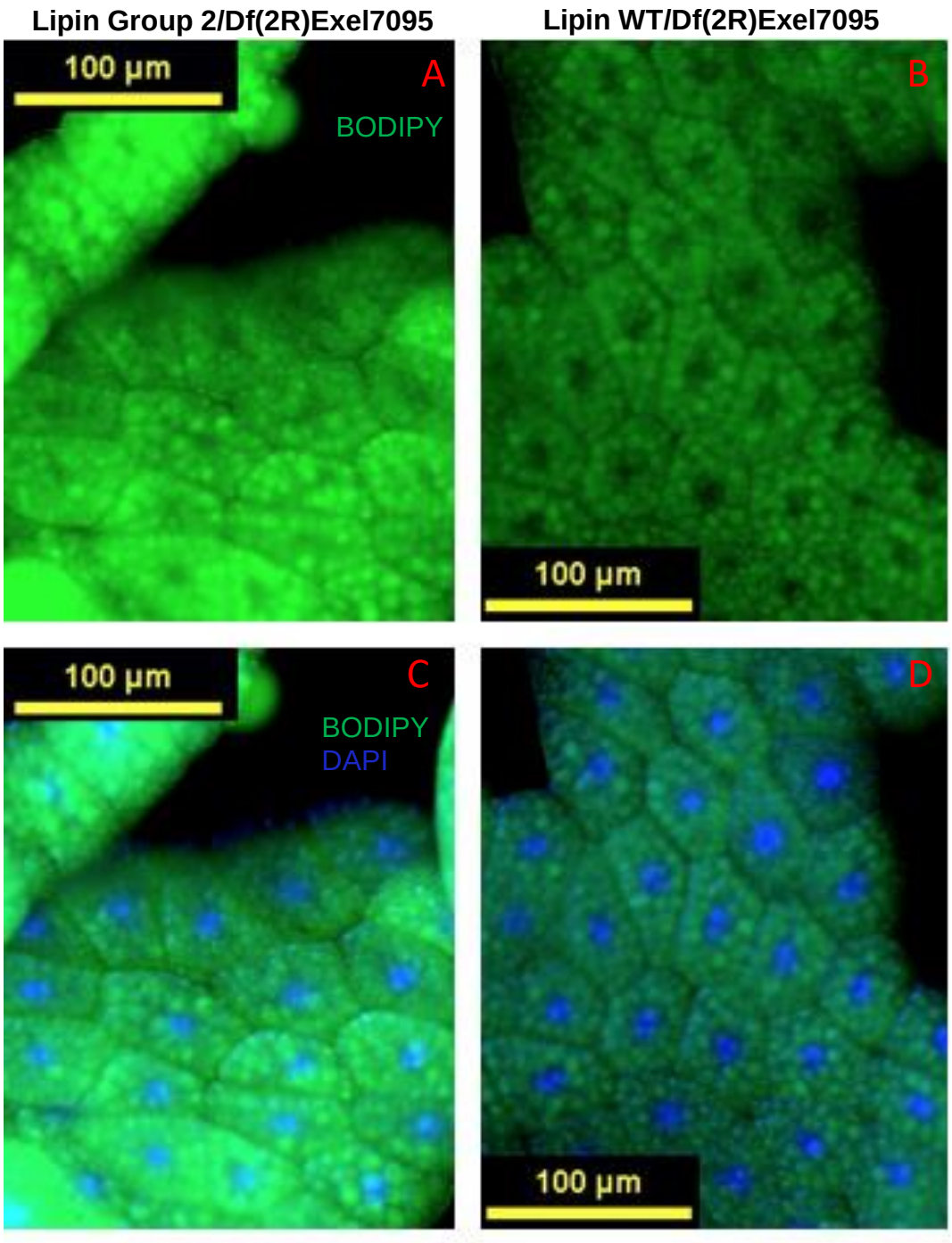

Fig 33. BODIPY 493/503 staining of Lipin Group 2 mutant fat body. Lipin Group 2 animals (A and C) have similar amounts of fat body when compared to the control animals, (B and D). Animals have comparable cell size. Intensity of the staining, however, appears more prominent in the experimental genotype.

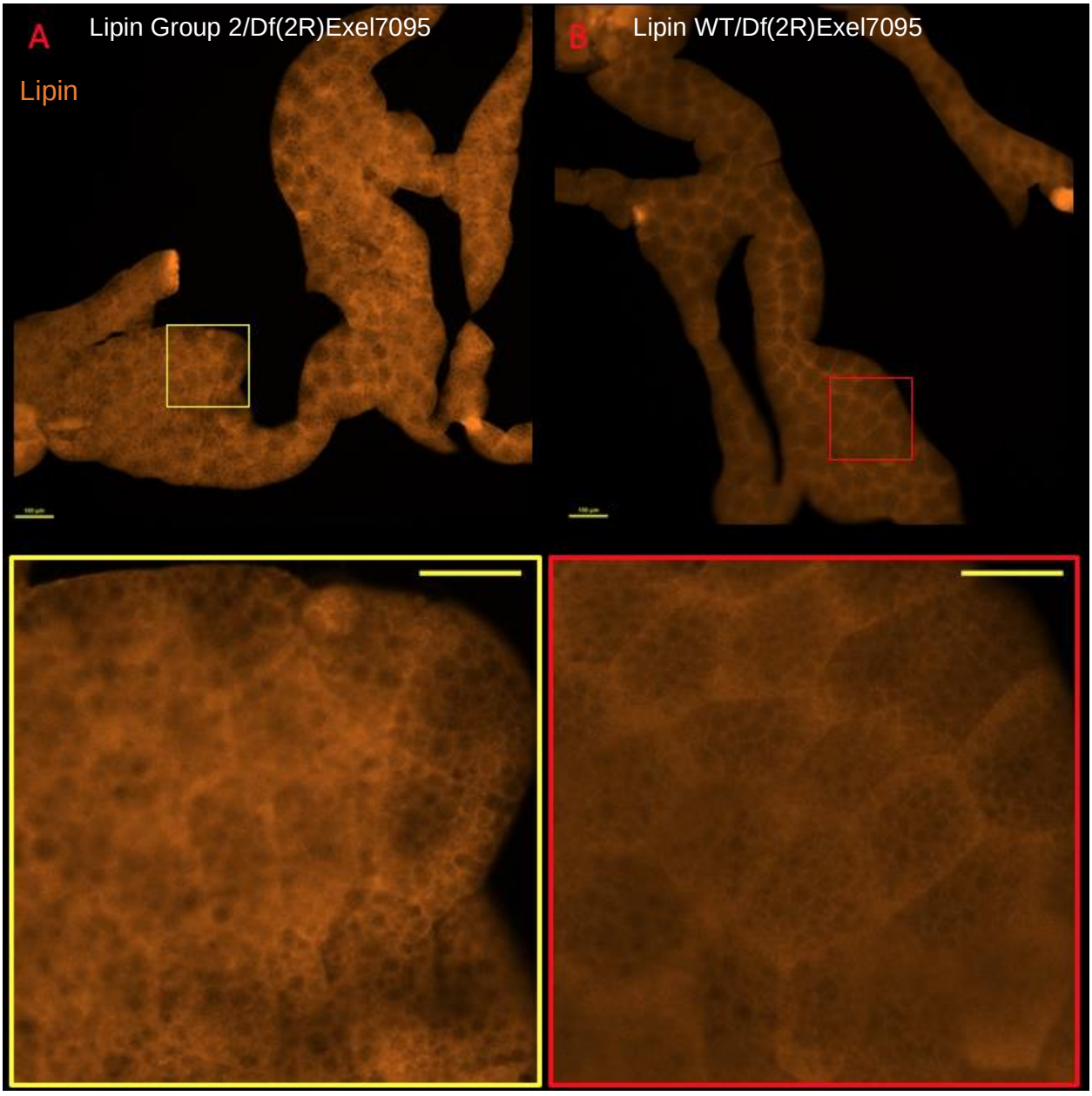

Fig 34. Lipin Antibody Staining of Lipin Group 2 mutant fat body. Lipin Group 2 animals (A) show an increased expression of Lipin compared to the control (B). Protein expression for all animals is predominantly cytoplasmic. Colored boxes indicate zoomed images. Scale bar zoomed images = 50 μm.

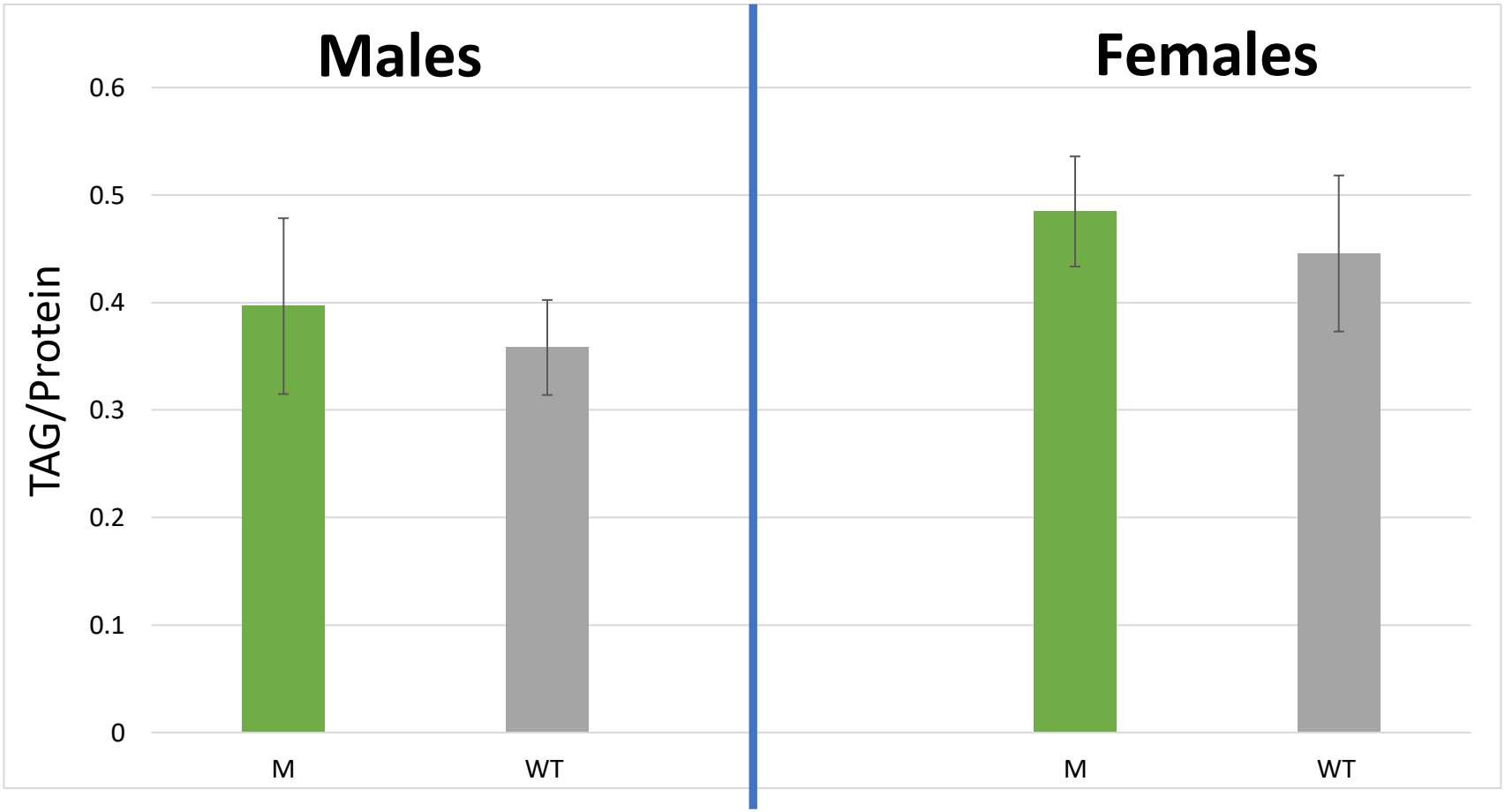

Fig 35. Triglyceride/total protein ratio of Lipin Group 2 mutants. Lipin Group 2 (green) males and females have comparable TAG/protein ratios to the control animals (gray). Differences are not statistically significant. Error bars: SD.

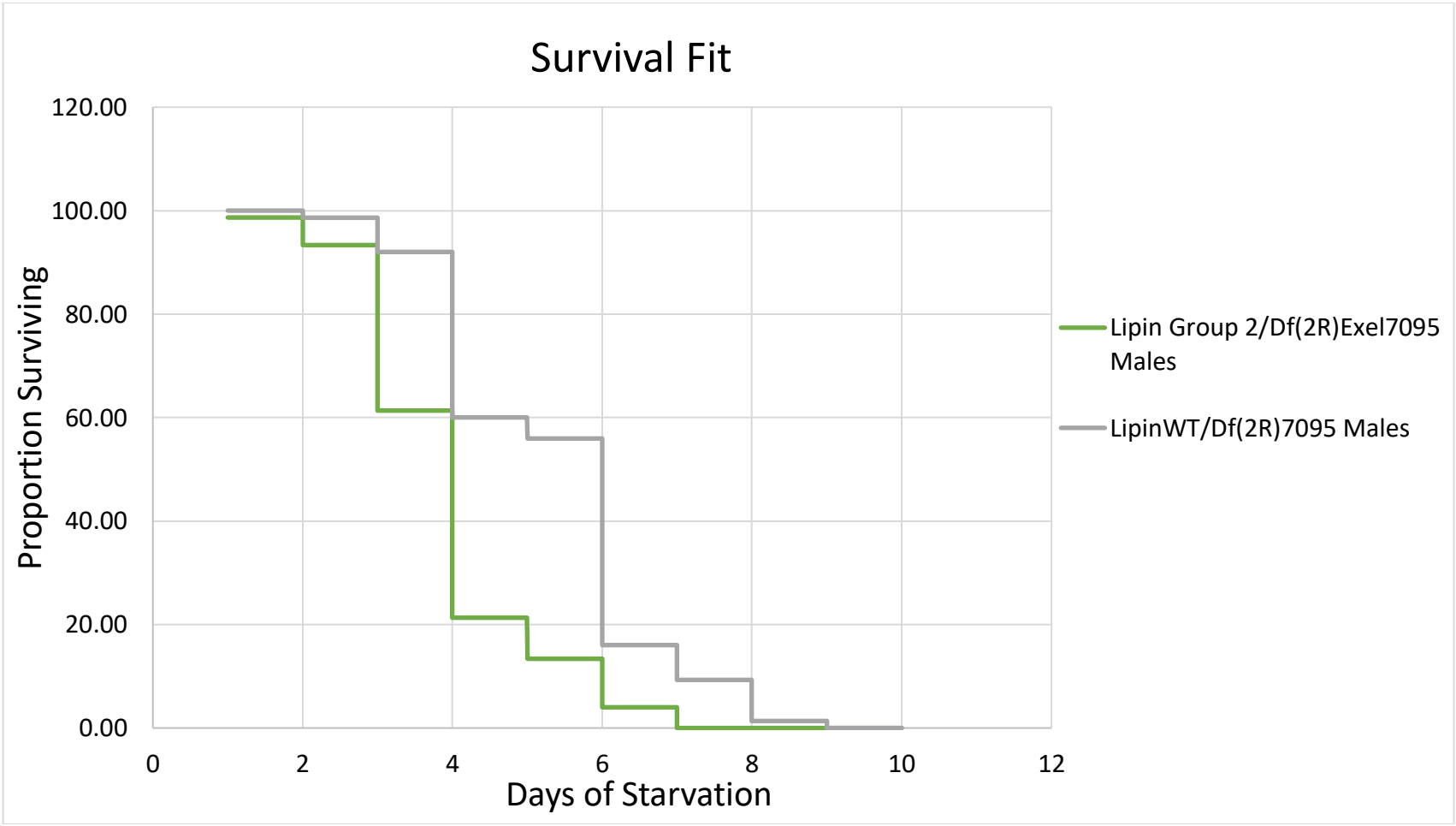

Fig 36. Starvation resistance of Lipin Group 2 mutant males. Lipin Group 2 (green) flies have less resistance to starvation than the control flies. Log-rank, $p < 0.0001$.

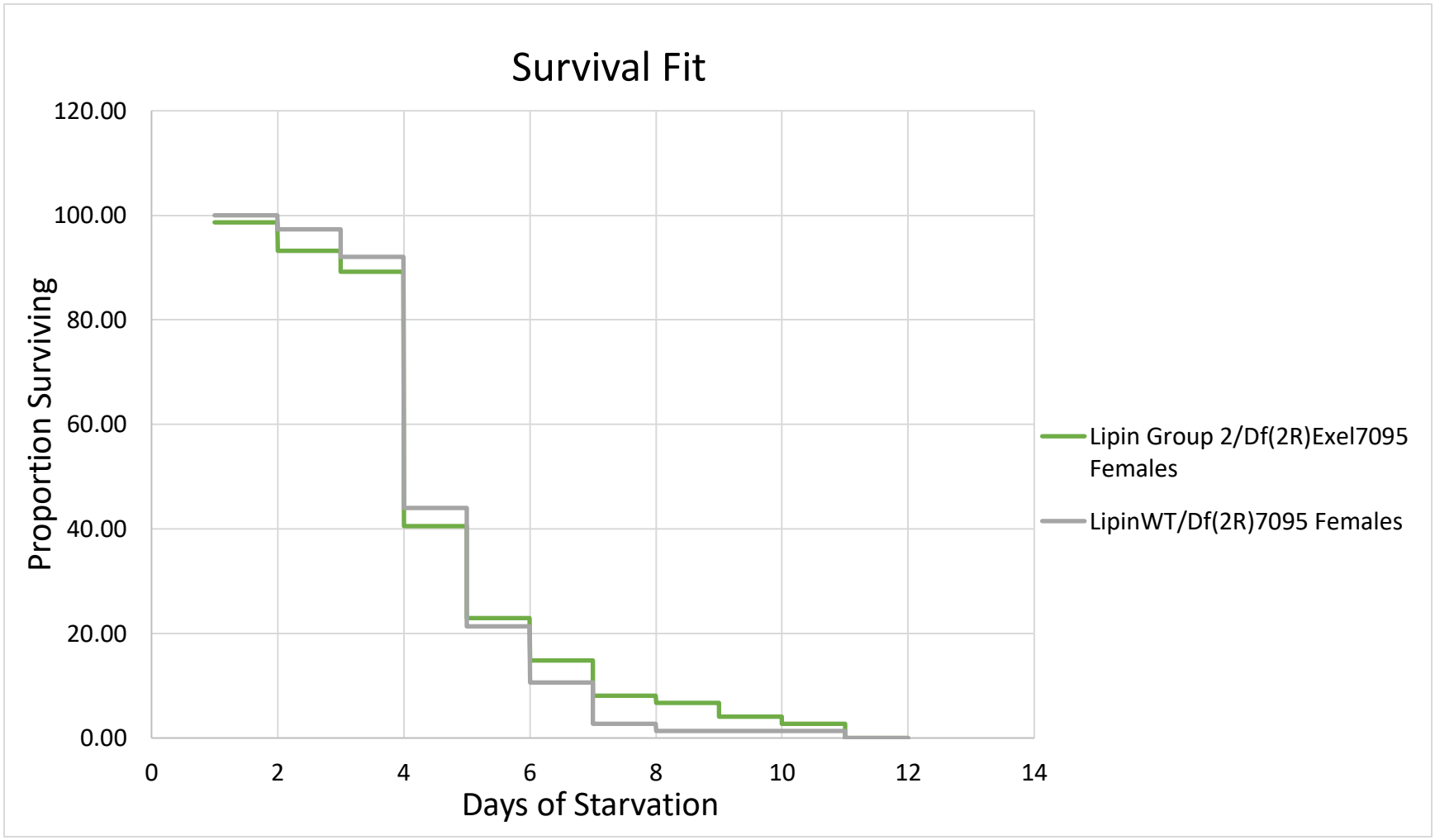

Fig 37. Starvation resistance of Lipin Group 2 mutant females. Lipin Group 2 (green) flies have a similar resistance to starvation as control flies (gray). Differences are not statistically significant.

2d. Lipin S820A

Amino acid residue S820 was of particular interest as it resides in the CLIP domain of the *Drosophila* Lipin protein and it is homologous to the residue at site S720 in mouse lipin1b. S820 is situated between the catalytic and transcriptional co-regulator motifs and therefore was suspected to be functionally important for the regulation of the protein.

The Lipin S820A mutant was not homozygous viable. However, Lipin S820A/Df(2R)Exel7095 animals were viable. These results indicate that lethality of the homozygotes was not caused by the Lipin allele but by homozygosity for a secondary site mutation on the mutagenized chromosome. Viability of animals carrying the Lipin S820A allele over the Lipin deficiency verifies that a single copy of Lipin S820A is sufficient for survival.

i. Developmental timing experiments

Developmental timing experiments for the Lipin S820A mutant showed a slight but statistically significant delay in pupariation (Fig. 38). There appeared to be no delay in eclosion or significant pupal lethality. Sample size: n (S820A) = 20; n (control) = 20.

ii. Fat droplet staining

BODIPY 493/503 staining of Lipin S820A mutants did not show any apparent differences in cell shape or size as compared to control animals (Fig. 39). Additionally, the number and size of fat droplets were similar between the animals.

iii. Lipin antibody staining

Increased levels of Lipin antibody staining were seen in Lipin S820A animals (Fig. 40). Fat body tissue appeared to have higher intensity and more homogenous Lipin staining in the Lipin S820A animals compared to the control. Lipin subsided in the cytoplasm in the experimental and control animals.

iv. Triglyceride and Protein assays

Lipin S820A males have similar ratios of TAG/protein as the control males (Fig. 41). However, Lipin S820A males have statistically significant differences in both the mean TAG (Fig. 42) and mean protein (Fig. 43) content per sample compared to wild-type animals.

Lipin S820A females, show a statistically significant decrease in TAG production compared to control females (Fig. 41). Mutant females also display a statistically significant decrease in mean TAG per sample when compared to the control females (Fig. 42).

v. Starvation assays

Starvation assays were completed for animals with Lipin S820A males and females. Mutant males and females both showed statistically significant decreases in starvation resistance as compared to the controls (Fig. 44 and Fig. 45), respectively.

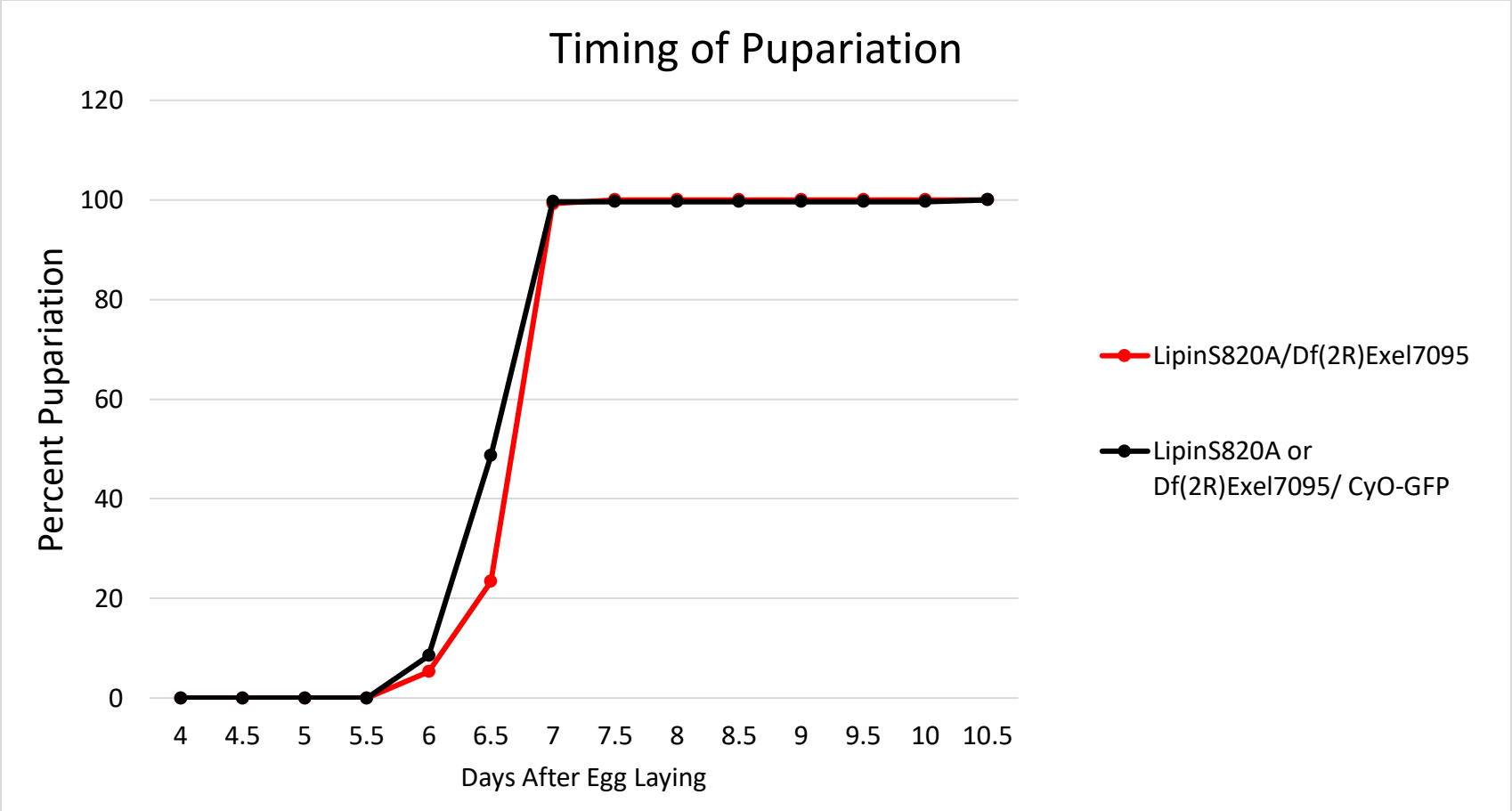

Fig 38. Timing of pupariation for Lipin S820A mutants. Lipin S820A (red) animals pupariate at a delayed rate as compared to the internal control (black). Differences are statistically significant. Log-rank, $p < 0.0001$.

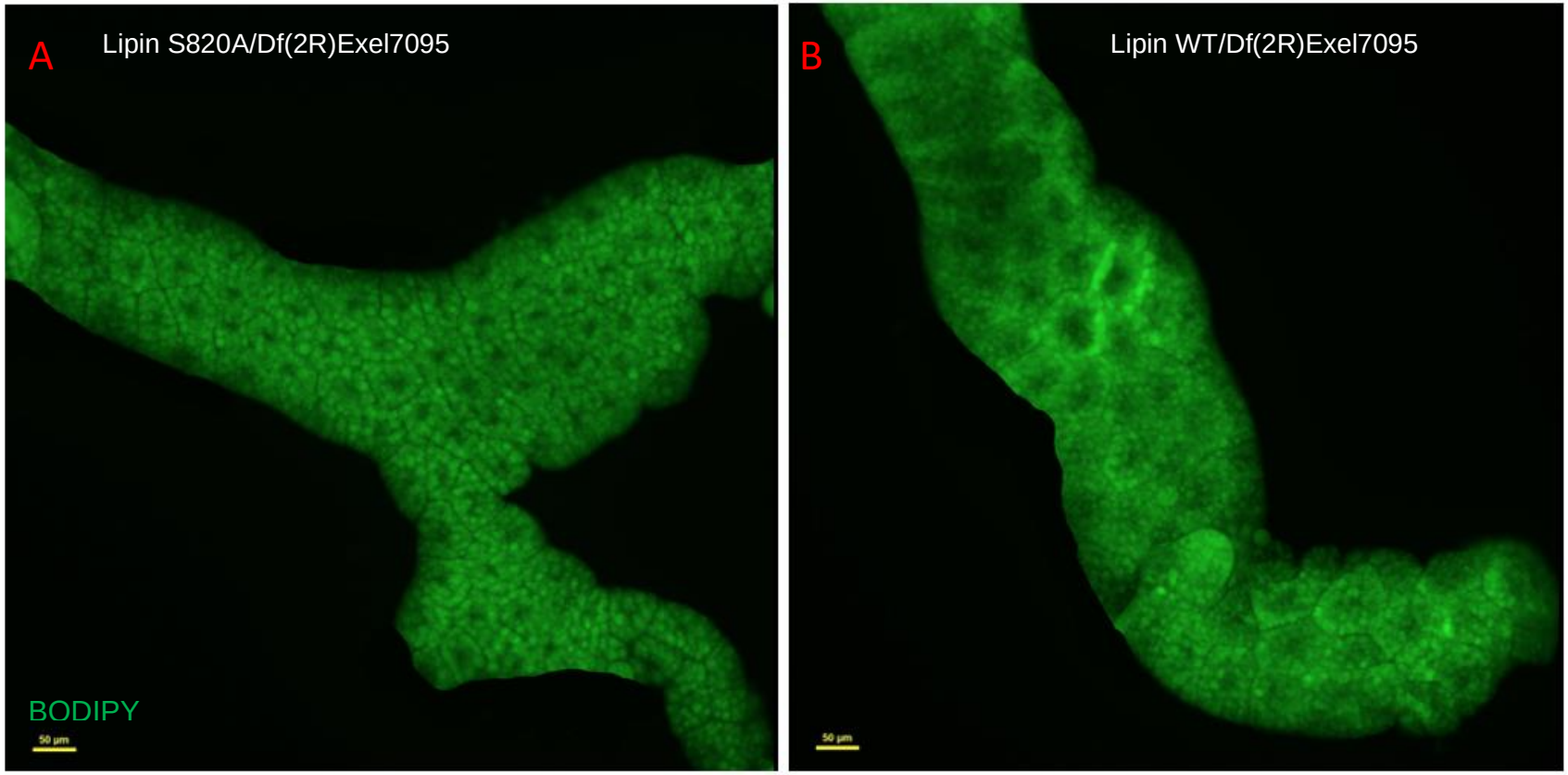

Fig 39. BODIPY 493/503 staining of Lipin S820A mutant fat body. Lipin S820A (A) mutants have similar fat body morphology when compared to the control (B). Animals have equivalent amounts of fat body and have comparable cell size. Scale bar = 50 µm.

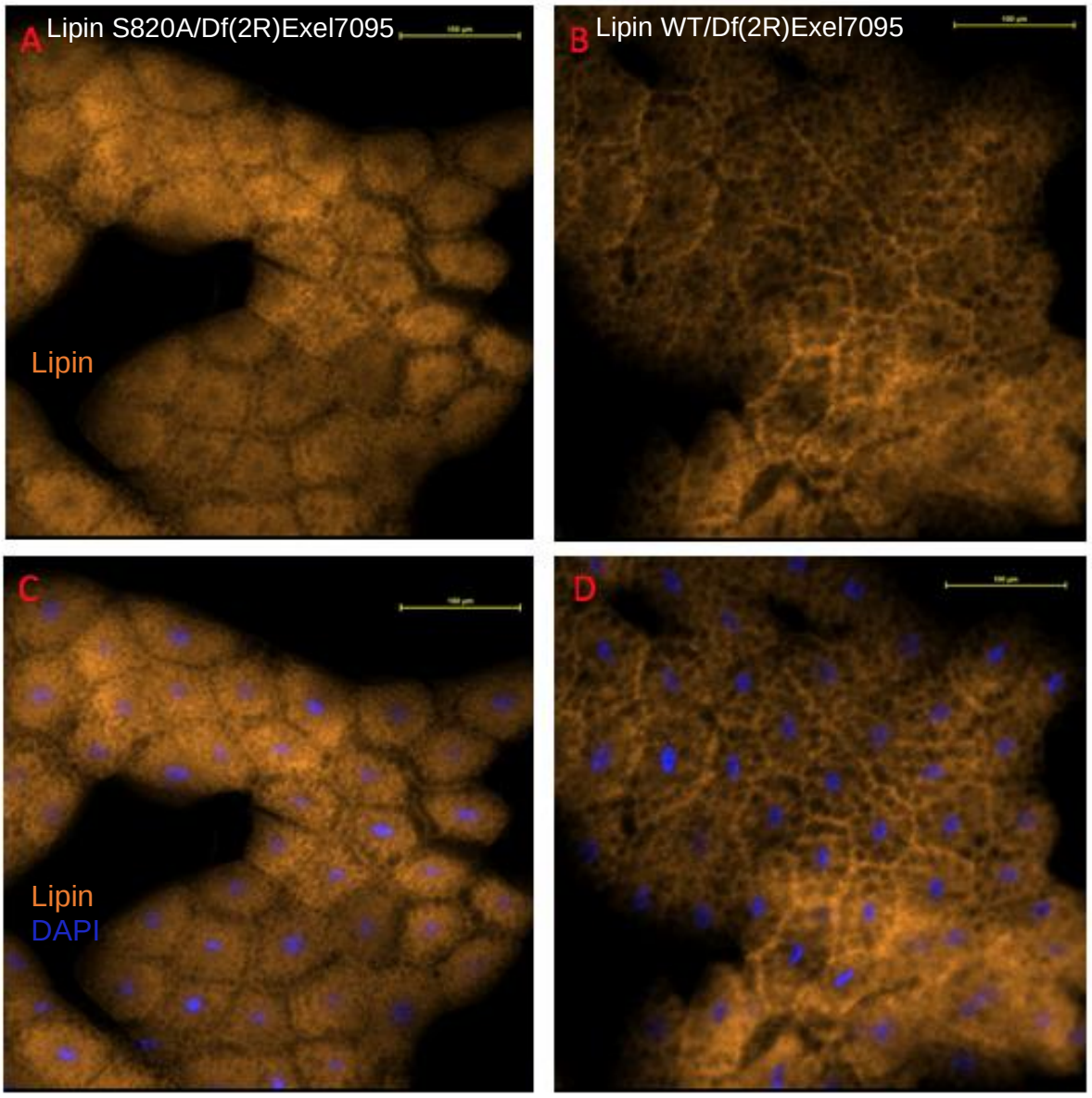

Fig 40. Lipin Antibody Staining of Lipin S820A mutant fat body. Lipin S820A mutants (A/C) have increased expression of Lipin compared to the control (B/D). Nuclear staining: DAPI (Blue). Scale bar = 100 μm.

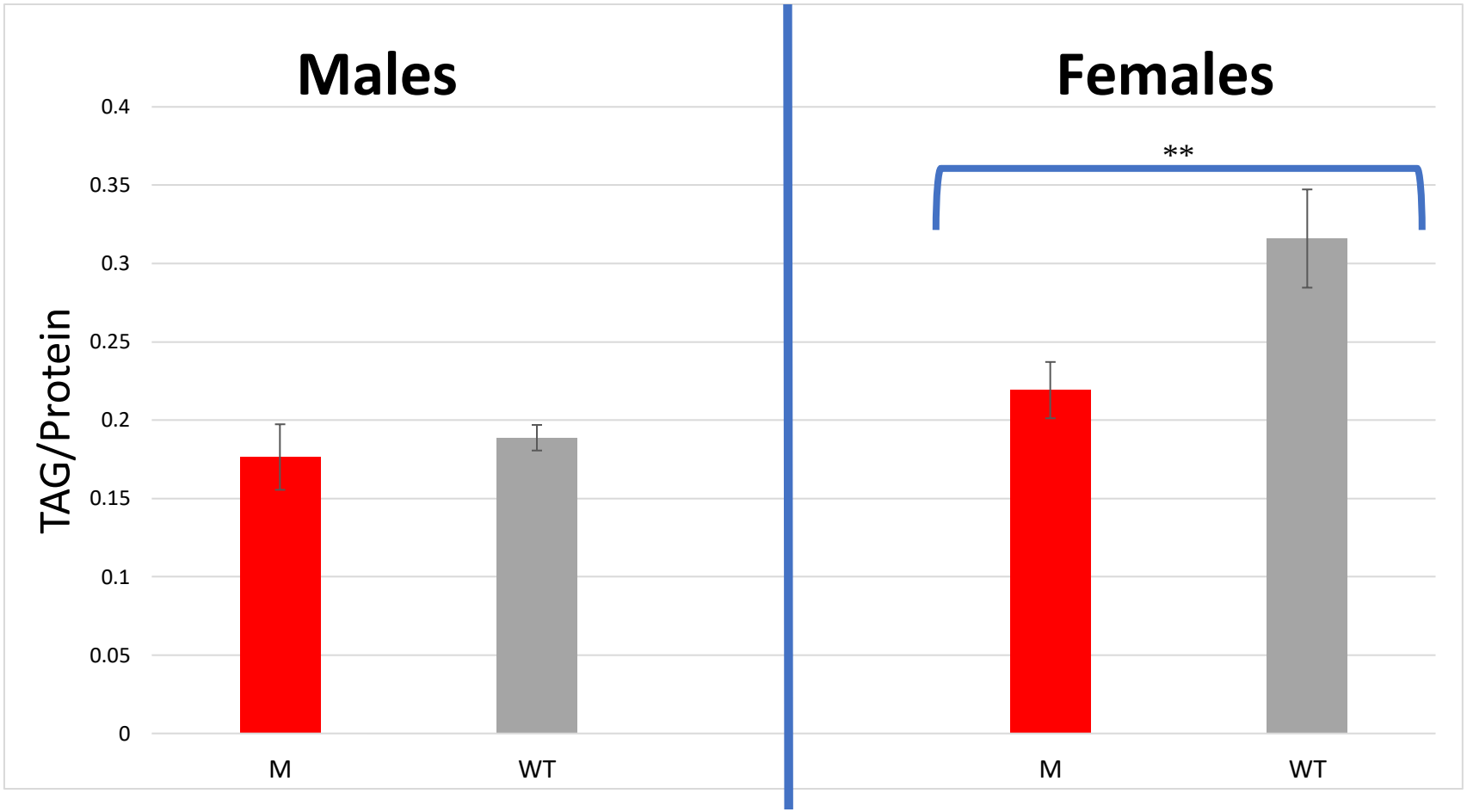

Fig 41. Triglyceride/total protein ratio of Lipin S820A mutants. Lipin S820A (red) females display a statistically significant decrease in TA 40/protein ratio when compared to control females (gray). Student's t-test, p =0.0098. However, Lipin S820A males have a similar TAG/protein ratio when compared to control males. Differences are not statistically significant. Error bars: SD.

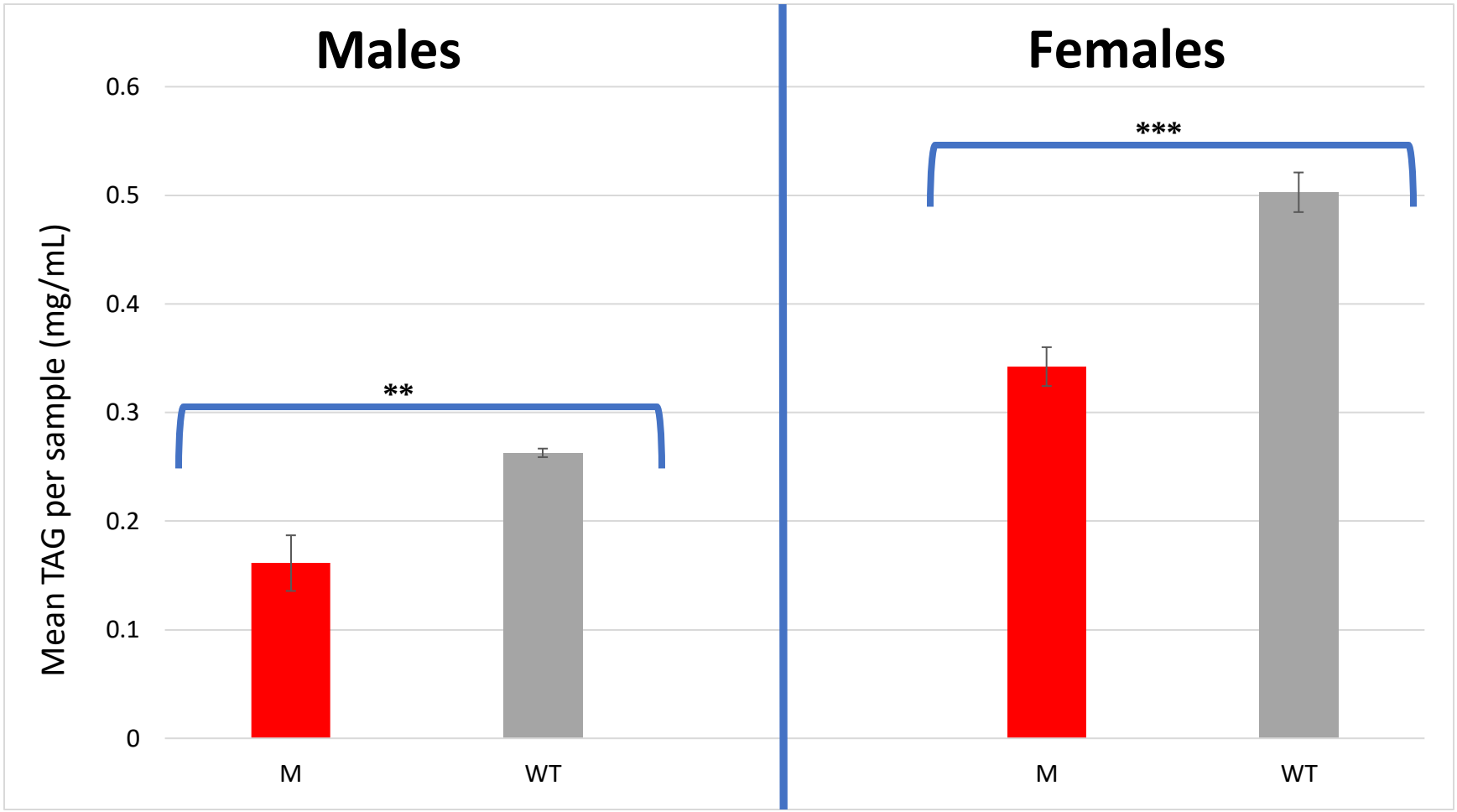

Fig 42. Mean TAG content per sample for Lipin S820A mutants. Lipin S820A (red) males and females have statistically significant lower TAG content than control animals (gray). Student's t-test, p = 0.0025 (males) and p = 0.0005 (females). Error bars: SD.

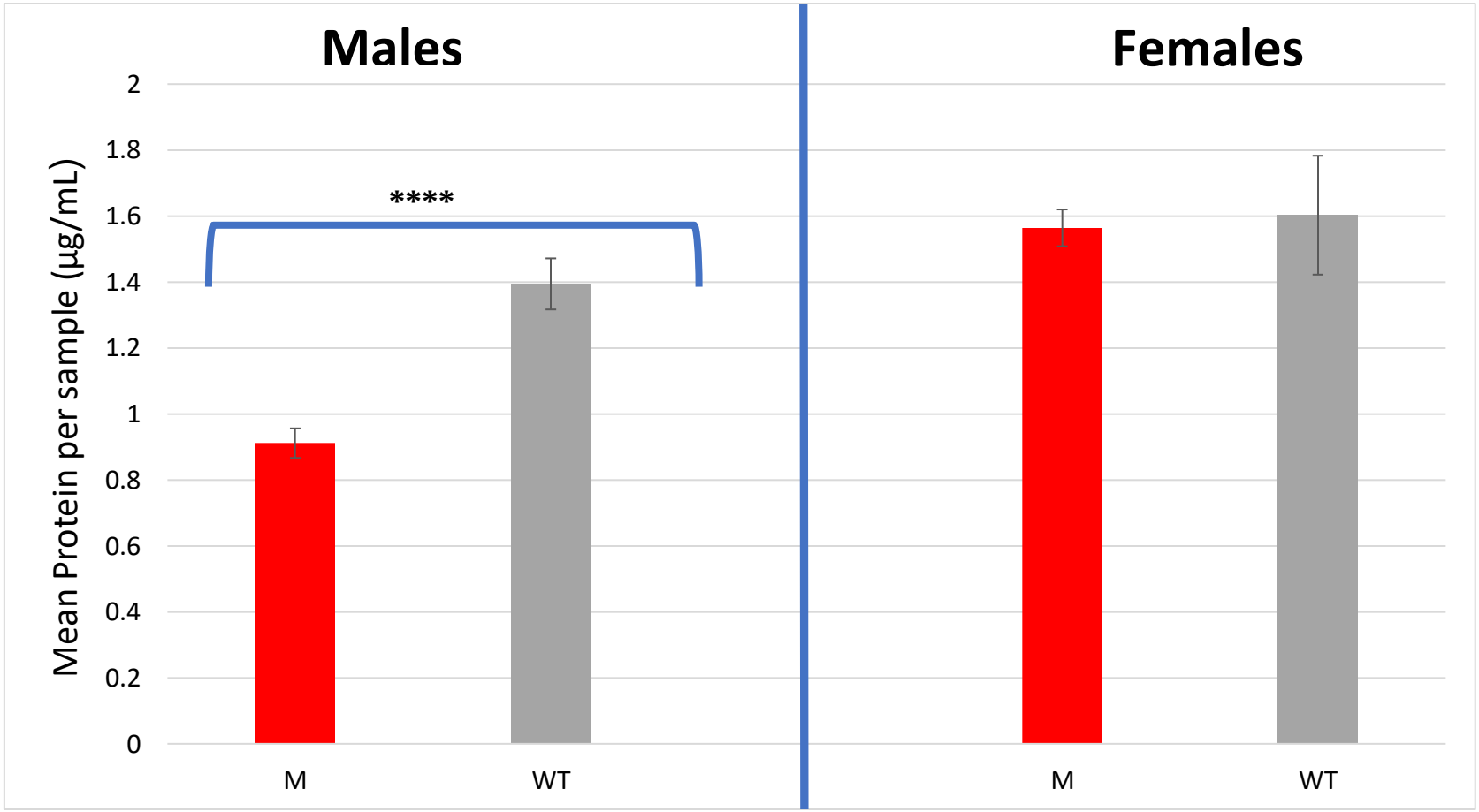

Fig 43. Mean protein content per sample for Lipin S820A mutants. Lipin S820A (red) males show a statistically significant decrease in total protein compared to control males (gray). Student's t-test, p =0.0007 (males). Mean protein content for Lipin S820A females showed no statistically significant differences compared to control females. Error bars: SD.

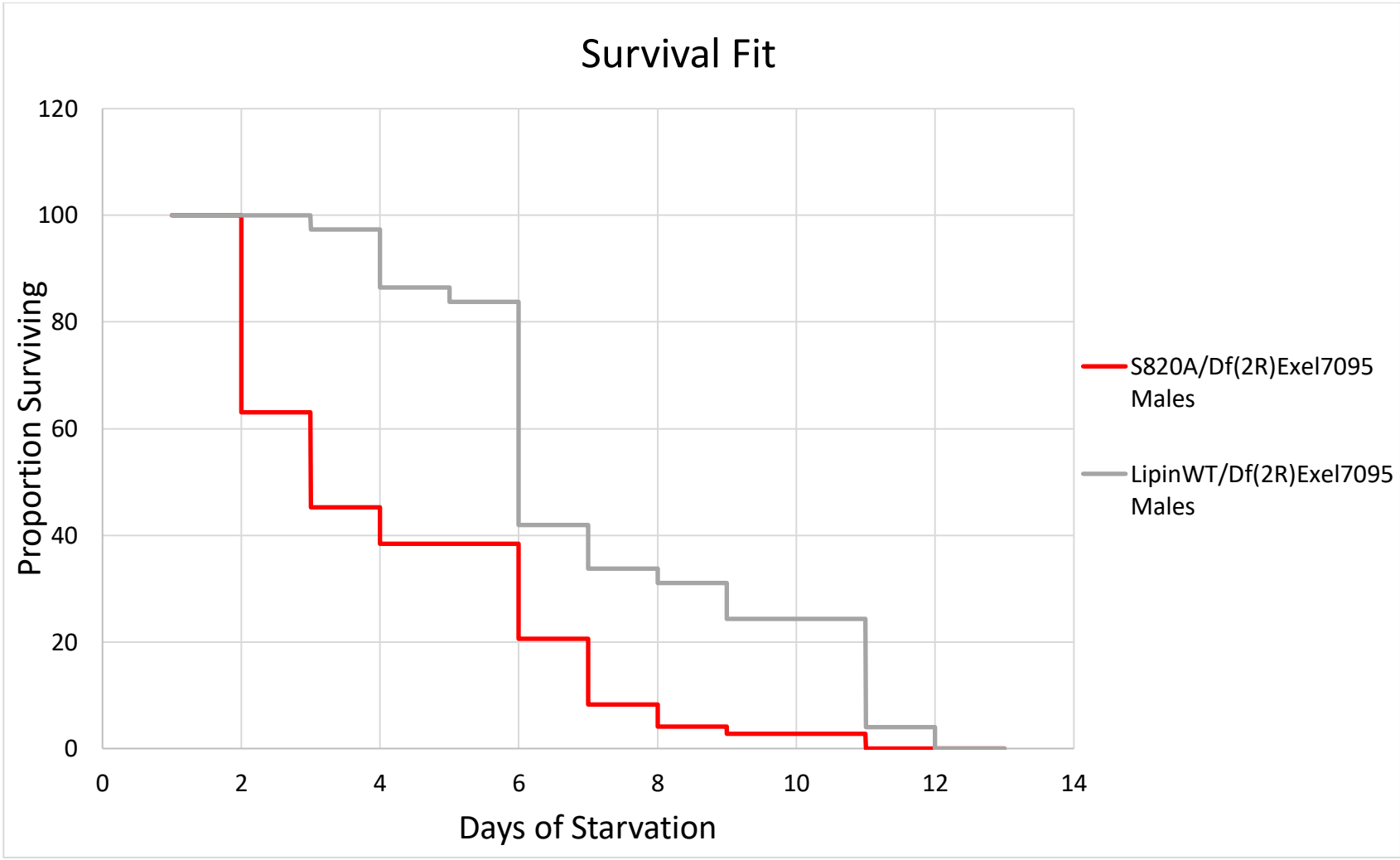

Fig 44. Starvation resistance of Lipin S820A mutant males. Lipin S820A (red) flies have a statistically significant decrease in starvation resistance when compared to the control (gray). Log rank, $p < 0.0001$.

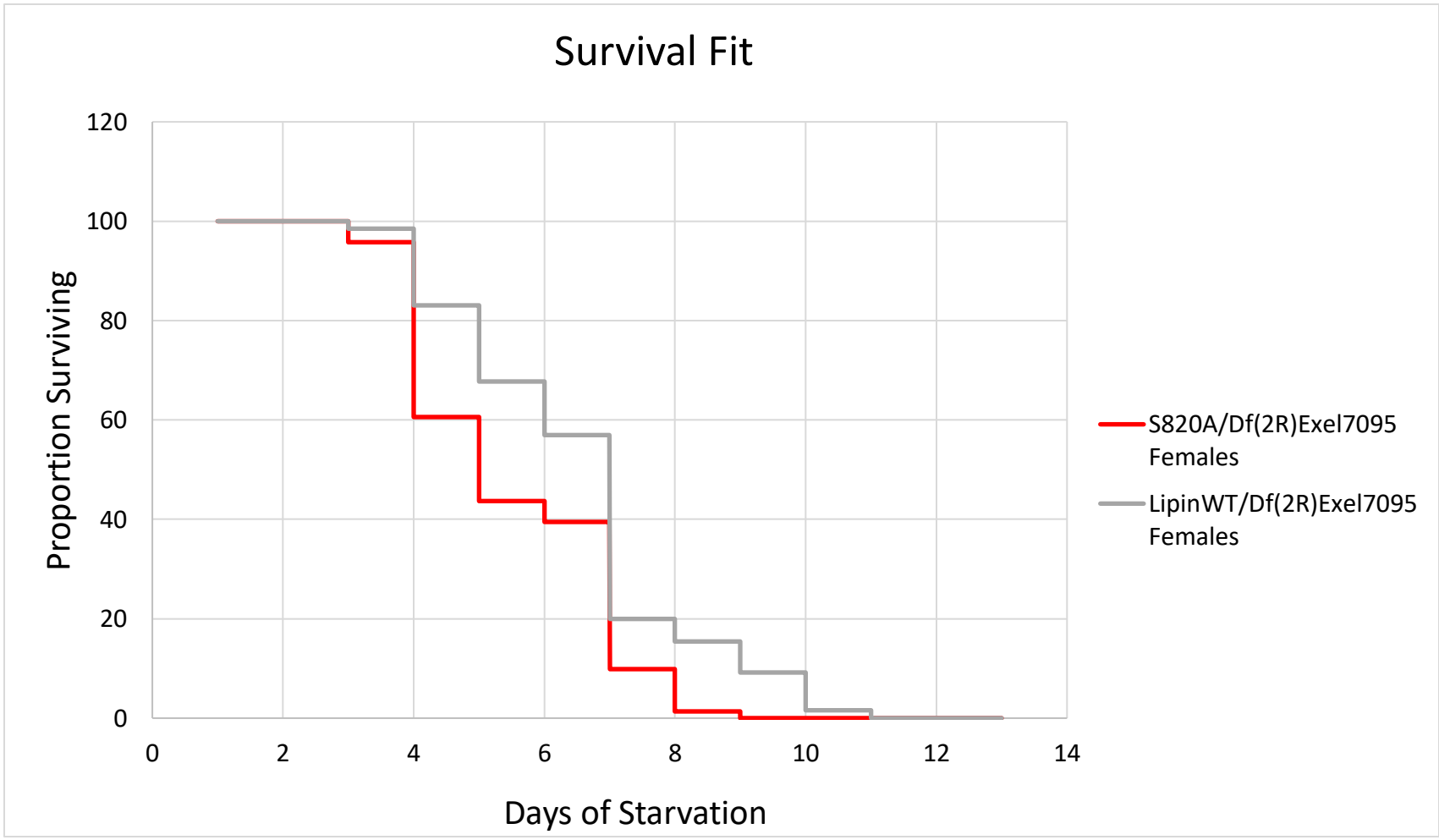

Fig 45. Starvation resistance of Lipin S820A mutant females. Lipin S820A (red) flies have a statistically significant decrease in starvation resistance when compared to the control (gray). Log-rank p <0.0012.

IV. Discussion

1. Characterization of the UAS-Lipin20S/T>A transgenic line

1a. *UAS-Lipin20S/T>A* expression in the fat body results in Lipin loss-of-function phenotype

Lipin is a highly phosphorylated protein containing many serine and threonine phosphorylation sites of unknown importance. Unlike mammalian lipin 1 (Peterson et al., 2011), *Drosophila* Lipin does not translocate into the nucleus when the majority of these serine and threonine phosphorylation sites are exchanged with alanine (Fig. 16). Here, I created a transgenic UAS reporter line, referred to as *Lipin20S/T>A*, where 20 of the 26-presumed serine/threonine phosphorylation sites of *Drosophila* Lipin were rendered non-phosphorylatable. When expressed using the *FB-GAL4* driver these animals had fat body cells which were extremely enlarged. These enlarged fat body cells sometimes contained two nuclei, experienced loss of cell adhesion, had minimal expression of Lipin, and contained few fat droplets (Fig. 16 & Fig. 15). The phenotypes displayed by animals with ectopic expression of *Lipin20S/T>A* in the fat body are similar to those of a Lipin loss-of-function mutant, which displays severely reduced fat body mass and fat droplet size (Ugrankar et al., 2011).

While the large fat body cells with ectopic expression of *Lipin20S/T>A* displayed minimal Lipin staining, clusters of small cells surrounding the fat body contained considerable amounts of Lipin (Fig. 16, A/C). Given the intensity of the Lipin antibody staining, these small surrounding cells are likely fat body cells which contain almost no cytoplasm, concentrating the protein. This phenotype has previously been observed in Lipin hypomorphic mutants, $dLipin_{e00680}$/ $dLipin_{e00680}$ (Ugrankar et al., 2011).

In addition to the dramatic decrease in the fat body amount, the larval size was severely reduced when *Lipin20S/T>A* was expressed in the fat body (Fig. 14). However, despite stunted

growth and reduced fat body, these animals were still able to pupariate. However, pupariation was delayed. Experimental animals began to pupariate 10 days after egg laying as compared to the control which began pupariation at day 7 (Fig. 13). Pupariation occurred later than normal in the control animals, which was likely due to overcrowding. Since the experimental conditions were the same for both genotypes, this experiment was not repeated. However, in the future, the developmental timing crosses should be set up with less animals to avoid overcrowding the vials. Since there was a small number of experimental animals which pupariated, they were collected to see if eclosion would occur. Of the pupae collected, only 23% eclosed, indicating a high percentage of pupal lethality.

Because there was such a robust phenotype when *Lipin20S/T>A* was driven by the *FB-GAL4* driver, a relatively strong fat body driver, additional experiments were performed to see if *Lipin20S/T>A* would translocate to the nucleus if expressed with a weaker driver. The *da-GAL4* driver was chosen as a weaker, ubiquitous driver, and could be used to express *Lipin20S/T>A* throughout the entire animal at lower levels. Lower, ubiquitous expression of the *Lipin20S/T>A* did not result in a loss-of-function phenotype. Lipin antibody staining revealed that fat body was similar in size, shape, and quantity when compared to the control (Fig. 17). Increased nuclear staining could not be observed. Use of a stronger ubiquitous driver, such as a tubulin driver, may yield different results.

Furthermore, the *Lsp-GAL4* driver, a fat body driver which is switched on specifically in 3rd instar larvae, was also chosen for additional experimentation. Since *Lipin20 S/T>A* would not be expressed until larvae enter their final stage before pupariation, animals would have normal functioning endogenous Lipin until they were done feeding. Despite fat body specific expression, these animals expressing *Lipin20S/T>A* under the control of the *Lsp-GAL4* driver lacked any

noticeable phenotype when compared to the control animals (Fig. 17). This result suggests that ectopic expression of *Lipin20S/T>A* in the fat body during later larval stages does not seem to impact development. Again, increased nuclear localization of Lipin could not be observed.

1b. Ectopic expression of *UAS-Lipin20S/T*>A results in a dominant-negative effect

Expression of a Lipin protein that constitutively localized to the nucleus was the motivation to create the *UAS Lipin20S/T>A* transgenic line. Previous experiments done using mammalian cell culture were successful in creating a nuclear form of Lipin (Peterson et al., 2011). In this mutant version of mammalian lipin 1, 17 serine/threonine phosphosites had been exchanged with alanine, rendering these sites non-phosphorylatable. The Lipin17 S/T>A mutant protein showed robust nuclear translocation in mammalian cell culture. The aim here was to recreate this affect with *Drosophila* Lipin to help better understand the nuclear function of Lipin and to learn how phosphorylation regulates the subcellular localization of Lipin. However, when *Lipin20 S/T>A* is expressed in the fat body of *Drosophila* during development, the animals experience a loss-of-function phenotype.

While the Lipin proteins of both mice and *Drosophila* have a similar distribution of phosphorylation sites (Fig. 4), there are still differences in both the distribution and number of these amino acid residues and, thus, possibly, their potential functions. It is possible that an amino acid residue or cluster of residues essential for the PAP function of Lipin in *Drosophila* were rendered non-phosphorylatable in these experiments, thus resulting in a Lipin loss-of-function phenotype. While these animals still express endogenous Lipin, the ectopic expression of *Lipin20 S/T>A* appears to exhibit a dominant negative effect. A dominant negative effect occurs when a mutant form of a protein forms an oligomer with the wild-type protein, altering the function of the protein. It has been previously shown in mammalians that lipin proteins self-

associate and exist predominately as stable homo and hetero oligomers (Liu et al., 2010). Induced mutations to mammalian lipin 1 did not affect the ability of the mutant to form oligomers (Liu et al., 2010). Thus, it seems likely that *Lipin20 S/T>A* could also from oligomers with the endogenous Lipin protein, resulting in a Lipin loss-of-function phenotype.

It was shown here that ectopic expression of *Lipin20 S/T>A* does not lead to nuclear translocation of Lipin (Fig. 16). Rather, these experiments demonstrated that at least some of the phosphorylatable amino acid residues of Lipin are essential for proper Lipin function. To further investigate the functional roles of Lipin phosphorylation, and in an additional effort to create a constitutively nuclear form of Lipin, mutants of individual and clusters of these putative phosphorylation sites were created using CRISPR/Cas9 mutagenesis.

2. Characterization and Analysis of Lipin Phosphosite Mutants

2a. Subcellular localization may be impacted in Lipin phosphosite mutants

The goal in creating these phosphosite mutants was to determine the functional importance of Lipin phosphorylation. The primary function of Lipin under normal feeding conditions is in triglyceride synthesis and in providing precursors for membrane lipids. Creating a subset of mutants that lack or mimic putative phosphorylation site(s) could provide valuable knowledge to better understanding the role that phosphorylation of Lipin has in energy homeostasis.

Nuclear translocation of *Drosophila* Lipin could not observed in any of the Lipin phosphosite mutants created here. It is known that serine/threonine phosphorylation of lipin 1 in response to insulin prompts the protein to translocate away from the ER membrane and out of the nucleus into the soluble fraction. However, it is dephosphorylation by unknown protein phosphatases that is responsible for directing lipin 1 to the nucleus or ER compartments (Harris et al., 2011). As increased nuclear localization of the mutant protein was not observed in any of the phosphosite mutants, it may be possible that these phosphorylation sites are targets of phosphatases responsible to shuttle the protein to the ER for fat droplet synthesis rather than being responsible for the nuclear localization of Lipin. Thus, these animals with S/T>A mutations may have lost their ability to disassociate from the ER as a result of the introduced mutations. Co-staining with an ER antibody and the Lipin antibody could verify this hypothesis as intracytosolic changes in Lipin localization are subtle (Liu et al., 2010).

Although there were no apparent differences in subcellular localization of the mutant protein in the Lipin antibody staining presented here, the images still provide important information. Antibody staining reveal increased intensity of mutant protein expression for all the

observed phosphosite mutants. The protein expression levels appeared more robust and homogenous in the mutant animals which should be further investigated. Increased Lipin expression levels may be a consequence of the decreased degradation of the mutant protein as a consequence of decreased phosphorylation of the mutant proteins (Kaushik et al., 2016). Western blot analysis should be done to confirm the increases in the protein levels seen with the antibody staining. Additionally, improved optical approaches are likely to help indicate any subtle differences that may have been overlooked. Confocal microscopy could provide higher resolution images that could help better indicate the subcellular localization of the mutant protein.

Additionally, expression levels of Lipin 1 are hypothesized to influence fat droplet size and number in mammals and lipins are predicted to aid in expanding fat droplet size in later adipogenesis. This requirement for lipins in lipid droplet biogenesis could result from the role lipins have in phospholipid metabolism (Sembongi et al., 2013). ER structure could be altered if the membrane composition is changed due to altered expression of lipins and could therefore effect the formation of lipid droplets at the ER, leading to an increase in lipid droplet formation. Initial examination of the fat body morphology of all the Lipin phosphosite mutants appeared apparently similar to the corresponding control animals. However, in two of the mutants, Lipin Group 1 and Lipin Group 2, fat droplet staining revealed increased levels of staining (Fig. 27 & Fig. 33). As BODIPY stains for neutral fats, these data suggest that the mutant animals may contain more fat within each fat body cell compared to the control. However, triglyceride assays do not support this hypothesis. Only Lipin Group 1 males experience a statistically significant increase in TAG levels when compared to Lipin wild-type males (Fig. 29). Additional assays, such as a buoyancy-based density assays could be done to determine if there is a difference in the

amount of fat body between the mutant animals and the control (Hazegh et al., 2016). Again, use of higher resolution microscopy may also be helpful in evaluating the BODIPY 493/503 staining. Higher resolution images would allow for measurements of individual fat droplets and could be used to quantify any differences suggested by the lower resolution images.

Finally, it should be noted that the use of LipinWT/Df(2R)Exel7095 animals may not have been the best choice for the control animals for the staining experiments. As was seen with the developmental timing experiments, the internal controls served as a better control than the LipinWT/Df(2R)Exel7095 animals which may also be the case here. Additional control stains should be considered for the BODIPY 493/503 and the Lipin antibody staining to help resolve any apparent differences.

2b. Phosphorylation impacts starvation resistance in Lipin phosphosite mutants

Knowing that the subcellular localization of Lipin determines the function of Lipin is key to understanding the phenotypes observed in the Lipin phosphosite mutants (Fig. 1). It has been shown previously that when TORC1 is downregulated by starvation or knocked-down by RNAi, there is a robust nuclear translocation of Lipin (Schmitt et al., 2015). Phosphorylation by TORC1 under normal metabolic homeostasis renders Lipin to the cytoplasm. However, there are many other kinases and phosphatases that are suggested to have functional importance for the regulation of Lipin and that could impact the subcellular localization of the protein. Many of the Lipin phosphosite mutants presented here exhibit differences in starvation resistance that may be explained by the subcellular localization of the protein. A statistically significant increase in starvation resistance was only seen in one of the phosphosite mutants: Lipin S147A females (Fig. 25). In contrast, statistically significant decreases in tolerance to starvation were seen in Lipin

S147E males (Fig. 24), Lipin Group 2 males (Fig. 36), and Lipin S820A males (Fig. 44) and females (Fig. 45).

The reduction of TAG levels may explain the reduced ability to withstand starvation for the Lipin S820A mutants (see section IV.2d: Functional importance of conserved Serine residue S820) (Fig. 42). However, for the additional phosphosite mutants presented, the inability to tolerate starvation is more likely a consequence of the subcellular localization of Lipin, rather than having to do with the total TAG levels of the animals. If Lipin is prevented from translocating into the nucleus, it cannot work as a transcriptional co-regulator where it helps in the transcription of metabolic genes. Therefore, regardless of the amount of Lipin available, if it is unable to translocate to the cell nucleus, it cannot work aid in gene regulation. The Lipin S147A females, which show a slightly higher resistance to starvation (Fig. 25), may have a more robust translocation of Lipin into the nucleus during starvation. Additionally, since Lipin S147E males display a statistically significant decrease in the ability to withstand starvation (Fig. 24), it is possible that by rendering the S147 phosphosite to glutamic acid that the ability for this mutant form of Lipin to enter the nucleus is reduced.

As phosphorylation is known to impact the subcellular localization of Lipin, it is possible that these phosphosite mutants are impaired in their ability to change subcellular localization (as described in section 4B.1). Additionally, it may be possible that Lipin is still able to translocate to the nucleus during times of starvation, however, the protein may have experienced a conformational change as a result of the mutation(s) that may impact how it binds to other transcription factors. Additional experiments to examine changes in subcellular localization of the mutant Lipin proteins during times of starvation should be done to address these possibilities.

2c. Effects of ectopic Akt expression in Lipin S147A mutants

Phosphorylation by TOR renders Lipin to the cytoplasm during fed conditions (Peterson et al., 2011; Schmitt et al., 2015). However, other serine/threonine protein kinases and phosphatases may also control the regulation of Lipin. One subset of kinases that are predicted to be involved in the regulation of Lipin are the insulin-sensitive kinases. Akt is an insulin-sensitive kinase that is responsible for the phosphorylation of FOXO in both mammals and *Drosophila* (DiAngelo et al., 2009). *Drosophila* Lipin has two amino acid residues that are putative targets of Akt including the serine residue at amino acid 147 and 1073 (Bridon et al., 2012).

To determine if Lipin site S147 is of functional importance, a Lipin S147A and Lipin S147E mutant were constructed. Lipin S147A was created to study the effects when this site was rendered non-phosphorylatable and Lipin S147E was made to study the site when made phosphomimetic. However, these mutants did not show altered TAG/protein ratios (Fig. 22). These data suggest that while Lipin site S147 may be a target of Akt, it is not required for Lipin to respond to Akt signaling.

Since there was no indication of any statistically significant differences in the TAG levels in the Lipin S147 mutant animals (Fig. 22), this prompted additional experiments to verify if amino acid residue S147 was only sensitive to high PI3K/Akt activity. Animals which expressed constitutively active Akt in both a Lipin S147A and Lipin wild-type background were generated using the GAL4/UAS system. Like the Lipin Sl47A mutants expressing normal levels of Akt, animals that expressed constitutively active Akt in the Lipin Sl47A background did not have a TAG/protein ratio that was statistically different from that of the corresponding control animals (Fig. 23).

Lipin S147A mutants expressing active Akt in the fat body were then compared to mutants expressing normal levels of Akt. Lipin S147A males, but not females, expressing constitutively active Akt had a statistically significant increase ratio of TAG/protein (Fig. 23). Lipin S147A males expressing constitutively active Akt showed a clear increase in TAG production. This result did not support the hypothesis that the S147 site was required for proper responses of Lipin to insulin-Akt signaling. Animals of all genotypes showed a response to the ectopic Akt expression (Fig. 23), which is consistent with previous work where the insulin receptor was activated ectopically, leading to increased triglyceride storage (DiAngelo et al., 2009).

While Lipin S147A males with normal Akt expression showed no differences in tolerance to starvation, the Lipin S147E males showed a strongly decreased starvation resistance (Fig. 24). Reduced starvation resistance cannot be attributed to reduced fat stores, as TAG levels were not different from those of the control males (Fig. 22). Again, while these data do not eliminate site S147 of Lipin as a target of Akt, they suggest that site S147 does not play an essential role in the control of *Drosophila* Lipin by insulin-Akt signaling. Rather, it seems more likely that this site is a target of TOR given that the Lipin S147E mutant males experience such a robust decrease in survival rate when subjected to starvation. This site may act in concert with TOR to render Lipin to the cytoplasm, which may explain the increase in survival rate of the Lipin S147A females (Fig. 25).

To better understand the differences in starvation tolerance seen here between the Lipin S147A and Lipin S147E mutants, subsequent experimentation could be done. As the starvation assays provided the most sensitive results about these mutations, and starvation has been shown to cause nuclear translocation of Lipin (Schmitt et al. 2015), it would be prudent to examine the

fat bodies of starved larvae with both lipin antibody and fat droplet staining. These experiments will help indicate the subcellular localization of the mutant protein during times of starvation and any apparent changes in fat droplet morphology as a result of nutrient deprivation.

2d. Functional importance of conserved Serine residue S820

Of the Lipin phosphosite mutants examined only one mutant, Lipin S820A, showed a small, but statistically significant, developmental timing delay (Fig. 38). Located in the conserved CLIP domain, this serine residue is homologous to mammalian lipin 1 residue, S720 (Fig. 4). Interestingly, this residue has been identified as being phosphorylated in mouse but not *Drosophila* (Harris et al., 2007). Since serine residue 820 is located within the conserved CLIP domain between the enzymatic (PAP) and transcriptional co-regulator (TRX) motifs of Lipin, the location of the putative phosphorylation site may have functional importance. S820 is just 3 amino acids downstream of the PAP motif and 2 upstream of the TRX motif. Thus, the presence of this residue may be of importance for both functions, PAP and TRX, in Lipin. While the S820 residue in *Drosophila* is homologous to S720 of mammalian lipin 1, lipin 1 in mammals has an additional phosphorylation site, T722, which may also be functionally important. Additionally, proximity to the TRX motif may imply that this residue also functions to control the transcriptional activity of Lipin (Reue, 2009).

Both males and females of the Lipin S820A mutant have decreased tolerance to starvation (Fig. 44 & Fig. 45). This may be caused by lower levels of TAG in the animals (Fig. 42). While there was a statistically significant difference seen in the TAG/protein ration in Lipin S820A mutant females, males had similar ratios of TAG/protein (Fig. 41). Reduction in the overall TAG levels, however, were statistically significant for both sexes (Fig. 42). However, mutant males also have less protein per animal (Fig. 43), suggesting that Lipin S820A males may

have a growth defect and/or a defect in protein synthesis. The presence of a growth defect is supported by an apparent reduction in body weight of the Lipin S820A males, although this decrease was not statistically significant.

To further investigate the functional importance of S820, an additional mutant could be created, Lipin S820E, in which S820 is replaced by a phosphomimetic amino acid residue. The results yielded by the Lipin S820A mutant are likely either a consequence of the inability of S820 to be phosphorylated or a repercussion of introducing an amino acid exchange in a region that may be important for proper folding of the protein in its PAP and TRX domains. Further, a Lipin S820E mutant would be particularly interesting as this site, as previously mentioned, is phosphorylated in mammals but has not been identified as being phosphorylated in *Drosophila*.

V. Summary

Lipin is a dual functioning protein whose function varies based on subcellular localization. During times of sufficient food supply, Lipin works in the cytoplasm as a phosphatidate phosphatase enzyme, required for lipid synthesis. However, during times of starvation, Lipin translocates into the cell nucleus functioning as a transcriptional co-regulator to promote the expression of metabolic genes. What causes this shift in subcellular localization is only partly understood. Phosphorylation of Lipin by serine/threonine kinases is predicted to be one of the major regulators for these changes in protein localization within the cell. In my thesis, I used both the GAL4/UAS system and CRISPR-Cas9 mutagenesis to examine the functional roles of putative phosphorylation sites of the *Drosophila* Lipin protein. My results support the hypothesis that phosphorylation of specific serine and threonine residues of Lipin is of different functional importance. Phosphorylation of these sites can both increase and decrease pupariation rates, starvation resistance, and TAG production. Additionally, increased Lipin protein expression were seen for all Lipin phosphosite mutants. From these data, additional experimentation should include Lipin antibody staining of starved animals, and higher resolution microscopy, such as confocal, to detect subtle differences in fat body morphology and intracellular distribution of the mutant protein.

VI. References

Alfa R, Kim SK. Using *Drosophila* to discover mechanisms underlying type 2 diabetes. 2016. Di Mod Mech 9(4): 365-376.

Bodenmiller B, Campbell D, Gerrits B, Lam H, Jovanovic M, Picotti P, Schlapbach R, Aebersold R. 2008. PhosphoPep—a database of protein phosphorylation sites in model organisms. Nat Biotechnol 26:1339–1340.

Bridon G, Bonneil E, Muratore-Schroeder T, Caron-Lizotte O, Thibault P. 2012. Improvement of phosphoproteome analyses using FAIMS and decision tree fragmentation. application to the insulin signaling pathway in Drosophila melanogaster S2 cells. J Proteome Res 11:927–940.

Cavaliere V, Donati A, Hsouna A, HsuT, Gargiulo G. 2005. dAkt Kinase Controls Follicle Cell Size During *Drosophila* Oogenesis. Dev Dyn 232(3):845-854.

Chen Y, Rui B-B., Tang L-Y, HµC-M. 2015. Lipin Family Proteins- Key Regulators in Lipid Metabolism. Ann Nutr Metab 66:10-18.

Choi H-S, Su W-M, Morgan JM, Han G-S, XuZ, Karanasios E, Siniossoglou S, Carman GM. 2011. Phosphorylation of phosphatidate phosphatase regulates its membrane association and physiological functions in Saccharomyces cerevisiae: identification of SER(602), THR(723), AND SER(744) as the sites phosphorylated by CDC28 (CDK1)-encoded cyclin-dependent kinase. J Biol Chem 286:1486–1498.

Choi H-S, SµW-M, Han G-S, Plote D, XµZ, Carman GM. 2012. Pho85p-Pho80p phosphorylation of yeast Pah1p phosphatidate phosphatase regulates its activity, location, abundance, and function in lipid metabolism. J Biol Chem 287:11290–11301

Csaki LS et al. 2013. Lipins, Lipinopathies, and the Modulation of Cellular Lipid Storage and Signaling. Prog Lipid Res. 52(3):305-316.

DiAngelo JR et al. 2009. Regulation of Fat Cell Mass by Inuslin in *Drosophila melanogaster*. Molecular and Cellular Biology. 29(24): 6341-6352.

Finck BN, Gropler MC, Chen Z, Leone TC, Croce MA, Harris TE, Lawrence JC Jr, Kelly DP. 2006.Lipin 1 is an inducible amplifier of the hepatic PGC-1alpha/PPARalpha regulatory pathway. Cell Metab 4(3):199-210.

Friedman AA, Tucker G, Singh R, Yan D, Vinayagam A, Hu Y, Binari R, Hong P, Sun X, Porto M, Pacifico S, Murali T, Finley RL, Asara JM, Berger B, Perrimon N. 2011. Proteomic and Functional Genomic Landscape of Receptor Tyrosine Kinase and Ras to Extracellular Signal-Regulated Kinase Signaling. Science Signaling 4:rs10–rs10.

Harris TE, Huffman TA, Chi A, Shabanowitz J, Hunt DF, Kumar A, Lawrence JC. 2007. Insulin controls subcellular localization and multisite phosphorylation of the phosphatidic acid phosphatase, lipin 1. J Biol Chem 282:277-286.

Harris TE, Finck BN. 2011. Dual function lipin proteins and glycerolipid metabolism. Trends in Endocrinology & Metabolism. 22, 6:226-233.

Hazegh KE, Reis T. 2016, A Buoyancy-based Method of Determining Fat Levels in *Drosophila*. J Vis Exp. 117:54744.

Kaushik S. et al. AMPK-dependent phosphorylation of lipid droplet protein PLIN2 triggers its degradation by CMA. Autophagy. 12(2):432-438.

Kockel L, et al. 2010. Dynamic Switch of Negative Feedback Regulation in *Drosophila* Akt-TOR signaling. PLoS Genetics. E1000990.doi:10.1371/journal.pgen.1000990.

Kühnlein R. 2012. Lipid droplet-based storage fat metabolism in *Drosophila*. J Lipid Res. 53(8):1430-1436.

Lee G, Park JH. 2004. Hemolymph Sugar Homeostasis and Starvation-Induced Hyperactivity Affected by Genetic Manipulations of the Adipokinetic Hormone-Encoding Gene in *Drosophila melanogaster*. Genetics 167:1 311-323.

Lehmann M. 2018. Endocrine and physiological regulation of neutral fat storage in *Drosophila*. Mol Cell Endocrinol. 461L165-177.

Liu GH, et al. 2010. Lipin proteins form homo- and hetero- oligomers. Biochem J. 432(1):65-76.

Liu J, et al. 2012. Synphilin-1 alters metabolic homeostasis in novel *Drosophila* obesity model. International Journal of Obesity. 36:1529-1536.

Liu Z, et al. 2013. Lipid metabolism in *Drosophila*: development and disease. Acta Biochimica et Biophysica Sinica. 45(1):44-50.

Makarova M, GµY, Chen J-S, Beckley JR, Gould KL, Oliferenko S. 2016. Temporal Regulation of Lipin Activity Diverged to Account for Differences in Mitotic Programs. Curr Biol 26:237–243.

Park S, Alfa RW, Topper Sm, Kim GES, Kockel L, Kim S. 2014. A Genetic Strategy to Measure Circulating *Drosophila* Insulin Reveals Gene Regulating Insulin Production and Secretion. PLoS Genet 10(8): e1004555.

Péterfy et al. 2001. Lipodystrophy in the *fld* mouse results from mutation of a new gene encoding a nuclear protein, lipin. Nat. Genet. 27, 121–124

Péterfy et al. 2010. Insulin-stimulated Interaction with 14-3-3 Promotes Cytoplasmic Localization of Lipin-1 in Adipocytes. J Biol Chem. 285(6):3857-64.

Peterson TR, Sengupta SS, Harris TE, Carmack AE, Kang SA, Balderas E, Guertin DA, Madden KL, Carpenter AE, Finck BN, Sabatini DM. 2011. mTOR complex 1 regulates lipin 1 localization to control the SREBP pathway. Cell 146:408–420.

Peti W, Page R. 2013. Molecular basis of MAP kinase regulation. Protein Sci 22:1698–1710.

Pool AH, Scott K.2014. Feeding regulation in *Drosophila*. Current Opinion in Neurobiology 24:57-63.

Reue K, et al. 2000. Adipose tissue deficiency, glucose intolerance, and increased atherosclerosis result from mutation in mouse fatty liver dystrophy (fld) gene. The Journal of Lipid Research. 41, 1067-1076.

Reue K. 2009. The Lipin Family: Mutations and Metabolism. Curr Opin Lipidol. 20(3):165-170.

Reue K, Dwyer J. 2009. Lipin proteins and metabolic homeostasis. J Lipid Res. 50(Suppl): S109-S114).

Richardson CD et al. 2016. Enhancing homology-directed genome editing by catalytic active and inactive CRISPR-Cas9 using asymmetric donor DNA. Nature Biotechnology. 34, 339-344.

Saltiel et al. 2001. Insulin signaling and the regulation of glucose and lipid metabolism. Nature. 414l 799-806.

Schmelzle et al. 2000. TOR, a Central Controller of Cell Growth. Cell. 103(2),253-262.

Schmitt S, Ugrankar R, Greene SE, Prajapati M, Lehmann M. 2015. *Drosophila* Lipin interacts with insulin and TOR signaling pathways in the control of growth and lipid metabolism. J Cell Sci 128:4395–4406.

Sembongi H, et al. 2013. Distinct Roles of the Phosphatidate Phosphatases Lipin 1 and 2 during Adipogenesis and Lipid Droplet Biogenesis in 3T3-L1 Cells. Journal of Biological Chemistry. 2888: 34502-513.

Su W-M, Han G-S, Casciano J, Carman GM. 2012. Protein kinase A-mediated phosphorylation of Pah1p phosphatidate phosphatase functions in conjunction with the Pho85p-Pho80p and Cdc28p-cyclin B kinases to regulate lipid synthesis in yeast. J Biol Chem 287:33364–33376.

Steinhauer, J. 2017. Co-Culture Activation of MAP Kinase in *Drosophila* S2 Cells. Methods Mol Biol 1487: 235-241.

Tennessen JM, Barry WE, Cox J, Thummel CS. 2014. Methods for studying metabolism in Drosophila. Methods 68:105–115.

Ugrankar R, LiμY, Provaznik J, Schmitt S, Lehmann M. 2011. Lipin is a central regulator of adipose tissue development and function in *Drosophila melanogaster*. Mol Cell Biol 31:1656.

Vinayagam A, et al. An Integrative Analysis of the InR/PI3K/Akt Network Identifies the Dynamic Response to Insulin Signaling. Cell Reports 16(11): 3062-3074.

Xue Y, Li A, Wang L, Feng H, Yao X. 2006. PPSP: prediction of PK-specific phosphorylation site with Bayesian decision theory. BMC Bioinformatics 7:163.

Zhang H, et al. 2000. Regulation of cellular growth by the *Drosophila* target of rapamycin *dTOR*. Genes Dec, 21: 2712-2724.